NATIONAL BUREAU OF STANDARDS REPORT

9387

MEASUREMENTS OF THE THERMAL CONDUCTIVITY AND ELECTRICAL RESISTIVITY OF PLATINUM FROM 373 TO 1373° K

by

D. R. Flynn
Environmental Engineering Section
Building Research Division
Institute for Applied Technology
National Bureau of Standards

and

M. E. O'Hagan
School of Engineering and Applied Science
The George Washington University

U. S. DEPARTMENT OF COMMERCE
NATIONAL BUREAU OF STANDARDS

THE NATIONAL BUREAU OF STANDARDS

The National Bureau of Standards[1] provides measurement and technical information services essential to the efficiency and effectiveness of the work of the Nation's scientists and engineers. The Bureau serves also as a focal point in the Federal Government for assuring maximum application of the physical and engineering sciences to the advancement of technology in industry and commerce. To accomplish this mission, the Bureau is organized into three institutes covering broad program areas of research and services:

THE INSTITUTE FOR BASIC STANDARDS . . . provides the central basis within the United States for a complete and consistent system of physical measurements, coordinates that system with the measurement systems of other nations, and furnishes essential services leading to accurate and uniform physical measurements throughout the Nation's scientific community, industry, and commerce. This Institute comprises a series of divisions, each serving a classical subject matter area:

—Applied Mathematics—Electricity—Metrology—Mechanics—Heat—Atomic Physics—Physical Chemistry—Radiation Physics—Laboratory Astrophysics[2]—Radio Standards Laboratory,[2] which includes Radio Standards Physics and Radio Standards Engineering—Office of Standard Reference Data.

THE INSTITUTE FOR MATERIALS RESEARCH . . . conducts materials research and provides associated materials services including mainly reference materials and data on the properties of materials. Beyond its direct interest to the Nation's scientists and engineers, this Institute yields services which are essential to the advancement of technology in industry and commerce. This Institute is organized primarily by technical fields:

—Analytical Chemistry—Metallurgy—Reactor Radiations—Polymers—Inorganic Materials—Cryogenics[2]—Materials Evaluation Laboratory—Office of Standard Reference Materials.

THE INSTITUTE FOR APPLIED TECHNOLOGY . . . provides technical services to promote the use of available technology and to facilitate technological innovation in industry and government. The principal elements of this Institute are:

—Building Research—Electronic Instrumentation—Textile and Apparel Technology Center—Technical Analysis—Center for Computer Sciences and Technology—Office of Weights and Measures—Office of Engineering Standards Services—Office of Invention and Innovation—Clearinghouse for Federal Scientific and Technical Information.[3]

---

[1] Headquarters and Laboratories at Gaithersburg, Maryland, unless otherwise noted; mailing address Washington, D. C., 20234.

[2] Located at Boulder, Colorado, 80302.

[3] Located at 5285 Port Royal Road, Springfield, Virginia, 22151.

NATIONAL BUREAU OF STANDARDS REPORT

NBS PROJECT
421.03-40-4212231

NBS REPORT
9387

August 22, 1966

MEASUREMENTS OF THE THERMAL CONDUCTIVITY AND ELECTRICAL RESISTIVITY OF PLATINUM FROM 373 TO 1373 °K

by

D. R. Flynn
Environmental Engineering Section
Building Research Division
Institute for Applied Technology
National Bureau of Standards

and

M. E. O'Hagan
School of Engineering and Applied Science
The George Washington University

U. S. DEPARTMENT OF COMMERCE
NATIONAL BUREAU OF STANDARDS

ABSTRACT

Measurements have been made of the thermal conductivity and the electrical resistivity of commercial grade platinum (99.98% pure) in the temperature range 373 to 1373 °K. The measurements have been made with a view to providing accurate data on the thermal conductivity of platinum to serve as a basis for establishing platinum as a thermal conductivity standard reference material.

Two methods of measuring the thermal conductivity have been employed, one an electrical method and the other a non-electrical method. In the electrical method, a direct current passed through a necked-down portion of the specimen and the thermal conductivity was determined in terms of the temperature and electrical potential distribution in the necked-down region. The second method was of the absolute guarded longitudinal heat flow type. The experiment was designed to permit measurements by both methods in the same apparatus and on the same specimen thereby providing as direct a comparison as possible between the methods.

The data given by the two methods agree within experimental error and show the thermal conductivity of platinum to be a smoothly increasing function of temperature in the measured range. The data are considered to be accurate to better than 1% and indicate that platinum could be adopted as a thermal conductivity standard reference material.

TABLE OF CONTENTS

ACKNOWLEDGMENTS

This research was the subject of a dissertation submitted by Malcolm O'Hagan to the Faculty of The School of Engineering and Applied Science, The George Washington University, in partial satisfaction of the requirements for the degree of Doctor of Science.

This work was supported in part by Engelhard Industries, Inc., Newark, New Jersey, who supplied the platinum and financial assistance in the form of a Grant to the National Bureau of Standards. We thank Henry G. Albert and A. V. Lincoln, both of Engelhard Industries, Inc., for their support and advice.

Malcolm E. O'Hagan was supported in part by Grant AFOSR-1025-66 from the Air Force Office of Scientific Research and in part by the Institute for Industrial Research and Standards, Dublin, Ireland.

We thank Henry E. Robinson, Chief, Environmental Engineering Section, NBS, and Adjunct Professor of Engineering, The George Washington University for his advice and support.

The intricate and difficult machining required for this project was done by Raymond Chidester, Section 145.01 NBS. Much good advice in matters of fabrication came from John Hettenhouser, Section 145.01 NBS.

LIST OF TABLES

LIST OF ILLUSTRATIONS

INTRODUCTION

Standards and standard reference materials are the basis of a consistent and accurate measuring system. The need for standard reference materials in thermal conductivity measurements is two-fold. In the first place, such materials are required for comparative measurements in which the thermal conductivity of the material under test is determined in terms of that of the standard reference material. Secondly, such materials are required in evaluating the accuracy of apparatus designed for thermal conductivity measurements. The degree to which the measured value of the thermal conductivity of the standard reference material agrees with the accepted value is a check on the accuracy of the apparatus in which the measurements were made.

The basic requirements for any standard reference material are that it be stable, reproducible and appropriate for the measurements at hand, and that the property in question be uniform throughout the material. In the case of standard reference materials for thermal conductivity other desirable requirements are that the standard be usable over a wide range of temperature, that it be chemically inert so as not to be affected by or affect other materials in the system and that the thermal conductivity of the reference material be close in value to that of the materials which are to be measured in terms of it. For a more complete discussion of thermal conductivity reference standards the reader is referred to reference [1].[1/]

The advantages of using pure platinum as a thermal conductivity reference material have been pointed out by Powell and Tye [2] and by Slack [3].

1/ Numbers in square brackets refer to references listed at the end of the paper.

Platinum is a face-centered-cubic metal available in high purity (easily evaluated by electrical resistivity measurements) in pieces of substantial size. It has a fairly high melting point (2042°K on the 1948 IPTS), is optically opaque, and is relatively stable chemically in air and other atmospheres, with the exception of hydrogen, even at high temperatures [4, 5]. It is readily machinable and is not prohibitively expensive. Its thermal conductivity, although relatively high for use as a standard with non-metals, is about the geometric mean for metals and alloys (circa 0.7 W/cm deg); it has no known transition points. Powell and Tye [2] have pointed out the particular advantages of using a reference material that is also one of the most frequently used thermocouple elements.

An obvious objection one might raise concerning the use of platinum as a thermal conductivity reference material is that the thermal and electrical conductivities of ultra-pure elements at low temperatures are markedly affected by the first traces of impurity. However, small amounts of impurity would not be expected, on present theoretical grounds, to seriously affect thermal or electrical conductivity at temperatures in the vicinity of the Debye temperature or above. The stability of the electrical conductivity of platinum is evidenced by the fact that the International Practical Temperature Scale is defined by a platinum resistance thermometer in the temperature range +90.18 to 903.65°K [6, 7], and that studies are currently under way at NBS [8] and other laboratories to investigate the possibility of extending to the gold point (1336.15°K) the range over which a platinum resistance thermometer is used to define the temperature scale. The work at NBS, although not complete, appears to indicate that a properly constructed platinum resistance thermometer can be used at temperatures up to the gold

point with very good stability. The electrical resistance of very fine platinum wires (0.00127-cm diameter) has been observed [9] to be very stable in several different atmospheres at temperatures up to 1300°K. Changes in room-temperature resistance of fine wires which had been heated to temperatures in excess of 1300°K have been observed [9], however.

Stability studies on the platinum-10% rhodium:platinum thermocouple, which is currently used to define the International Practical Temperature Scale from 903.65 to 1336.15°K, have indicated that the thermoelectric power of 0.05-cm diameter platinum wire is quite stable to 1500°K in air, inert atmospheres, or vacuum [10, 11].

Platinum appears to be, in every way save one, an ideal material to use as a thermal conductivity reference standard. The exception is that the spread among the literature values for the thermal conductivity of platinum above room temperature is considerable, to say the least.

Referring to Figure 3 we see that at 1200°K the spread in the data is 25%. The need for further independent and more accurate determinations of the thermal conductivity of platinum above room temperature is obvious and it is this need that has led to the present investigation. The objective of this investigation then is to provide accurate data on the thermal conductivity of platinum above room temperature to permit the use of platinum as a thermal conductivity standard reference material. Data of this nature are also of interest to theoretical physicists in checking theoretical predictions.

CHAPTER 1

PREVIOUS INVESTIGATIONS

The thermal conductivity of platinum has been the subject of a number of investigations with the first reported values dating back to the nineteenth century. While a great variety of methods have been employed by the different investigators it is possible to classify them into two general groups. In the first group an electric current flows in the specimen generating heat therein. In the second group there is no current flowing in the specimen, and the heat is supplied from an external heat source as opposed to being generated within the specimen. For the purposes of this paper methods of the first group will be referred to as electrical methods or indirect methods since they require a knowledge of the electrical resistivity of the specimen, whereas methods of the second group will be referred to as non-electrical methods or direct methods.

The methods in the first group are based on the differential equations describing the steady-state distribution of temperature and electrical potential in a conductor carrying an electric current. In the absence of thermoelectric effects these equations can be written [see Chapter 3] as:

$$\nabla \cdot k\nabla T + \frac{1}{\rho} \nabla\phi \cdot \nabla\phi = 0, \qquad (1\text{-}1)$$

$$\nabla \cdot \frac{1}{\rho} \nabla\phi = 0, \qquad (1\text{-}2)$$

where k is the thermal conductivity of the material, ρ its electrical resistivity, T the temperature and ϕ the electrical potential. If heat losses from the surface of the conductor are rendered negligible (1-1) and (1-2) reduce to a simple equation:

$$V^2 = 8\int_{T_o}^{T_m} k\rho dT, \qquad (1\text{-}3)$$

where V is the voltage drop measured between two isothermal surfaces in the conductor at temperature T_o, and T_m is the maximum temperature in the conductor.

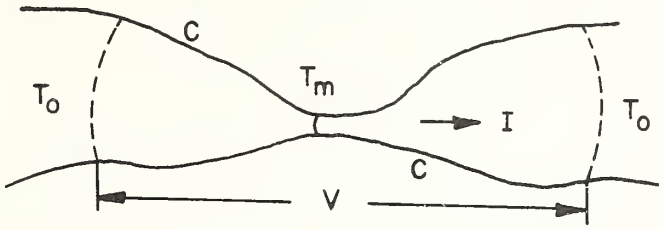

Figure 1. Conductor carrying an electric current.

Equation (1-3) is developed in detail in Chapter 3. It is independent of geometry provided heat losses from the surface, (C), are negligible. From (1-3) we see then that, in the case of negligible heat losses, the thermal conductivity is determined by measuring the voltage drop, V, in the specimen, the end temperatures, T_o, the maximum temperature, T_m, and the electrical resistivity, ρ.

The works of Jaeger and Diesselhorst [12], Meissner [13], Holm and Stormer [14], Hopkins [15], Hopkins and Griffith [16], and Cutler, et al [17] are all based on equation (1-3). Differences between these investigations arise mainly with respect to the following:

1. Generation and measurement of T_o.
2. Measurement of T_m.
3. Method of rendering heat losses negligible.
4. Analysis of the data, e.g. treatment of $k\rho$ as a function of temperature, etc.

Jaeger and Diesselhorst [12] measured on a platinum rod 1.5 cm in diameter using currents up to 350 amps. The specimen was covered with thermal insulation to minimize heat losses from its surface. The ends of the rod were in thermal contact with two constant temperature water baths thereby maintaining the ends at constant temperature T_o.

Meissner [13] measured on a wire 2 mm in diameter and 6.3 cm long. The measurements were made in vacuum in the temperature range from 20.7 to 373°K where heat losses by radiation are negligible. The maximum temperature rise, $(T_m - T_o)$, was measured by using the specimen as its own resistance thermometer. To a first approximation it can be shown [13, 18] that

$$\theta_m = \frac{3}{2}\left(\frac{R - R_o}{\alpha_o R_o}\right) \qquad (1\text{-}4)$$

where $\theta_m = T_m - T_o$, R is the measured resistance at current I, R_o is the resistance extrapolated to I = 0, or in other words the resistance of the specimen at $T = T_o$, and α_o is the temperature coefficient of resistance at $T = T_o$. More exact expressions relating θ_m to the measured resistances are developed by Meissner [13], Holm [18] and in Chapter 3 of this paper.

Holm and Störmer [14] were the first to apply the method to high temperature thermal conductivity measurements, measuring in the temperature range from 292 to 1293°K. While Meissner could employ a long specimen due to small radiation losses at the lower temperatures, a long specimen can no longer be used at the higher temperatures where radiation becomes significant. This consideration led Holm and Störmer to adopt a short necked-down specimen as shown in Figure 2.

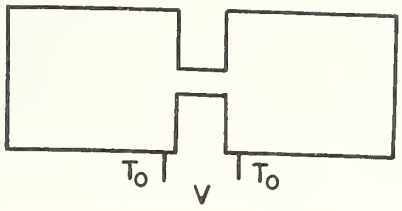

Figure 2. Necked-down Sample

Their sample was 1.0 cm diameter by 2.5 cm long with a neck 0.7 mm diameter by 5 mm long machined at the center of it. The specimen was located in a furnace where the whole specimen could be brought to the temperature T_o. The temperatures T_o were measured with Pt/Pt 10% Rh thermocouples and the maximum temperature rise $T_m - T_o$ was measured using the specimen as its own resistance thermometer similar to Meissner. The data analysis differs from that of Meissner, and is developed in full by Holm [19]. The measurements were made in a nitrogen atmosphere using currents up to 60 amps. A correction was applied for heat losses from the neck by convection and radiation.

In their experiments at high temperatures (1473 - 2580°K) Hopkins [15] and Hopkins and Griffith [16] used a simulated necked-down sample. A platinum wire 5 cm long and 0.193 mm diameter was clamped symmetrically between platinum clamps over nearly half its length at each end so as to leave 0.5 mm exposed at the middle thereby simulating a necked-down sample as used by Holm and Störmer. The clamps consisted of pairs of platinum semicylinders (0.635 cm diameter and 2.5 cm long) fitted accurately into semicylindrical channels in water-cooled copper blocks which maintained the ends of the specimen at the temperature of the cooling water, (T_o). The maximum temperature, T_m, was measured by optical pyrometry. Measurements were made in vacuum, in air, in nitrogen and in hydrogen, using currents up to 87 amps. It is

worth noting the extreme temperature gradients and current densities that existed in the neck, the former reaching values of 9200°C/cm and the latter being as high as 3×10^5 amps/cm^2. In reducing their data Hopkins and Griffith differentiate (1-3) and write:

$$V \frac{\partial V}{\partial T_m} = 4k\rho_{(T_m)} \qquad (1\text{-}5)$$

where $k\rho$ is evaluated at $T = T_m$. The thermal conductivity is thus determined by measuring V and ρ as functions of T_m, T_o being held constant.

Cutler and his associates [17, 20, 21, 22, 23, 24] simulated a necked-down sample by welding a section of 5-mil platinum wire between two blocks of the same material. The sample was suspended in a furnace which was used to bring the specimen to temperature, T_o. The maximum temperature T_m was measured using the specimen as its own resistance thermometer. The change in resistance per se was not measured, but, rather, the corresponding voltage change. They write:

$$\delta R = \frac{V^2}{12k\rho} \frac{dR}{dT} , \qquad (1\text{-}6)$$

and

$$\delta V = \frac{V^3}{12k\rho T} \frac{d(\ell n\ R)}{d(\ell n\ T)} , \qquad (1\text{-}7)$$

where $d(\ell n\ R)/d(\ell n\ T)$ is nearly unity.

Equation (1-6) follows from (1-3) and (1-4) using the approximation $V^2 = 8k\rho\theta_m$. With the entire specimen at uniform temperature, T_o (measured by a Pt/Pt 10% Rh thermocouple) the current is switched on. There is an instantaneous voltage drop V across the specimen before it has time to heat up. Superimposed on this is a transient voltage due to the change in

resistance as the neck heats up. The change in voltage δV corresponding to the change in resistance δR is observed on an oscilloscope as the peak of the transient. Measurements were made in vacuum from room temperature to 1400°K.

In the case of one-dimensional conduction where heat losses are present (1-1) and (1-2) can be written in the form [25, Sec. 4.10]:

$$\pi a^2 k \frac{d^2T}{dx^2} + \rho \frac{I^2}{\pi a^2} - 2\pi a f(T-T_a) = 0, \qquad (1\text{-}8)$$

where a is the radius of the conductor, $f(T-T_a)$ is the heat loss per unit area, I the electric current and T_a the ambient temperature. The first term in (1-8) represents the net amount of heat conducted from an element of the specimen, the second term represents the Joule heat generated in the element and the third term represents the heat loss from the surface of the element. The works of Kannuluik and Carman [26, 27], Krishnan and Jain [28], and Bode [29] are based essentially on equation (1-8). In all cases the measurements were conducted in vacuum so that heat losses from the surfaces of the conductor were by radiation and an appropriate form for $f(T-T_a)$ was used.

In their experiments Kannuluik and Carman [26, 27] used a platinum wire that was nominally 1.5 mm diameter and 11.6 cm long. The wire was mounted in a closed coaxial cylindrical tube so that the ends of the wire and the walls of the tube were at the same temperature, $T_o = T_a$. The tube was evacuated. Measurements were made at five fixed-point temperatures in the range 90 to 579°K; the thermal conductivity apparatus being immersed in fixed-point baths at each of the five temperatures. Kannuluik and Law [30] developed a solution to (1-8) in terms of measured resistances rather than

temperatures, and that solution was applied in deriving the thermal conductivity of platinum.

Krishnan and Jain [28, 31] measured on a platinum wire 0.5 mm diameter. They give no details of their apparatus. They give two approximate solutions to (1-8), one in terms of the temperature distribution near the center of a short filament, and the other in terms of the temperature distribution in regions slightly removed from the center of a long filament. Measurements were made in the temperature range 1300 to 1800°K using alternating current and measuring the temperature distributions along the wires with an optical pyrometer.

Bode [29] derived a solution to (1-8) giving the thermal conductivity in terms of the rate of change with current of the resistance and the maximum temperature in the conductor. The heat losses were evaluated by adjusting the current through the specimen until its temperature was uniform throughout and there was no temperature gradient in it. Under these conditions the first term in (1-8) is zero and the third term in (1-8), the heat loss term, is readily evaluated. The measurements were made on a wire 1 mm in diameter and 5-10 cm long, using direct currents ranging from 8 to 13 amps. The wire was mounted concentrically in an evacuated, water-cooled glass cell and the temperature distribution along it measured with an optical pyrometer.

The second group of methods mentioned at the beginning of the chapter can be considered in terms of the partial differential equation describing the one-dimensional flow of heat in a rod or bar in the absence of an electric current [25, Chapter 4]:

$$\pi a^2 k \frac{\partial^2 T}{\partial x^2} - 2\pi af(T-T_a) = \pi a^2 wc \frac{\partial T}{\partial t} , \qquad (1-9)$$

where w is the density of the material, c its specific heat and $\partial T/\partial t$ the time variation of temperature. The other parameters are as defined above. Equation (1-9) describes a transient state with the term on the right hand side representing the rate of accumulation of heat. The solution to (1-9) yields the thermal diffusivity, $\varkappa$, = k/wc, whence the thermal conductivity is determined from a knowledge of the density, w, and the specific heat, c. Wheeler [32], Martin and Sidles [33], Zolotukhin [34], Schulze [35] measured the thermal diffusivity of platinum and used their results to compute thermal conductivity.

In his measurements Wheeler used a method proposed by Cowan [36]. The specimen, in the form of a thin solid plate, is mounted in a vacuum chamber and heated uniformly to incandescence by bombarding one face with a beam of electrons from an electron gun. The electron beam is amplitude modulated to vary sinusoidally with time, and the phase difference between the resulting temperature fluctuations on the two faces of the plate yields a solution for the thermal diffusivity. Heat loss is by radiation and the fourth power radiation law is assumed. The platinum plate was 1 mm thick with face area of 0.3 - 1.3 cm^2. The phase difference was measured in terms of the phase difference between the signals from two photocells trained on the opposite surfaces of the plate. Temperature measurements were made with an optical pyrometer.

Martin and Sidles [33] used a modified Angstrom method in measuring the thermal diffusivity of platinum. A sinusoidally varying temperature was

applied to one end of a long rod (10-12 inches long and 3/16 inches in diameter). The temperature oscillations produced at the end of the rod were propagated along it. From temperature measurements at two locations along the rod the velocity of propagation of the temperature wave was determined as well as the amplitude decrement of the wave between the two measuring stations. The amplitude of the temperature oscillation in the specimen did not exceed 5°C so that Newton cooling could be assumed. Under these conditions Sidles [37] has shown that the solution to (1-9) yields a simple expression for the thermal diffusivity:

$$K = \frac{LV}{2 \ell n\, q} \quad , \qquad (1\text{-}10)$$

where L is the separation of the measuring stations, V is the velocity of propagation of the temperature wave and q is the amplitude decrement of the wave between the measuring stations. The period of the oscillations was 60 seconds, and temperatures were measured with Pt/Pt 10% Rh thermocouples. Measurements were carried out from room temperature to 1200°K on two samples of platinum, one of commercial purity and one of high purity. The measurements were made in vacuum except at the lower temperatures where a helium atmosphere was used.

Zolotukhin [34] apparently used a method of the Angstrom type [38] but no details of his work are available to the author.

In measuring the thermal diffusivity of platinum at room temperature Schulze [35] allowed the specimen to assume a constant temperature. One end of the rod was then cooled suddenly and the temperature observed at regular time intervals a short distance from that end. The solution to (1-9) under

these conditions is

$$T = 1 - \text{erf} \frac{x}{2\sqrt{\kappa t}} \qquad (1\text{-}11)$$

where erf denotes the error function. A discussion of this method and the solution is given in reference [25, Sec. 2.10].

For steady-state conditions the term on the right-hand side of (1-9) is zero and we can write:

$$\pi a^2 k \frac{d^2T}{dx^2} - 2\pi a f(T-T_a) = 0. \qquad (1\text{-}12)$$

Barratt [39] measured the thermal conductivity of platinum on a wire 1 mm in diameter and 35 cm long at 290 and 373°K. Heat was supplied at a constant rate to one end of the wire. The heat was conducted down the wire and lost from the surface of the wire to the surrounding medium. The temperature of the hot end of the wire did not exceed that of the surrounding medium by more than about 10°C so that Newton cooling could be assumed, i.e. $f(T-T_a) = (T-T_a)H$ where H is a constant. Under these conditions the solution to (1-12) gives

$$k = \frac{Q^2}{2\pi^2 a^3 H (T_H - T_a)^2} \coth^2 rL \quad , \qquad (1\text{-}13)$$

where Q is the amount of heat flowing into the wire at the hot end, T_H is the temperature of the wire at the hot end, L is the length of the wire and

$$r = \sqrt{\frac{2H}{ka}} \quad .$$

The temperatures were measured with platinum resistance thermometers. The surface conductance H was determined in a second experiment. All the heat generated in the center span of the wire when an electric current passed through it was assumed to be lost to the surrounding medium. The mean

temperature rise of the span above that of the surrounding medium was determined using the wire as its own resistance thermometer. Then $H = Q'/\theta'$ where Q' is the heat generated and θ' is the mean temperature rise.

Barratt and Winter [40] used essentially the same method as Barratt had used earlier with the exception that a shorter wire was employed and both its ends were held at fixed temperatures. For the solution see [25, Sec. 4.5].

If heat losses from the specimen are rendered negligible (by use of a guard), (1-9) further simplifies to the basic equation defining thermal conductivity

$$-\pi a^2 k \frac{dT}{dx} = Q \ , \qquad (1\text{-}14)$$

where Q is the heat flowing in the specimen and dT/dx is the temperature gradient therein. Thermal conductivity is measured most directly in terms of (1-14). In longitudinal heat flow methods a measured amount of heat flows in a bar of diameter large enough to permit accurate determination of its cross-sectional area. The temperature distribution along the bar is measured and used in computing the temperature gradient. A cylindrical tube is located coaxial with the specimen and bears a temperature distribution matching that on the specimen thereby minimizing lateral heat losses from the specimen. The space between the specimen and the guard cylinder can either be filled with thermal insulation, as is generally done at medium and high temperatures, or be evacuated, as is generally done at low temperatures. Any heat losses are then by conduction or radiation and can be satisfactorily analyzed. The guarded longitudinal heat flow method is potentially the most accurate means of measuring thermal conductivity, but, despite its apparent simplicity, it

is also one of the most difficult methods experimentally. Bode [41], Powell, Tye and Woodman [42] and Powell and Tye [2] measured the thermal conductivity of platinum in this way. Grüneisen and Goens [43], Mendelssohn and Rosenberg [44] and White and Woods [45] conducted their measurements at low temperatures in vacuum where use of a guard is not necessary.

Grüneisen and Goens [43] measured the thermal conductivity at 21.2 and 83.2°K on the same platinum as had been used earlier by Meissner [13]. A heater was attached to one end of the specimen and the temperatures were measured with thermocouples.

Mendelssohn and Rosenberg [44] measured on a rod about 5 cm long and 1 - 2 mm in diameter over the temperature range 2.4 to 31.7°K. A small electric heater was wound around one end of the rod and the other end was connected to the expansion chamber of a Simon helium liquifier. Helium gas thermometers were attached to the specimen by copper contacts 3 cm apart. The pressure difference in the thermometers corresponding to their temperature difference was read on a differential oil manometer.

White and Woods [45] used the same method as Mendelssohn and Rosenberg. Their specimen was 1.5 mm in diameter and 5 - 7 cm long.

Bode [41] measured the thermal conductivity of platinum on a bar 5 cm in diameter and 7 cm long in the temperature range 273 to 373°K. Details of the apparatus are given by Bode and Fritz [46]. The heat input was measured in terms of the electric power dissipated in a heater located at the hot end of the specimen. The temperature distributions in the specimen and guard were measured with copper-constantan thermocouples.

Powell, Tye and Woodman [42] and Powell and Tye [2] have made an extensive series of measurements on the thermal conductivity of platinum. They carried out their measurements on two samples using several variations of a comparative guarded longitudinal heat flow method. The first specimen was 0.635 cm in diameter and 6.1 cm long, and the second specimen 1.269 cm in diameter and 10.16 cm long. The thermal conductivities of both specimens were measured from 320 to 520°K using a comparative method in which the specimen was attached to a rod of Armco iron of known thermal conductivity at its upper end and to a water-flow calorimeter at its lower end. The heat in-flow to the specimen was measured in terms of the temperature gradient established in the iron, and the heat out-flow by means of the water-flow calorimeter. The thermal conductivity of the platinum was thus determined in terms of that of the Armco iron, with heat loss corrections applied from the two heat-flow measurements.

For measurements above 520°K the calorimeter was not used, and the assembly was inverted so that the platinum was uppermost and at the higher temperature. Two series of measurements were made. In one the Armco iron rod had a diameter of 0.371 cm, in the other an Armco iron rod of 1.273 cm diameter was used. The measurements were made in vacuum with powder insulation between the specimen assembly and the guard.

A further series of measurements were made on the second specimen from 273 to 800°K. The assembly was the same as described above for the high temperature measurements but with a water-flow calorimeter attached to the lower end of the Armco iron rod to give a second measure of heat flow.

Other reported values of the thermal conductivity of platinum include those of Carter [47], Johansson and Linde [48] and Mikryukov [49]. No details of their works are available to the author. It is possible that the values reported by Carter have been referenced from Jaeger and Diesselhorst [12].

The available information pertaining to the characterization of the platinum specimens used by various investigators is summarized in Table 1 below so that differences in their specimens may be allowed for in comparing their results.

Table 1. Sample Characterization of Platinum Samples Used By Various Investigators.

Investigator	Ref	Source[1]	Purity	ρ_{273}[2]	ρ_o[3]	Density
			Pt%	$\mu\Omega$-cm	$\mu\Omega$-cm	gm/cm^3
Jaeger and Diesselhorst	12			10.12		21.39
Schulze	35	FH		10.0		
Barratt	39	JM	"pure"	9.77		
Meissner	13	FH	"high"	9.81	0.0162	
Grüneisen and Goens	43	FH	"high"	9.81	0.0162	
Holm and Störmer	14	FH	99.95	9.90		
Kannuluik and Carman	26			9.87		
	27			9.97		
Mendelssohn and Rosenberg	44	JM	99.999	~9.8	~0.01	
Krishnan and Jain	28	JM	"Spectro"			
White and Woods	45	Baker	99.99	9.79	0.0125	
Hopkins and Griffith	16	JM	99.999			
Mikryukov	49		99.99			
Bode	29	Degussa	99.9			
Cutler, et al	17		99.9			
Powell and Tye	2	JM	99.999[4]	9.85	0.013	21.5
Bode	41		99.98[4]			21.32
Martin and Sidles[5]	33	Bishop	99.999			
			99.9			
Wheeler[6]	32	JM	99.95			21.5

1/ FH - Firma Heraeus, Germany; JM - Johnson, Matthey and Co., England; Baker - Baker Platinum Co., USA; Degussa, Germany; Bishop - J. Bishop and Co., USA.

2/ Ice-point resistivity

3/ Residual resistivity.

4/ Spectrographic analysis given in reference.

5/ Martin and Sidles computed thermal conductivity from diffusivity using assumed density of 21.37 gm/cm^3 and specific heat data of Jaeger and Rosenbohm [50].

6/ Wheeler computed thermal conductivity from diffusivity using measured density of 21.5 gm/cm^3 and specific heat data of Kubaschewski and Evans [51].

- - -

The thermal conductivity data on platinum are summarized in Figures 3 and 4 and in Table 2. Reported values of the Lorenz Number are plotted in Figure 5.

Table 2. Thermal Conductivity of Platinum in the Temperature Range 273-373°K as Reported by Several Investigators.

Investigator	Ref.	Temperature °K		
		273	292[1/]	373
Jaeger and Diesselhorst	12		0.696	0.725
Schulze	35			
Barratt	39	0.691	0.690	0.711
Meissner	13	0.699	0.701	0.706
Johansson and Linde	48		0.690	
Holm and Störmer	14		0.699	0.715[2/]
Kannuluik and Carman	26	0.702		0.720
Mikryukov	49			.720
Cutler, et al	17		.609	
Powell and Tye	2	.733		.730
Bode	41	.702	.705	.710
Martin and Sidles	33			.701

1/ Nominal temperature - data points range from 290 to 294°K.

2/ Value interpolated from equation given in reference.

- - -

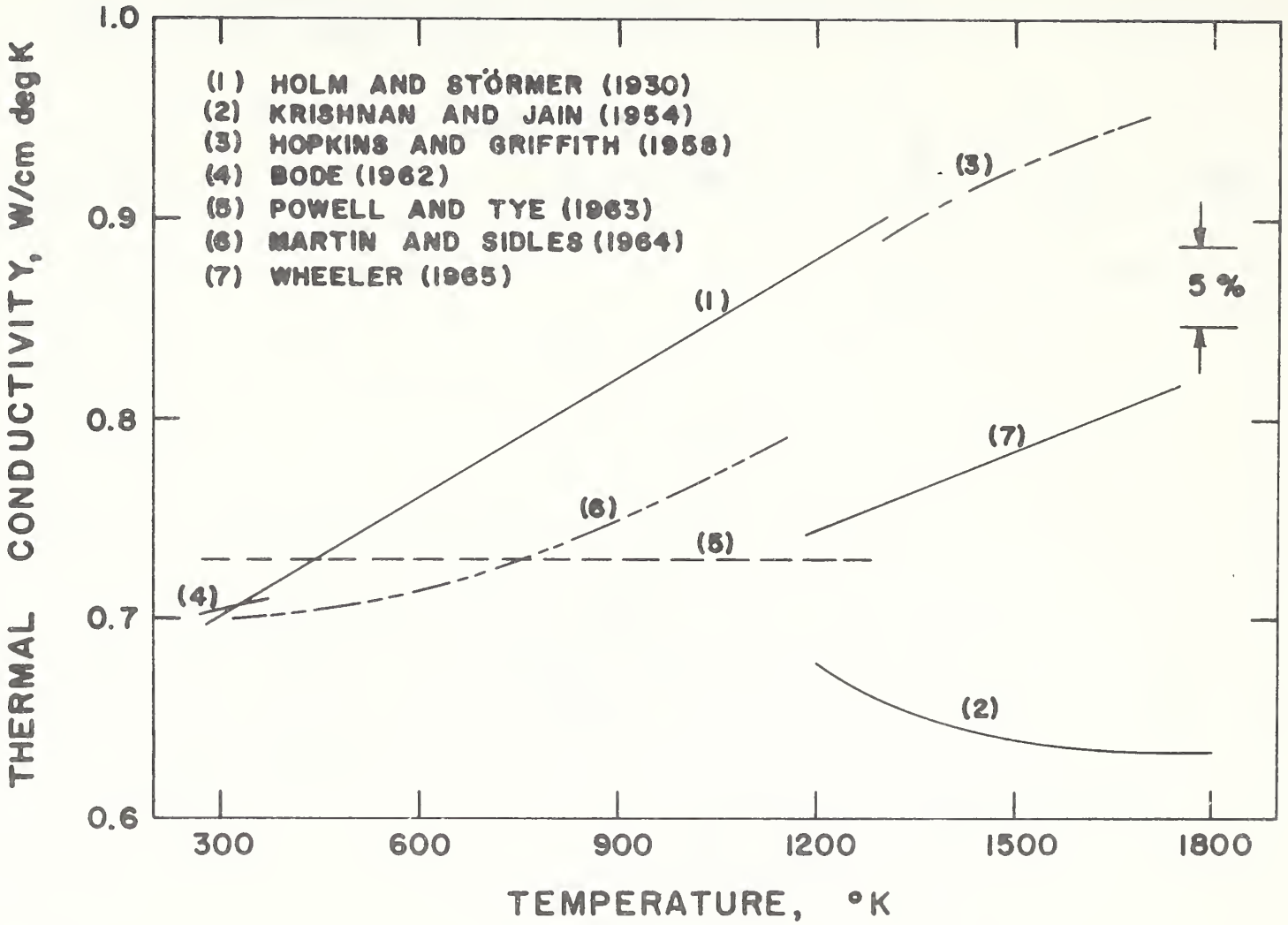

FIG. 3, THERMAL CONDUCTIVITY OF PLATINUM AS REPORTED BY SEVERAL INVESTIGATORS.

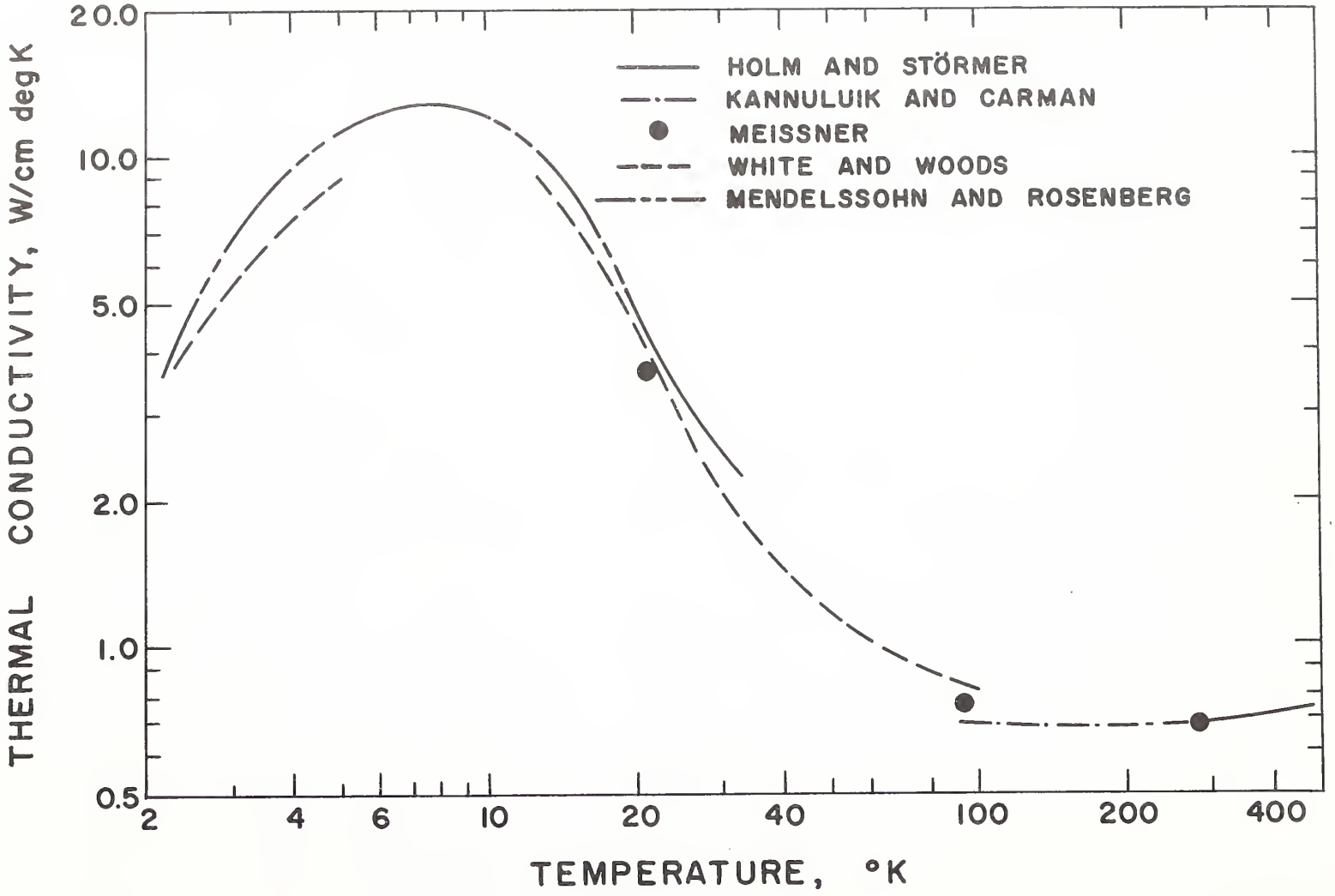

FIG. 4, LOW TEMPERATURE THERMAL CONDUCTIVITY OF PLATINUM AS REPORTED BY SEVERAL INVESTIGATORS.

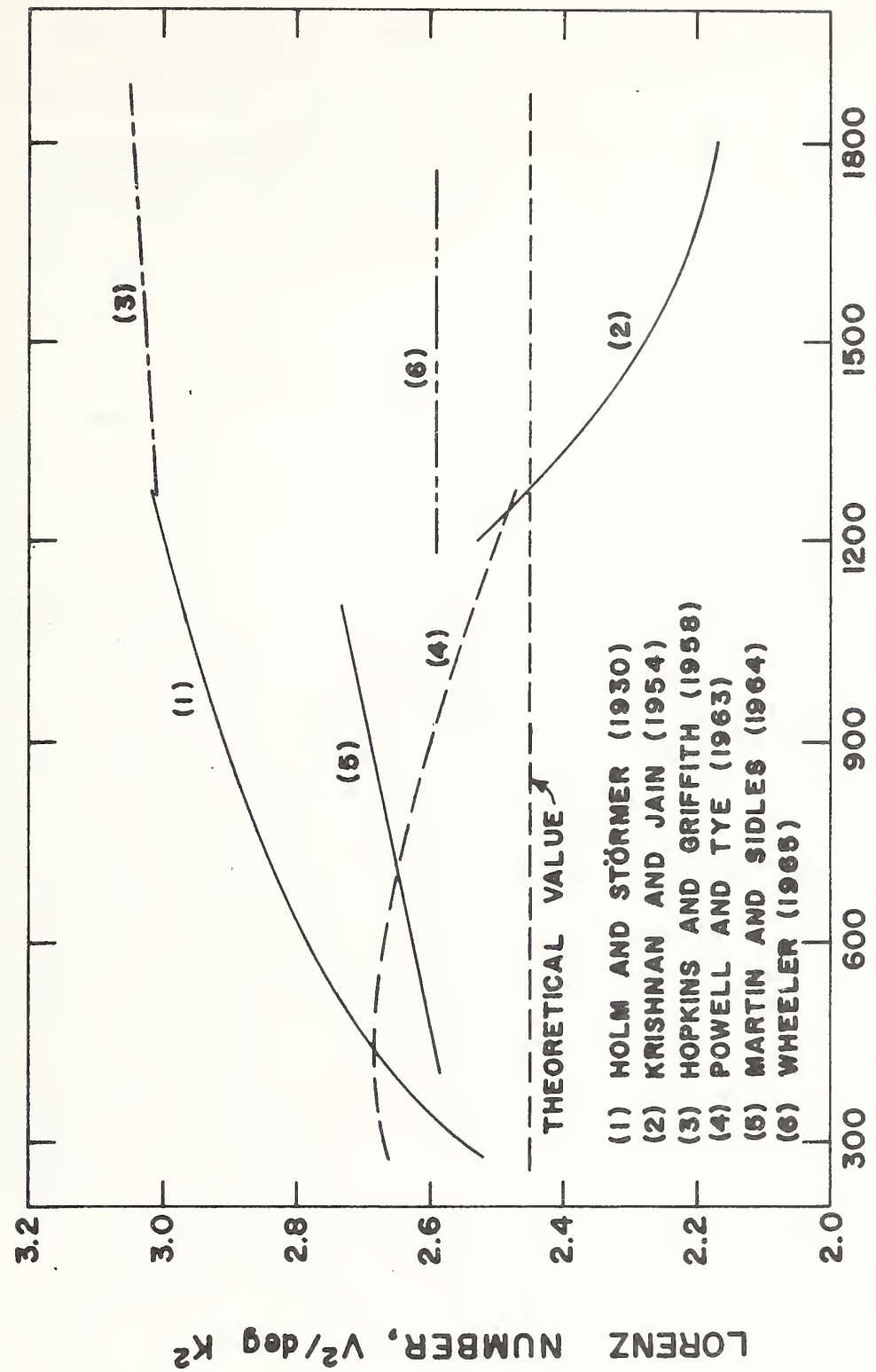

FIG. 5, LORENZ NUMBER FOR PLATINUM AS REPORTED BY SEVERAL INVESTIGATORS.

The agreement between the reported values for the thermal conductivity of platinum in the temperature range 273 - 373°K is quite good. Representative of these values are the results of Bode [41] which are quoted as being accurate to 0.5%. All the investigators, with two exceptions, Cutler, et al and Powell and Tye, agree with Bode to within 2%. Cutler, et al report four values at room temperature with scatter of 14% indicating the inaccuracy of these results. The results of Powell and Tye, representing as they do a large number of determinations by well established methods [52, 53], are about 4% higher than those of Bode. This may be due to the higher purity and higher density of the samples used by Powell and Tye.

Some of the high temperature thermal conductivity data on platinum are plotted in Figure 3. The data of Meissner, Kannuluik and Carman, and Mikryukov all fall within 2% of Holm and Störmer's curve. The data of Bode [29] which he refers to as preliminary, and those of Cutler, et al, show considerable scatter but tend to agree also with the results of Holm and Störmer. As shown in Figure 3, values of thermal conductivity computed from the Lorenz number reported by Hopkins and Griffith, using the resistivity values of Vines [79], tend to confirm those of Holm and Störmer at the higher temperatures. The results of Holm and Störmer are thus representative of those of a number of people all of whom measured the thermal conductivity by an electrical method. However, these results as a group differ significantly from the results of Powell and Tye, Martin and Sidles, and Wheeler, all of whom used a non-electrical method. The results of Krishnan and Jain fall in a category by themselves showing the thermal conductivity of platinum to be a decreasing function of temperature.

The low temperature thermal conductivity results are in good agreement when one allows for differences in sample purity as the thermal conductivity is strongly dependent on purity at low temperatures. The data of Grüneisen and Goens [43] are not shown in Figure 2 but they are essentially in agreement with the results of Meissner.

CHAPTER II

DESCRIPTION OF THE APPARATUS

It has been pointed out in Chapter 1 that all the data above room temperature, with the exception of that of Krishnan and Jain, derived from investigations using electrical methods are in fairly good agreement. However, the values given by the electrical methods are considerably higher than those given by non-electrical methods. Although there is a great deal of variation in published data, there is some evidence to indicate that electric methods tend to give higher values of thermal conductivity than do non-electric methods for some of the other transition metals also, notably tungsten [38]. This immediately raises the question as to whether or not there are some inherent differences in the values of thermal conductivity yielded by the two types of methods. Two possible reasons for such differences come to mind.

1. The analyses of electrical methods may be subject to errors of omission or logic.
2. Thermal conductivity may be significantly dependent on electric current density, at least for some materials.

In view of the differences just noted it was decided to conduct the present investigation using both an electrical and a non-electrical method. As we have seen in Chapter 1, a necked-down sample is an appropriate form for high temperature measurements by an electrical method. Moreover, this is the sample configuration utilized by Holm and Störmer, Hopkins and Griffith and Cutler, et al, with whom we wish to compare data. Consequently, it was decided to use such a sample configuration for the electrical method.

As regards a non-electrical method it was decided to use the guarded longitudinal heat flow method. This method, while cumbersome, is the most direct and most accurate method of measuring thermal conductivity for high conductivity materials.

To give a direct and accurate comparison between the two methods it was considered desirable to combine both sets of measurements in one apparatus and on the same specimen thereby eliminating a number of uncertainties which would arise in comparing data derived from measurements in different apparatus and on different specimens.

The above considerations led to the specimen configuration shown in Figure 12. The specimen (A) is raised to the desired temperature level by means of the heaters Q_1 and Q_3. In the non-electrical method, or the direct method as it will be referred to in the remainder of the paper, the heater, Q_2, located slightly above the center of the bar is energized so as to cause heat to flow down the bar. Heat from this heater is prevented from flowing up the bar by adjusting the top heater so that there is no temperature difference across the necked-down region of the specimen. Lateral heat losses from the bar are minimized by matching the temperature distribution along the guard to that along the specimen. Thermal conductivity is determined from the measured temperature distribution along the lower portion of the bar, the power input to the central heater and the geometry.

In the electrical method or the indirect method as it will be referred to, an electric current is passed through the specimen. The electrical potential drop across the necked-down region of the specimen is measured

as a function of current, while the maximum temperature rise in the neck is determined from the change in electrical resistance (due to a given change in current) and the temperature coefficient of resistance of the material. The thermal conductivity is determined from the voltage drop across the neck, the maximum temperature rise in it, and the electrical resistivity of the material. The electrical resistivity is determined from potential drops in the lower part of the specimen at the lowest current setting.

The apparatus is described in detail in this chapter and the methods are discussed at length in Chapters 3 and 4.

Mechanical Configuration

The mechanical configuration of the apparatus is illustrated diagrammatically in Figures 6 and 9 and described in detail below.

Specimen: The specimen (A) is a bar 0.7864 inch (~ 2 cm) diameter by 7.25 inches long with a 0.045-inch diameter by 0.130-inch long neck machined in it 1.622 inches from the upper end (Figure 7). A special technique, described in Appendix A, had to be developed for machining the neck due to its structural weakness.

Molybdenum extensions (B) of the same diameter as the specimen are screwed to the specimen (A) at both ends. These extensions consist of bars approximately 3 1/2 inches long bored from one end to a depth of 3 inches, leaving a 0.040-inch thick wall. The open ends are brazed to copper blocks (C) that act as heat sinks. The molybdenum extensions are filled with high purity coral alumina.

The lower end of the specimen assembly (B-A-B) is bolted to, but electrically insulated from, a brass flange which is welded to a water-cooled brass column (D). This column is firmly bolted to plate (E) which serves as a base for the apparatus.

One of the major problems with the necked-down specimen is that of protecting the neck from mechanical strain due to tension, compression, torsion or bending. Any clamp supporting the neck would have to be electrically insulated from the specimen and differential thermal expansion between the clamp and specimen would introduce strain in the neck. As an alternative to a clamp it was decided to counterbalance the load on the

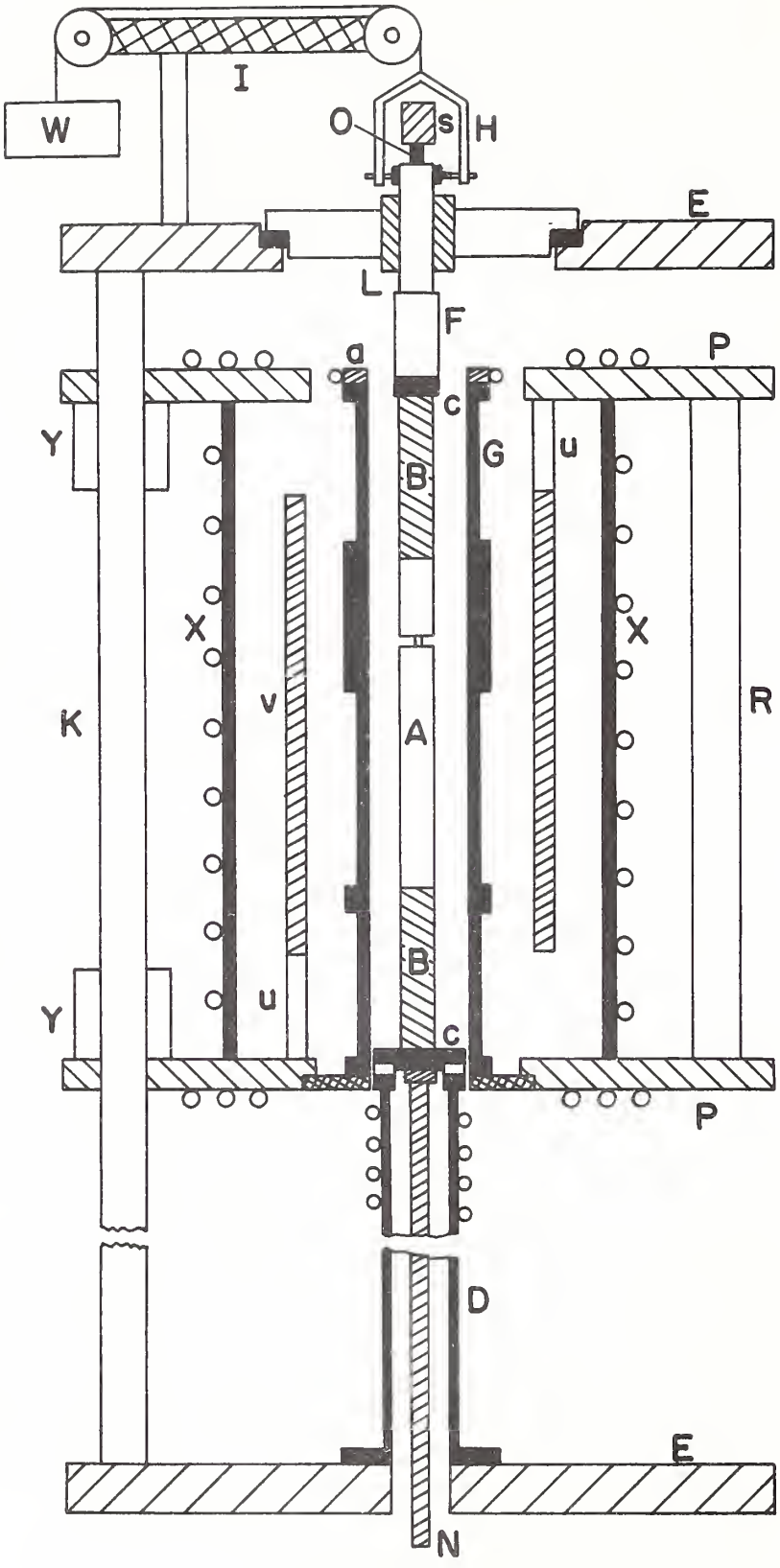

Figure 6, The Apparatus (Components are Identified in the Text)

Figure 7. Upper end of the platinum specimen showing the neck, the outer set of thermocouples and the specimen heater. The upper heater and part of the upper molybdenum extension also appear.

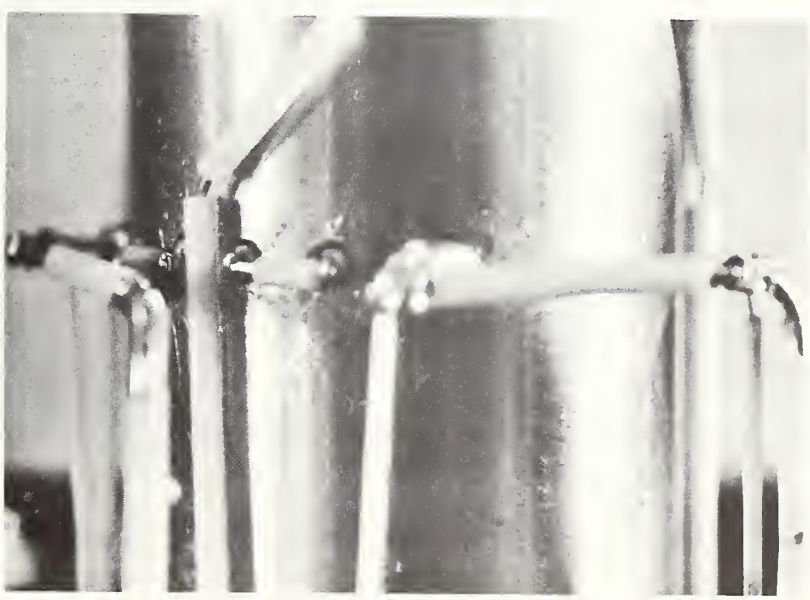

Figure 8. Close up view of the specimen heater. The two current leads can also be seen along with the two potential leads welded to the right-hand current lead. The two wires coming from above the specimen are thermocouple wires.

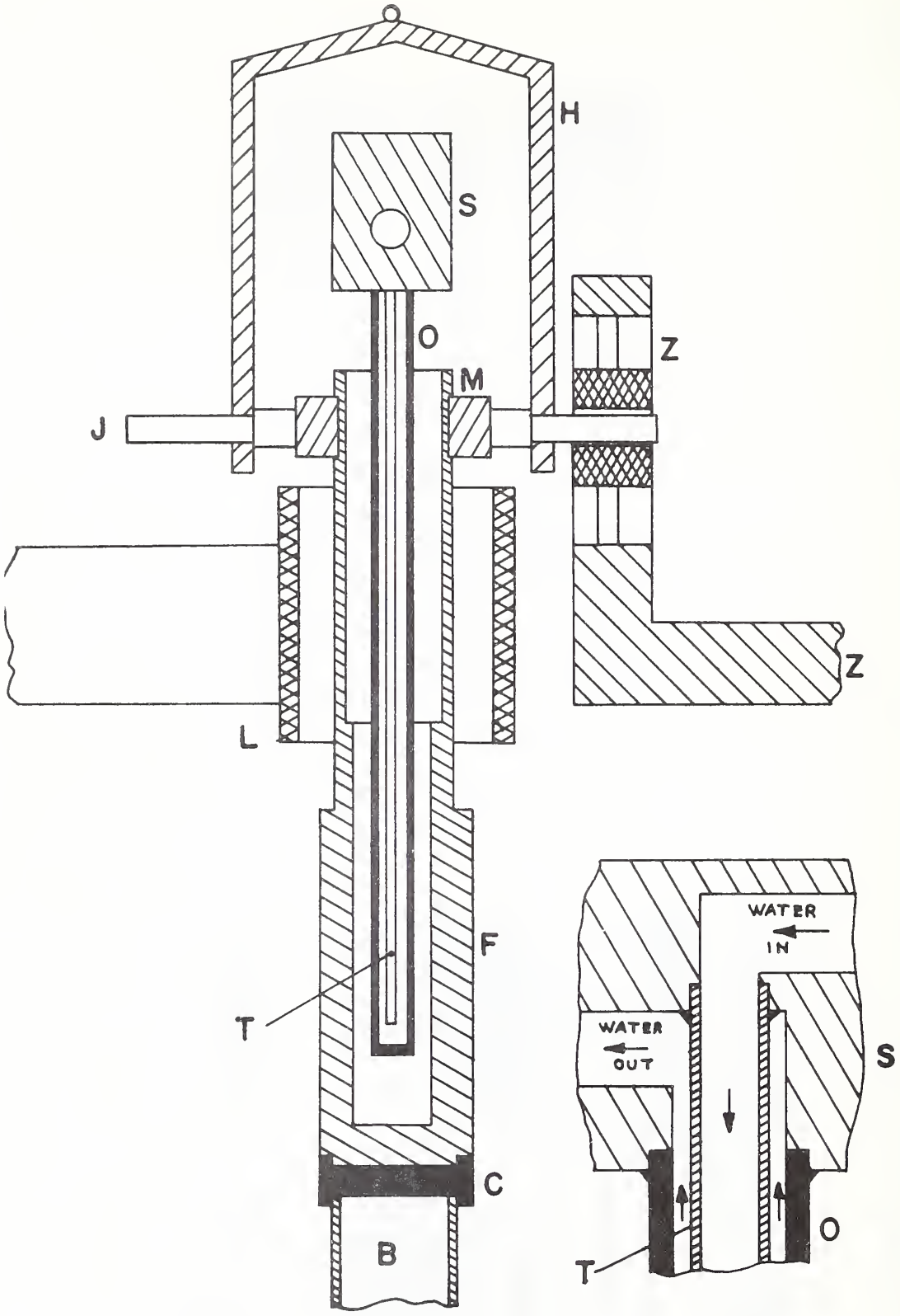

Figure 9. Details of the Suspension System and the Upper Assembly. (Components are Identified in the Text).

neck due to the weight above it so that there would be no net force on the neck. The weight of platinum above the center of the neck was computed from dimensional measurements and from the measured density of the specimen, and the components extending from the upper end of the specimen were weighed before assembly.

The counterweight (W) is suspended from a string which passes over two pulleys and attaches to an aluminum hanger (H). The pulley wheels are mounted on ultra-high-precision, low-friction, bearings of 1/8-inch diameter bore and have a starting force of less than 1 g each. The hanger pulls on two pins (J) projecting from a split aluminum collar (M) clamped to a molybdenum well (F) which is brazed to the upper copper block (C). The molybdenum well passes through a 3/4-inch linear bearing (L) which serves to maintain the upper part of the specimen in precise alignment with the lower part, and presents negligible resistance to the free vertical motion of the specimen resulting from thermal expansion. The bearing is mounted on the upper plate (E) but electrically insulated from it. The two 15 3/4-inch diameter by 1-inch thick aluminum plates (E,E) are connected by three 1-inch diameter stainless steel tie bars (K) to form a rigid framework for maintaining proper specimen alignment. The overall length from the inside of one plate to the inside of the other is 30 1/2 inches. One of the pins (J) projecting from the aluminum collar is constrained in a device (Z) consisting essentially of two fixed vertical pillars and two horizontal plates which can be moved up and down (Figures 9 and 10). The vertical pillars prevent lateral motion of the pin and thereby prevent the upper part of the specimen from rotating

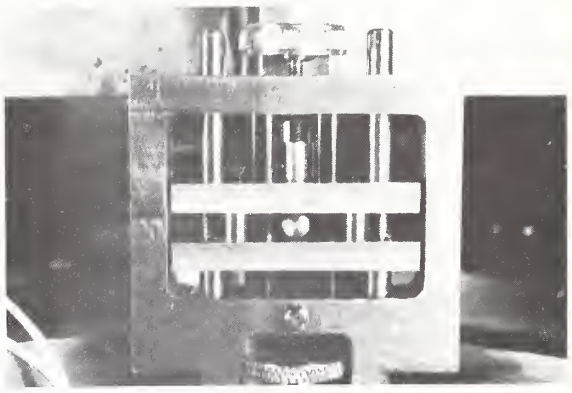

Figure 10. Device for constraining the upper part of the specimen. The end of the pin can be seen between the two horizontal plates and the two vertical pillars.

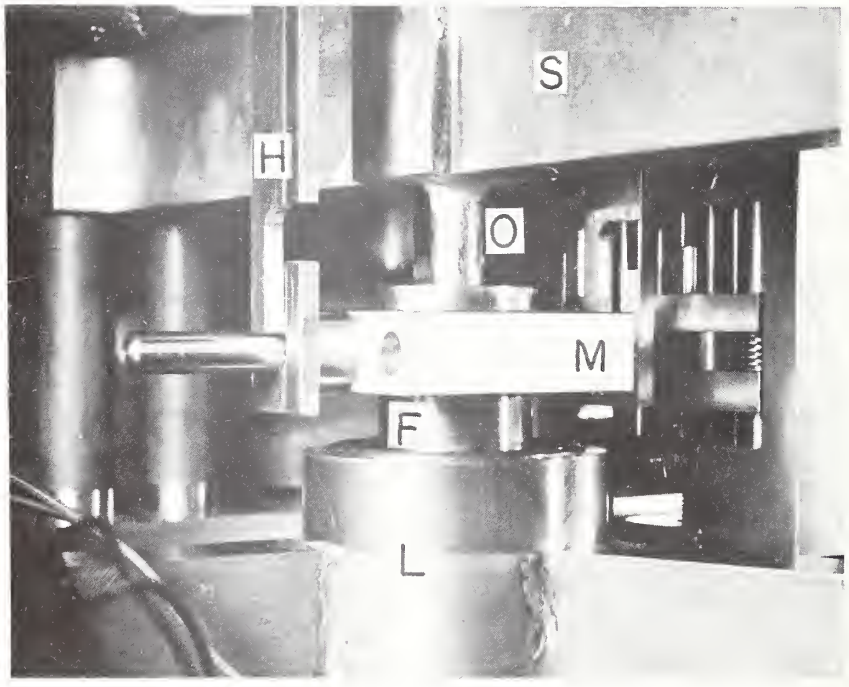

Figure 11. Close up view showing the linear bearing housing (L), the upper end of the molybdenum well (F), the clamp (M), the hanger (H), the molybdenum electrode (O) and the copper support (S).

relative to the lower part. The horizontal plates can be located so as to prevent up or down motion of the pin and consequently of the upper part of the specimen. The horizontal plates are maintained in the constraining position to protect the specimen except when tests are in progress and the specimen must be free to contract and expand thermally.

Current is introduced to the specimen through a 3/8-inch diameter copper rod (N) at the lower end and through a molybdenum electrode (O) at the upper end (Figures 9 and 11). The electrode is a 1/4-inch outside diameter by 3/16-inch inside diameter tube closed at one end and brazed to a copper support (S) at the other. The copper support is fastened to the upper plate (E) but electrically insulated from it. The molybdenum well (F) contains a liquid metal into which the electrode dips thereby affording a flexible current connection. The buoyant force of the liquid metal on the electrode contributes to the load on the neck and must be compensated for in the counterweight. The electrode is fixed but the molybdenum well moves upwards with the specimen due to thermal expansion during test runs. This changes the buoyant force and consequently puts a load on the neck. The maximum change in buoyant force is only 3 grams however and so the neck is not strained significantly. The liquid metal used was a gallium-indium eutectic alloy chosen primarily for its low vapor pressure and its comparatively low freezing temperature of 15.7°C. The requirement for low vapor pressure was dictated by a need to evacuate the system. Preliminary tests were run to evaluate the uncertainty in buoyant force due to surface tension and sticking of the gallium-indium to the molybdenum surfaces. A very definite hysteresis effect was observed

as the electrode was moved relative to the well and then returned to its initial position. The largest uncertainty in buoyant force was determined to be about 4 grams. The choice of molybdenum as the electrode and well material stems from its compatability with gallium which reacts with most other metals, and from the fact that molybdenum is wetted by gallium.

The current feed-in system serves also as a heat sink for the upper part of the specimen assembly. Water flows down a 1/8-inch diameter thin-wall stainless steel tube (T) within and concentric with the molybdenum tube and flows back out between the two so that the electrode acts as a heat exchanger transferring the heat from the liquid metal to the cooling water. The inner tube is also brazed to the copper support as shown in Figure 9. The water is pumped from a tank through a closed system and its temperature is always well above the freezing point of the gallium-indium eutectic alloy.

Furnace: The furnace skeleton (Figure 6) consists of two brass plates (P), 1/2-inch thick by 15 3/4 inches in diameter, joined by three 1-inch diameter stainless steel tie rods (R). The outer shell of the furnace (X) is a brass tube 8 1/2 inches outside diameter by 1/8-inch wall thickness. It slips over a ring fastened to the lower brass plate but is not connected to the ring. Copper coils for water cooling the furnace are soft soldered to both plates and to the outer shell.

The inner core (G) of the furnace, or the guard as it is called, is a molybdenum tube 15 inches long by 2 1/4 inches inside diameter. Molybdenum was selected as the most suitable metal from a standpoint of high-temperature thermal and mechanical properties, compatability with other materials in the

system, and cost. Since the inner core acts as a thermal guard to prevent heat losses from the specimen, it was considered more desirable to make it from metal rather than from ceramic so that the temperature distribution along it could be more easily controlled and more accurately measured. In the gradient section at each end and in the central gradient section, the wall thickness of the guard is 1/16 inch. For a span of 3 1/4 inches opposite the neck region on the specimen the wall thickness increases to 3/8 inch to assist in making that region isothermal as desired in the experiment. There is a second span of 1/2 inch where the wall thickness is 3/8 inch to allow grooves to be machined in the tube to accommodate a heater winding. The space between the specimen and the molybdenum guard is filled with high purity aluminum oxide powder of very low thermal conductivity (0.43 mW/cm deg C in air at 22°C) and low density (0.16 gm/cm^3). The guard sits on a brass plate which is fastened to the lower furnace plate, and can be removed for inspection or repair without disturbing the remainder of the furnace. Attached to the upper end of the guard is a brass ring (a) having the same inside and outside diameters as the guard itself. The ring has a copper cooling coil soldered to it to maintain the end of the guard at room temperature. It also has a terminal strip screwed to it to which the heater leads are connected. Two-mil[2/] indium foil is used at all interfaces to enhance thermal contact.

The outer furnace core (V) is an aluminum oxide tube 5 inches inside diameter by 5 3/4 inches outside diameter by 10 inches long supported on three 3/8-inch diameter aluminum oxide rods (U).

[2/] 1 mil = 0.001 inch.

Attached to the upper plate of the furnace is a split nut. This nut engages a lead screw mounted between the plates (E,E) and by turning the screw the furnace can be moved up or down. Ready access to the specimen is thereby afforded. The three tie rods (K) act as guide rods for the furnace. Six linear bearings (Y) attached to the furnace plates ensure alignment and permit the furnace to move up and down freely. The correct vertical location of the guard relative to the specimen is determined when a probe attached to the upper end of the guard makes electrical contact with a plate attached to the molybdenum well at the upper end of the specimen assembly. When the furnace has been positioned the indicating probe attached to the guard is removed.

Environmental System: The entire apparatus is mounted on the base plate of a 4-inch vacuum station, the base plate being 26 inches in diameter by 1 inch thick. A 4-inch high by 24-inch diameter aluminum feed-through ring with twelve ports accommodates power, thermocouple, water, gas and vacuum-gage feed-throughs. The thermocouple feed-throughs were made by passing the wires with flexible fiber-glass sleeving on them through a brass elbow section and filling it with hot low vapor pressure vacuum wax[3/] which formed a vacuum seal upon solidification. A 24-inch diameter by 26-inch high stainless steel bell jar sits on the feed-through ring and encloses the complete apparatus. The bell jar has two 4-inch diameter viewing ports and is counterweighted to enable it to be raised and lowered.

The system can be evacuated and measurements made in vacuum. However,

---

3/ The wax used was Hard "W" Apiezon wax.

preliminary tests run in vacuum on the type of heater used for heating the specimen, as described below, showed that the mean temperature of the heater winding was approximately 1000°C above that of the test bar in which the heater was located when the test bar was at room temperature and the heater was delivering only 7 watts. Similar tests in nitrogen atmosphere showed the mean temperature of the heater winding to be approximately 600°C above that of the test bar with the latter at 300°C when the heater was delivering 110 watts. In view of these tests, it was obvious that the specimen could not be run in vacuum. As molybdenum is easily oxidized, an inert atmosphere had to be used. Argon was chosen on account of its low thermal conductivity.

Thermal Configuration

Specimen: The heater and thermocouple locations on the specimen and guard are shown in Figure 12.

End heaters, Q_1, and Q_3, are located in the molybdenum extensions (B), 3/8 inch from the platinum-molybdenum interfaces. Each heater consists of six helical coils of 8-mil diameter Pt 30% Rh wire, the coils having an outside diameter of 31 mils and a pitch of 15 mils. The individual coils are slipped into single-bore, high purity, alumina tubes of 32 mils bore and 47 mils outside diameter. The tubes are placed in 48-mil diameter holes eloxed in the molybdenum extensions and located so as to uniformly introduce the heat over the cross-sectional area. The tubes are a snug fit in the holes giving reasonably good thermal contact. The coils are torch welded to 15-mil diameter platinum jumpers which connect them in series. The jumpers are insulated in alumina tubes. Current leads of 20-mil diameter

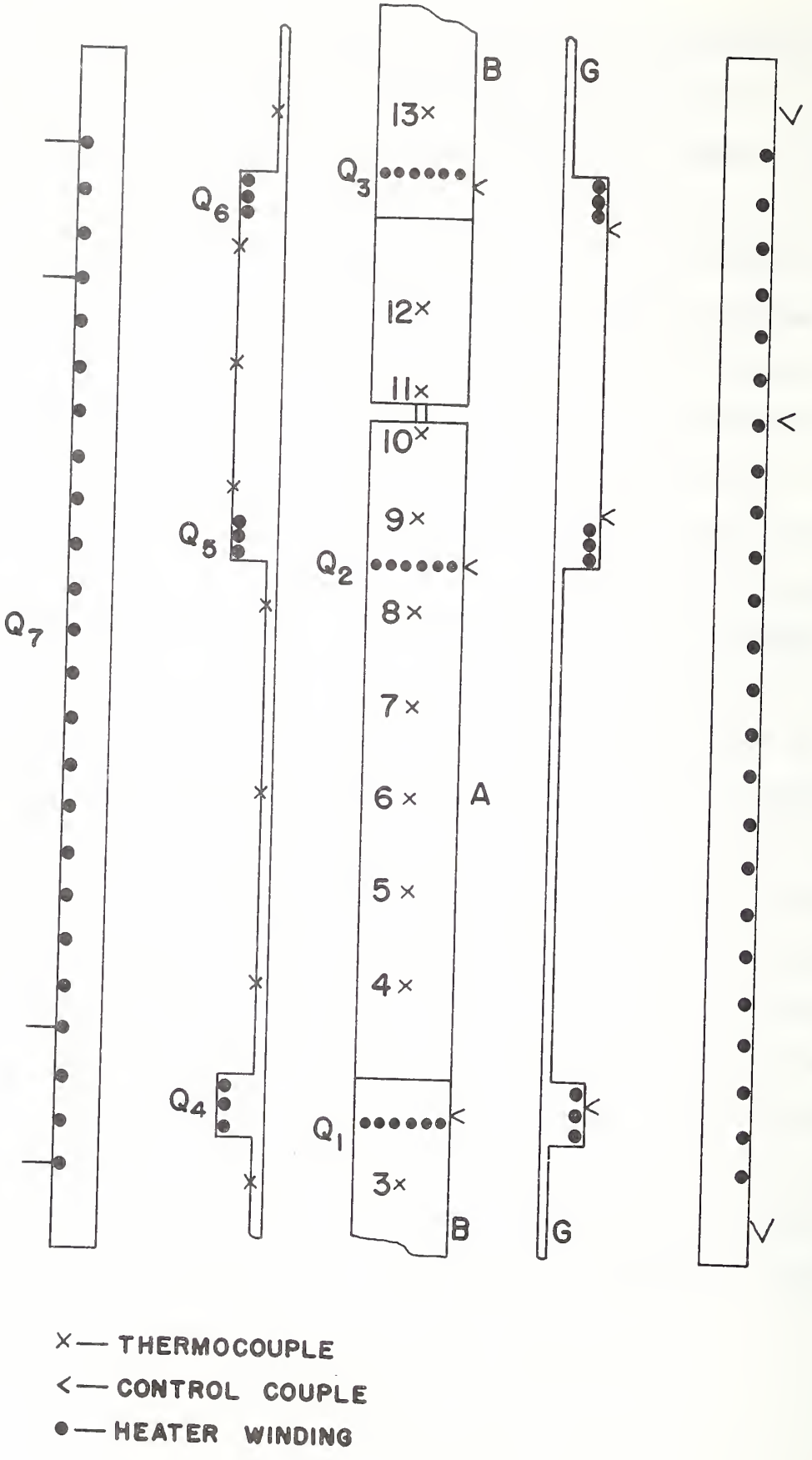

Figure. 12, Heater and Thermocouple Locations.

platinum wire are welded to the heaters at each end and are insulated by 24-mil bore alumina tubing. Eight-mil Pt 30% Rh potential taps are also welded to the heaters so that the heaters may be used as resistance thermometers to measure their own mean temperature. Twenty-mil Platinel [4/] control couples with butt-welded junctions are pressed into slits in the bars adjacent to the heaters.

The central heater, Q_2, is contained in six holes drilled through the platinum bar similar to the end heaters, Q_1, and Q_3, (See Figure 8). The inner four holes are 40 mils in diameter and accommodate helical elements contained in thin-wall ceramic tubes. The elements are made from 5-mil diameter Pt 10% Rh wire, the outside diameter of the helix being 18 mils and the pitch 10 mils. The outer two holes are 63 mils in diameter and accommodate "swaged elements" having Pt 10% Rh sheaths insulated from Pt 10% Rh heater wires by compacted MgO powder insulation. The swaged elements are a snug fit in the holes so that there is good thermal contact between the sheath and the bar, and consequently good thermal coupling

---

4/ Platinel is a new all noble metal thermocouple developed by Englehard Industries, Inc. It has high thermal emf, approximately that of Chromel-Alumel, and can be used up to 1300° C. The negative leg of the thermocouple is 65% Au, 35% Pd alloy (Platinel 5355) and the positive leg is 55% Pd, 31% Pt and 14% Au (Platinel 7674). For further information see references [54, 55, 56 and 57].

between the heater and the bar. The six elements are connected in series as in heaters Q_1 and Q_3. Platinum heater leads, 20 mils in diameter, are welded to the ends of the swaged elements. The good thermal contact in the swaged elements ensures that the temperature at the ends of the heater closely approximates that of the specimen. Moreover, the current leads extend radially from the heater in an isothermal plane. The combined result is to minimize heat losses out the leads. Two 8-mil Pt 10% Rh potential leads are welded to each of the current leads, one at the junction of the heater and the current lead, and the other about 1/2 inch back along the current lead. The two Pt 10% Rh potential leads together with the intervening section of platinum current lead serve as a differential thermocouple to determine the temperature gradient in the current lead. By taking potential readings with the current flowing in the forward and reverse directions the IR drop in the leads can be eliminated and the temperature gradients therein determined. This data is used in computing heat flows along the leads. The potential drop across the inner taps is used in computing the power generated in the heater. The distances from the heaters to the nearest thermocouples and potential taps are such that perturbations in heat flow and electric current flow generated by the presence of the heaters have decayed to an insignificant level at the position of the thermocouples or potential taps as discussed in Appendix B.

Located in the gradient zone of the specimen are five 8-mil Pt/Pt 10% Rh thermocouples spaced 0.787 inch (one specimen diameter) apart, with the first one 0.787 inch from the cold end of the specimen.

The thermocouple wires are annealed in air at 1450° C for 1/2 hour and then butt-welded [5/] together. They are pressed into 7-mil wide by 9-mil deep slits in the specimen thereby replacing the metal removed in machining the slits. By virtue of the fact that the specimen is fairly pure platinum with essentially the same absolute thermoelectric power as the Pt leg of the thermocouple the junction of the thermocouple is effectively at the point where the Pt 10% Rh leg first makes contact with the specimen, and the temperature measured is the temperature at that point. Since the Pt leg of the thermocouple leaves the specimen at another point there is only the Pt 10% Rh leg to conduct heat away from the junction. Temperature measurement is consequently more accurate. The Pt 10% Rh wire emerging from its groove extends a short way around the specimen in the same isothermal plane--insulated from the specimen in broken ceramic tubing--so as to minimize the amount of heat conducted away from the junction.

Similar thermocouples are located in the molybdenum extensions, three in each, to measure the temperature distribution along them. This information is essential to the mathematical analysis of the system.

Additional thermocouples are located on either side of the neck, one

---

5/ To butt-weld the thermocouples, the two wires are held in a jig with a small gap between their ends. The ends of the wires are heated with an oxygen-gas torch and expand toward each other. If the original spacing is correct and the heat is applied carefully the wires will just be at the right temperature for them to fuse when thermal expansion brings them together. Junctions made in this way were so even that it was hard to find them even under a microscope.

set 0.875 inch from the center of the neck, the other set 0.090 inch from the center of the neck. These are 15-mil Pt/Pt 10% Rh thermocouples contained in 14-mil wide by 16-mil deep slits. In addition to measuring temperature, the couples are cross-wired at the selector switches so that the Pt legs can be used to measure voltage drops across the neck when an electric current is flowing. With no current flowing the Pt 10% Rh legs, in conjunction with the platinum neck, can be used as a differential thermocouple to control the differential temperature across the neck in the direct mode of measurement.

Guard: The guard (Figure 13) has three heaters Q_4, Q_5, and Q_6 at positions corresponding to those on the specimen assembly. All three are swaged heaters with Pt 10% Rh sheaths and heating elements, and MgO insulation. They are pressed into grooves machined in the guard (Figure 14) giving good thermal contact. The end heaters (Q_4 and Q_6) have a 62-mil O.D. sheath and a 20-mil diameter heating wire and they are used to bring the guard to the desired temperature. The central heater (Q_5) has a 40-mil O.D. sheath with a 15-mil heating wire and it is used to produce a temperature gradient in the guard matching that in the specimen. Forty-mil platinum heater leads, insulated in ceramic tubing go to the end heaters while 30-mil leads go to the central heater. The guard is electrically grounded but the heaters are floating. Platinel control thermocouples are peened into the guard adjacent to each of the heaters.

Twelve thermocouples are located on the guard, three in the gradient zone, three in the isothermal zone and three in each of the end zones. All the thermocouples are 15-mil Pt/Pt 10% Rh with the junctions pressed into

Figure 13. The guard. The thermocouple wires emerge from slits and go around the guard in ceramic tubing.

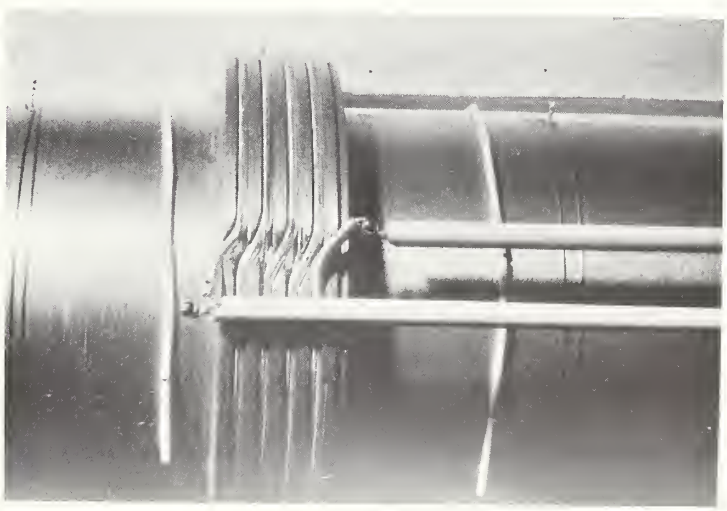

Figure 14. Guard heater. The swaged heater can be seen pressed into grooves machined in the guard. The heater leads are welded to the ends of the heater and are insulated in ceramic tubing.

slits machined in the guard. The thermocouple wires are taken one turn around the guard in broken ceramic tubing in an isothermal plane and cemented to the guard with high purity alumina cement. This helps to temper the thermocouple leads and reduce the amount of heat conducted away from the junction by the leads. Within the furnace all the thermocouples are insulated in single-bore ceramic tubes. For the remainder of their lengths the wires are insulated in flexible fiber-glass sleeving.

All the thermocouples, both from the guard and the specimen assembly, go to a junction box mounted on the inside of the feedthrough ring. There they are torch welded to identical wires which are taken through the vacuum feedthroughs to an ice bath.

All the Platinel control couples go to terminal strips on the upper plate of the furnace. There they are spot-welded to Chromel-Alumel wires coming from the controllers.

The alumina core (V) has a 40-mil molybdenum heater winding (Q_7) located in 1/16-inch wide by 3/32-inch deep by 3/8-inch pitch grooves terminated 1/2 inch from each end of the core. The winding is cemented over with alumina cement. The function of this heater is to bring the furnace as a whole to temperature and to reduce the heat losses from the molybdenum guard and the power load on its heaters. The heater has four current taps, one at each end of the winding and one 1-inch from each end, to enable the power density at the ends of the winding to vary from that over the central span, and thereby compensate for end heat losses. A Platinel control couple is mounted on the core.

Instrumentation

Temperature Control: In the direct method of measuring the thermal conductivity the Pt 10% Rh legs of the outer pair of thermocouples in the neck region are used in conjunction with the necked-down portion of the specimen as a differential thermocouple to control the power to heater Q_3, and maintain zero temperature differential across the neck. The signal from this thermocouple is amplified by a breaker-type d-c amplifier and fed into a current-adjusting-type proportional controller incorporating automatic reset control and rate control. The output of the proportional controller regulates the power to the heater by means of a transistorized power amplifier fed by a regulated d-c power supply. In the indirect mode an electric current flows through the specimen and the above system of control cannot be employed. In this case the Platinel control couple adjacent to heater Q_3 is put in series opposition with a signal from an adjustable constant voltage source and the resultant signal fed to the proportional controller which regulates the power to Q_3. The external signal is adjusted to give zero temperature differential across the neck.

The specimen heater (Q_2) is fed constant voltage from a regulated 10 A d-c power supply. Regulation is better than 0.01%.

Power to heater Q_1 and to the three guard heaters (Q_4, Q_5 and Q_6) is supplied by variable-voltage transformers, which in turn are fed by voltage-regulating isolation transformers. Power to each heater is pulsed high-low by individual thermocouple-actuated controllers.

Power to the heater winding (Q_7) on the alumina core is supplied by a variable-voltage transformer fed by a voltage-regulating isolation transformer. The current is manually ratioed among the three heater sections. The total power to this heater is pulsed high-low by a single thermocouple-actuated controller.

All heaters are supplied by separate isolating transformers or power supplies to minimize current leakage effects.

Temperature Measurement: The noble metal leads of the thermocouples are brought to an ice bath, where they are individually joined to copper leads. The copper leads go in shielded cables to a bank of double-pole selector switches of the type used in precision potentiometers. The selector switches are housed in a thermally insulated 3/8-inch thick aluminum box. The copper leads are thermally grounded to the switch box to minimize heat transfer directly to the switches. The emfs of the specimen thermocouples are read on a calibrated 6-dial high-precision potentiometer to 0.01μV, using a photocell galvanometer amplifier and a secondary galvanometer as a null detector. The emfs of all other themocouples are read on a second precision potentiometer to 0.1μV using an electronic null detector.

Power Measurement: Power input to the specimen heater (Q_2) is determined by measuring the d-c current through the heater and the voltage drop across the potential taps. These measurements are made by means of the 6-dial potentiometer.

Resistance Measurement: All electrical resistance measurements are made by measuring the current (from a 0-100 A regulated d-c power supply) flowing through the specimen, utilizing a calibrated 0.001 ohm shunt, and measuring

the appropriate voltage drop in the specimen. The selector switches mentioned above are cross-wired so that the voltage drops between corresponding legs of the specimen thermocouples may be read on either potentiometer.

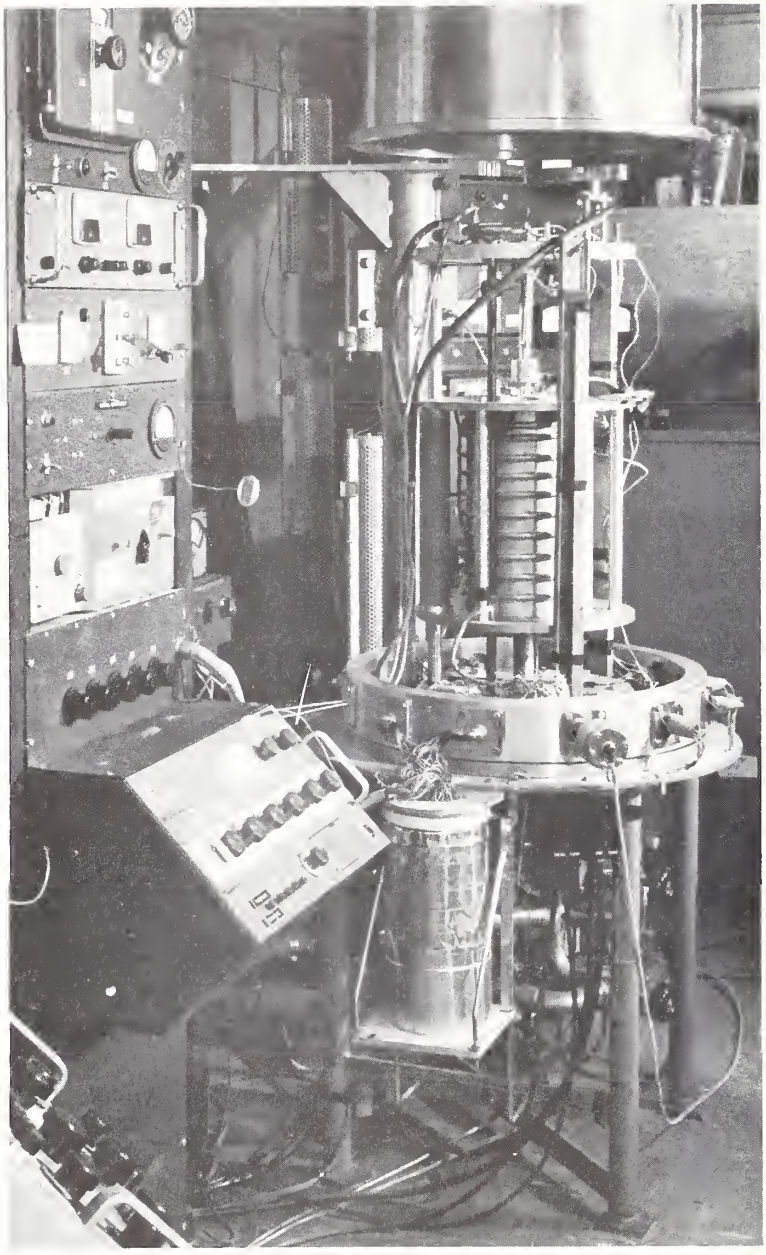

Figure 15 . General view of the apparatus. The apparatus proper stands on a round table with the vacuum system suspended below the table. The furnace is shown in the down position just prior to taking the clamp off the specimen. The bottom of the bell jar appears at the top of the picture. The ice bath can be seen in the lower center of the picture. The thermocouple feed-throughs are just above it. The 6-dial potentiometer and a small section of the instrumentation are housed in the relay rack to the left of the picture. The second potentiometer appears in the lower left-hand corner.

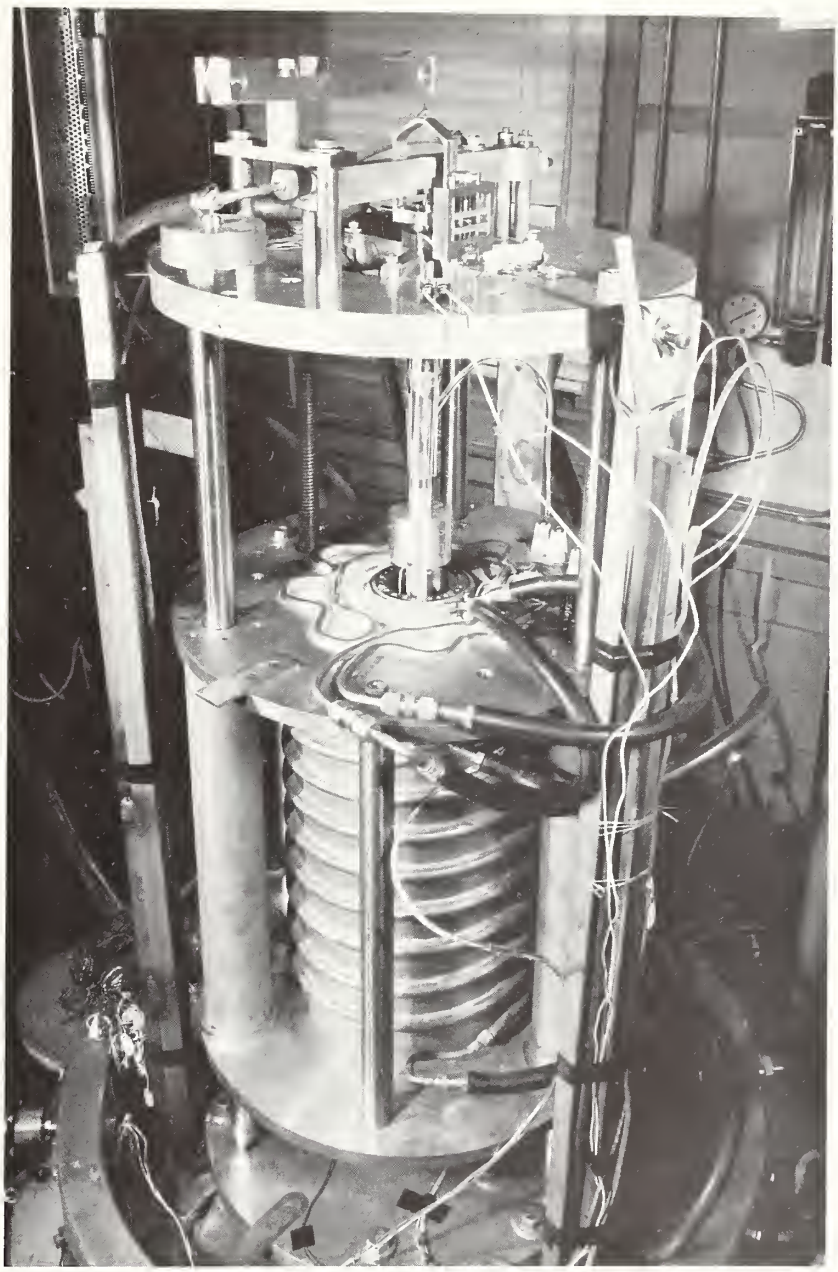

Figure 16. Close up view of the apparatus. The specimen is in place with the clamp still on. After the clamp is removed, the furnace is cranked up to the operating position. The furnace has already been filled with insulating powder. The counterweight hangs in position at the top of the picture. The pulley stand, the copper support, the hanger and the constraining device can all be seen.

CHAPTER III

THEORY OF THE INDIRECT METHOD

In the indirect method the specimen supports an electrical potential gradient, as well as a temperature gradient, and the corresponding thermoelectric effects must be analyzed. This is done most conveniently by the methods of irreversible thermodynamics, applying the Onsager Reciprocal Relations [58, 59, 60, 61, 62, 63, 64, 65, 66]. The application of the relations to steady-state processes involves an approximation; but as Callen [58] points out, it is an excellent approximation and is completely justifiable in this case.

We define a set of current densities $\vec{J}_i$:

$$\vec{J}_i = \sum_j L_{ij} \vec{X}_j \quad , \tag{3-1}$$

where $\vec{X}_j$ are the "conjugate forces," such that

$$R(S) = \sum_i \vec{J}_i \cdot \vec{X}_i \quad , \tag{3-2}$$

where R(S) is the rate of production of entropy in the system. Then the Onsager Reciprocal Theorem [67, 68] states that

$$L_{ij} = L_{ji} \tag{3-3}$$

in the absence of a magnetic field. The rate of entropy production R(S) is uniquely defined by the system under consideration, but since R(S) can be split into a sum of products in many ways, one is left with a choice of current densities and conjugate forces [59].

We define an electric current density $\vec{J}$, an energy current density $\vec{W}$, and an entropy current density $\vec{S}$, so that the divergence of each of these current densities is the rate of change per unit volume of the corresponding

thermodynamic variable. Since thermal expansion is negligible in our system we can write [58, equation 12]:

$$T\vec{S} = \vec{W} - \frac{\mu}{e}\vec{J} \quad , \tag{3-4}$$

where T is the absolute temperature, μ is the electrochemical potential, e is the electronic charge and $\vec{J}$, the electric current density, is equal to the electron current density times the electronic charge. We are considering the electron current to be the only mass current. Mass transport and the associated entropy flows due to electromigration (preferential migration of ions in a solid when a direct current is passed through the solid) and due to the Soret effect (mass transport in a solid due to a temperature gradient) are not considered. The reader is referred to [69, 70, 71] for discussions of these two effects.

We are concerned with steady-state conditions for which:

$$\nabla\cdot\vec{W} = 0 \quad , \tag{3-5}$$

$$\nabla\cdot\vec{J} = 0 \quad , \tag{3-6}$$

and

$$\nabla\cdot\vec{S} = R(S) \quad . \tag{3-7}$$

From (3-4) and (3-7) we can write

$$R(S) = \vec{J}\cdot\left[-\frac{\mu}{e}\nabla\left(\frac{1}{T}\right) - \frac{1}{T}\nabla\left(\frac{\mu}{e}\right)\right] + \vec{W}\cdot\nabla\left(\frac{1}{T}\right) \quad . \tag{3-8}$$

Using the identity

$$\nabla\left(\frac{1}{T}\right) = -\frac{1}{T^2}\nabla T \quad , \tag{3-9}$$

we can write the current densities in terms of the "conjugate forces:"

$$\vec{J} = L_{11}\left[\frac{\mu}{eT^2}\nabla T - \frac{1}{T}\nabla\left(\frac{\mu}{e}\right)\right] + L_{12}\left[-\frac{1}{T^2}\nabla T\right] \quad ; \tag{3-10}$$

$$\vec{W} = L_{12}\left[\frac{\mu}{eT^2}\nabla T - \frac{1}{T}\nabla\left(\frac{\mu}{e}\right)\right] + L_{22}\left[-\frac{1}{T^2}\nabla T\right] \quad . \tag{3-11}$$

The electrochemical potential μ is given by

$$\mu = \zeta + e\phi \quad , \tag{3-12}$$

where ϕ is the electrostatic potential, and ζ is the chemical potential, which in the case of a metal is simply the Fermi energy [72]. Since the Fermi energy is a function of temperature only, we can write

$$\nabla\left(\frac{\mu}{e}\right) = \frac{1}{e}\frac{\partial\zeta}{\partial T}\nabla T + \nabla\phi \quad . \tag{3-13}$$

We now proceed to evaluate the coefficients L_{11}, L_{12} and L_{22}.

The electrical conductivity is defined under isothermal conditions (i. e., $\nabla T = 0$) as

$$\sigma = \left[\frac{-\vec{J}}{\nabla\phi}\right]_{\nabla T=0} = \left[\frac{-\vec{J}}{\nabla\left(\frac{\mu}{e}\right)}\right]_{\nabla T=0} \quad , \tag{3-14}$$

since for $\nabla T = 0$, $\nabla\left(\frac{\mu}{e}\right) = \nabla\phi$. From (3-10) it follows that

$$L_{11} = \sigma T \quad . \tag{3-15}$$

The absolute thermoelectric power is defined (see [73]) as

$$S^{abs} = \left[\frac{-\nabla\left(\frac{\mu}{e}\right)}{\nabla T}\right]_{\vec{J}=0} \quad , \tag{3-16}$$

and from (3-10) it follows that

$$L_{12} = \sigma T\left[\frac{\mu}{e} + TS^{abs}\right] \quad . \tag{3-17}$$

The thermal conductivity is defined as

$$k = \left[\frac{-\vec{Q}}{\nabla T}\right]_{\vec{J}=0} = \left[\frac{-\vec{W}}{\nabla T}\right]_{\vec{J}=0} \quad , \tag{3-18}$$

where $\vec{Q}$ is the heat current density, since when $\vec{J} = 0$, $\vec{W} = \vec{Q}$.

From (3-10) and (3-11) we get

$$L_{22} = kT^2 + \sigma T\left[\frac{\mu}{e} + TS^{abs}\right]^2 \quad . \tag{3-19}$$

Substituting for L_{11}, L_{12} and L_{22} in (3-10) and (3-11), we can write $\vec{J}$ and $\vec{W}$ in terms of the defined thermoelectric parameters:

$$\vec{J} = -\sigma\left[\nabla\left(\frac{\mu}{e}\right) + S^{abs}\nabla T\right] \; ; \tag{3-20}$$

$$\vec{W} = -\sigma\left(\frac{\mu}{e} + TS^{abs}\right)\nabla\left(\frac{\mu}{e}\right) - \left[\sigma S^{abs}\left(\frac{\mu}{e} + TS^{abs}\right) + k\right]\nabla T$$

$$= \left[\frac{\mu}{e} + TS^{abs}\right]\vec{J} - k\nabla T \quad . \tag{3-21}$$

Taking the divergence of $\vec{W}$ and using (3-5) and (3-6)

$$\nabla\cdot\vec{W} = \vec{J}\cdot\nabla\left(\frac{\mu}{e} + TS^{abs}\right) - \nabla\cdot k\nabla T = 0 \quad . \tag{3-22}$$

Therefore

$$\vec{J}\cdot\left[\nabla\left(\frac{\mu}{e}\right) + T\nabla S^{abs} + S^{abs}\nabla T\right] - \nabla\cdot(k\nabla T) = 0 \quad . \tag{3-23}$$

In a homogeneous and isotropic medium, the parameter S^{abs} is a function of temperature only, and we can write

$$\vec{J}\cdot\left[\nabla\left(\frac{\mu}{e}\right) + \left(T\frac{\partial S^{abs}}{\partial T}\right)\nabla T + S^{abs}\nabla T\right] - \nabla\cdot(k\nabla T) = 0 \quad . \tag{3-24}$$

The coeffieient $T\frac{\partial S^{abs}}{\partial T}$ is defined [58] as the Thomson coefficient τ. From (3-20) and (3-24)

$$\vec{J}\cdot\left[\frac{-\vec{J}}{\sigma} + \tau\nabla T\right] - \nabla\cdot(k\nabla T) = 0 \quad . \tag{3-25}$$

At this point, it is convenient to introduce a pseudo-potential ψ such that

$$\vec{J} = -\sigma\nabla\psi \quad , \tag{3-26}$$

and $$\nabla\psi = \nabla\left(\frac{\mu}{e}\right) + S^{abs}\nabla T \quad . \tag{3-27}$$

Writing (3-25) in terms of ψ we get

$$\nabla\cdot(k\nabla T) + \sigma\nabla\psi\cdot\nabla\psi + \sigma\tau\nabla\psi\cdot\nabla T = 0 \quad . \tag{3-28}$$

Equation (3-28) can be considered as the generalized equation relating the temperature distribution and the electric potential distribution in an isotropic homogeneous medium carrying an electric current. We now proceed to solve that equation.

The second term in (3-28) can be written as $\nabla\cdot(\psi\sigma\nabla\psi)$ since

$$\nabla\cdot(\psi\sigma\nabla\psi) = \psi\nabla\cdot(\sigma\nabla\psi) + \sigma\nabla\psi\cdot\nabla\psi$$

$$= \sigma\nabla\psi\cdot\nabla\psi \text{ since } \nabla\cdot(\sigma\nabla\psi) = -\nabla\cdot\vec{J} = 0 \quad . \tag{3-29}$$

The third term in (3-28) can also be written in the form of a divergence, since

$$\nabla\cdot\left[\sigma\left(\int_{T^*}^{T}\tau dT\right)\nabla\psi\right] = \sigma\nabla\psi\cdot\nabla\int_{T^*}^{T}\tau dT + \left(\int_{T^*}^{T}\tau dT\right)\nabla\cdot(\sigma\nabla\psi)$$

$$= \sigma\nabla\psi\cdot\nabla\int_{T^*}^{T}\tau dT = \sigma\tau\nabla\psi\cdot\nabla T \quad , \tag{3-30}$$

where T^* is any arbitrary fixed temperature.

Using these identities (3-28) can be written as

$$\nabla\cdot\left[k\nabla T + \sigma\psi\nabla\psi + \sigma\left(\int_{T^*}^{T}\tau dT\right)\nabla\psi\right] = 0 \quad . \tag{3-31}$$

Integrating,

$$k\nabla T + \sigma\psi\nabla\psi + \sigma\left(\int_{T^*}^{T}\tau dT\right)\nabla\psi = \nabla\lambda + \vec{c} \quad , \tag{3-32}$$

where λ is any potential satisfying the Laplacian $\nabla^2\lambda = 0$ and $\vec{c}$ is a vector

constant. Since $\nabla\cdot(\sigma\nabla\psi) = 0$, we can write

$$\nabla\lambda = \psi_o\sigma\nabla\psi \quad , \tag{3-33}$$

where ψ_o is a constant which must satisfy the boundary conditions. Substituting for $\nabla\lambda$ in (3-32), we get

$$k\nabla T + \sigma(\psi - \psi_o)\nabla\psi + (\sigma\nabla\psi)\int_{T^*}^{T}\tau dT = \vec{c} \quad . \tag{3-34}$$

If $\vec{c} = 0$, it can be seen from (3-34) that ∇T and $\nabla\psi$ must be parallel at all points. This implies that if there is no electric current flow across a boundary, there can be no heat flow across that same boundary. Moreover, equipotential surfaces are also isothermal. More explicitly, the condition that $\vec{c} = 0$ requires that all the heat generated in an electrically insulated conductor must flow out the ends of the conductor, there being no heat losses from the sides. This condition can never actually be met in practice since there is no perfect or even near-perfect thermal insulator. However, by appropriate choice of geometry, as employed in the present experiments, heat losses can be made very small so that we can take $\vec{c} = 0$ as a valid statement of the boundary condition. Equation (3-34) then reduces to

$$k\rho\nabla T + (\psi - \psi_o)\nabla\psi + (\nabla\psi)\int_{T^*}^{T}\tau dT = 0 \quad , \tag{3-35}$$

where ρ is the electrical resistivity, $\rho = 1/\sigma$.

If there is a point in the medium where the temperature has a maximum value T_m, the gradient ∇T is zero at that point. Further, if we let

$$T^* = T_m \quad , \tag{3-36}$$

the first and third terms in (3-35) are zero at $T = T_m$. Since there is a

current flowing $\sigma\nabla\psi \neq 0$ and (3-35) is satisfied only if $\psi - \psi_o = 0$ at $T = T_m$. In other words

$$\psi = \psi_o \quad \text{at} \quad T = T_m \quad , \tag{3-37}$$

so that ψ_o is the value of ψ at the point of maximum temperature.

Integrating (3-35) along a line from one isothermal surface $S_1(T_1,\psi_1)$ to another isothermal surface $S_2(T_2,\psi_2)$ and substituting T_m for T^*,

$$\int_{S_1}^{S_2} k\rho\nabla T\cdot\vec{dr} + \int_{S_1}^{S_2}(\psi - \psi_o)\nabla\psi\cdot\vec{dr} + \int_{S_1}^{S_2}\nabla\psi\cdot\vec{dr}\int_{T_m}^{T}\tau dT = 0 \quad , \tag{3-38}$$

or, since $\nabla F\cdot\vec{dr} = dF$

$$\int_{T_1}^{T_2} k\rho\, dT + \int_{\psi_1}^{\psi_2}(\psi - \psi_o)d\psi + \int_{\psi_1}^{\psi_2} d\psi\int_{T_m}^{T}\tau dT = 0 \quad . \tag{3-39}$$

An arbitrary isotropic and homogeneous conductor is represented in Figure 17.

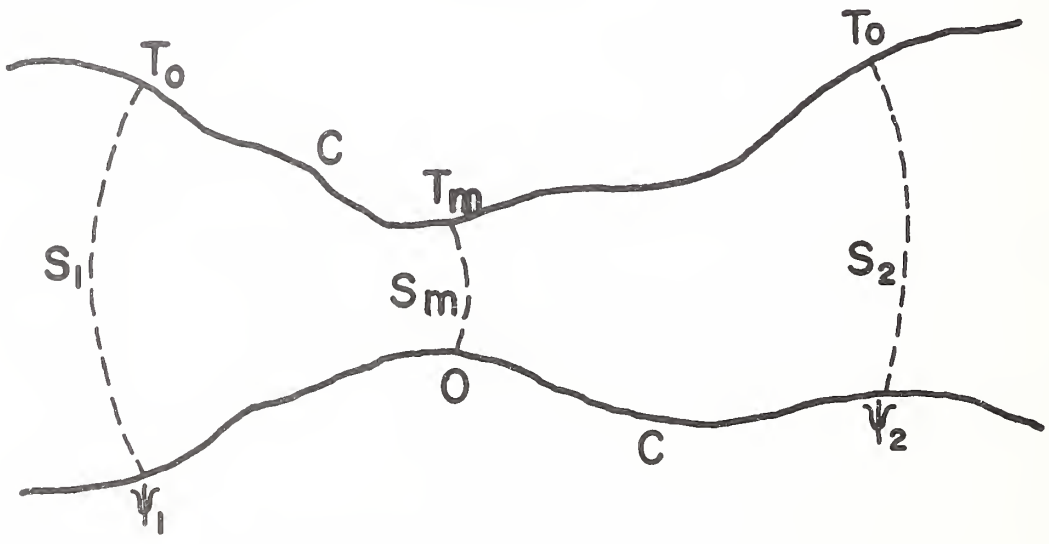

Figure 17. An electrical conductor with arbitrary geometry

There is no electric current flow across the boundary C and the geometry is selected to make heat losses from C negligible so that the condition for $\vec{c} = 0$ discussed above is satisfied. The isothermal surfaces S_1 and S_2 are taken to be at the same temperature, T_o, and the surface of maximum temperature is represented by S_m. In the absence of the Thomson effect, the surface of maximum temperature would bisect the reduced resistance between S_1 and S_2, the reduced resistance--a geometrical quantity--being the resistance of the medium for electrical conductivity of unity. However, the Thomson effect moves the surface of maximum temperature away from the symmetrical location, this effect being referred to as "the Thomson shift" [74]. It is analyzed in detail by Davidson [74] and discussed by Holm [18] and Llewellyn Jones [75]. It is convenient to define $\psi_o = 0$ and consider the integral (3-39) from S_m where $T = T_m$ and $\psi = 0$ to any other surface S where $\psi = \psi$, $T = T$. Rearranging we have

$$\int_o^{\psi} \psi \, d\psi = \int_T^{T_m} k\rho \, dT + \int_o^{\psi} d\psi \int_T^{T_m} \tau \, dT \qquad (3\text{-}40)$$

It is convenient to write (3-40) in the following form

$$\psi^2 - 2\epsilon\psi - F^2 = 0 \quad , \qquad (3\text{-}41)$$

where

$$F(T,T_m) = + \left\{ 2 \int_T^{T_m} k\rho \, dT \right\}^{1/2} \qquad (3\text{-}42)$$

and

$$\epsilon(T,T_m) = \frac{1}{\psi} \int_o^{\psi} d\psi \int_T^{T_m} \tau \, dT \quad . \qquad (3\text{-}43)$$

Solving the quadratic equation (3-41), we get

$$\psi = \epsilon \pm (\epsilon^2 + F^2)^{1/2} = \epsilon \pm F(1 + (\epsilon/F)^2)^{1/2} \quad . \qquad (3\text{-}44)$$

The Thomson effect is relatively small as shown in Appendix C, so that the second-order term $(\epsilon/F)^2$ in (3-51) can be neglected. Then

$$\psi = \epsilon \pm F \quad , \tag{3-45}$$

the plus and minus signs referring to the high and low potential sides of S_m respectively.

Referring to (3-43) we see that although T is a function of ψ, $\int_T^{T_m} \tau dT$ is independent of the sign of ψ since T_m is always greater than T. Consequently ϵ is an even function of ψ, having the same value at corresponding points on the high and low potential sides of S_m. At S_1 we have

$$\psi_1 = \epsilon(T_o, T_m) - F(T_o, T_m) \tag{3-46}$$

and at S_2

$$\psi_2 = \epsilon(T_o, T_m) + F(T_o, T_m) \quad . \tag{3-47}$$

Therefore

$$\psi_2 - \psi_1 = 2F(T_o, T_m) \quad . \tag{3-48}$$

From (3-27) and (3-13) we have

$$\nabla\psi = \nabla\phi + \frac{1}{e}\frac{\partial\zeta}{\partial T}\nabla T + S^{abs}\nabla T \quad . \tag{3-49}$$

Integrating from S_1 to S_2,

$$\psi_2 - \psi_1 = \phi_2 - \phi_1 + \frac{1}{e}\{\zeta_2 - \zeta_1\} + \int_{T_1}^{T_2} S^{abs} dT \quad . \tag{3-50}$$

In an isotropic and homogeneous medium ζ and S^{abs} are functions of temperature only. When the terminal temperatures are the same, as in the case we are considering; i. e., when $T_1 = T_2 = T_o$, we can write from (3-48) and (3-50)

$$\psi_2 - \psi_1 = \phi_2 - \phi_1 = V = 2F(T_o, T_m) \quad , \tag{3-51}$$

where V is the voltage drop between the surfaces S_1 and S_2. If the potential probes are not at the same temperature, a correction must be made as

indicated in (3-50). Writing F explicitly we finally get from (3-51) and (3-42)

$$\frac{V^2}{8} = \int_{T_o}^{T_m} k\rho\, dT = \int_{o}^{\theta_m} k\rho\, d\theta \quad , \qquad (3\text{-}52)$$

where $\theta = T - T_o$, $\theta_m = T_m - T_o$.

Equation (3-52) shows that the maximum temperature rise θ_m in an electrically-heated conductor with negligible lateral heat losses and with both its ends held at the same temperature is, to first order, a function only of the voltage drop V across it, and of the thermal and electrical conductivities of the material, and is independent of the geometry of the conductor provided the geometry is such as to make lateral heat losses negligible. If the maximum temperature rise can be measured as a function of the applied potential, $k\rho$ is readily determined.

Hopkins and Griffith [15,16] maintained the ends of their specimen at room temperature and measured the maximum temperature T_m directly by sighting on the specimen with an optical pyrometer.

The maximum temperature rise can also be measured indirectly using the specimen as its own resistance thermometer. This method was employed by Holm and Störmer [14] and Cutler et al. [17] and requires that the temperature coefficient of resistance of the material be known over the temperature range of interest and that it be large enough to yield sufficient sensitivity. Platinum satisfies both requirements very well and the resistance method of measuring the maximum temperature rise was adopted in the present experiments. We now proceed to relate the maximum temperature rise in a conductor to the measured resistance of the conductor. This problem is discussed at length by Holm [18, paragraph 18].

Consider two geometrically identical conductors, each carrying the same current, and differing only in that one conductor has temperature-dependent properties $\rho = \rho(\theta)$ and $k = k(\theta)$, while the other conductor has temperature independent or constant properties $\rho = \rho_o$ and $k = k_o$ where $\theta = T - T_o$ is the temperature measured from any arbitrary reference temperature T_o. Let ψ and θ be the potential and the temperature respectively in the conductor having temperature-dependent properties, and let ψ_o and θ_o refer to the corresponding variables in the conductor having constant properties. Then if $d\psi$ and $d\psi_o$ are the potential differences between corresponding equipotential surfaces in the two conductors, we can write from (3-26)

$$\frac{d\psi_o}{d\psi} = \frac{\rho_o}{\rho} \quad . \tag{3-53}$$

Neglecting terms arising from the Thomson effect, we have from (3-41):

$$\psi = \pm F \quad , \tag{3-54}$$

and from (3-35):

$$k\rho \frac{d\theta}{d\psi} = -\psi \quad . \tag{3-55}$$

Combining the last three equations,

$$d\psi_o = \pm \frac{k\rho_o d\theta}{F} \quad . \tag{3-56}$$

Integrating,

$$\psi_o = \int_{\theta}^{\theta_m} \frac{k\rho_o d\theta}{F} \quad . \tag{3-57}$$

Since both conductors are assumed to carry the same current,

$$\frac{R_o}{R} = \frac{\psi_o}{\psi} \quad , \tag{3-58}$$

and we have

$$\frac{R_o}{R} = \frac{1}{F}\int_{\theta}^{\theta_m} \frac{k\rho_o d\theta}{F} \quad . \tag{3-59}$$

Assuming that k and ρ are both linear functions of temperature--a valid assumption over small temperature intervals--we can write:

$$\rho = \rho_o(1 + \alpha_o\theta) \quad , \tag{3-60}$$

$$k = k_o(1 + \beta_o\theta) \tag{3-61}$$

and

$$k\rho = k_o\rho_o(1 + \eta_o\theta) \quad , \tag{3-62}$$

where α_o is the temperature coefficient of resistance evaluated at $T = T_o$, β_o is the temperature coefficient of thermal conductivity evaluated at $T = T_o$ and $\eta_o = \alpha_o + \beta_o$. The term in $\alpha_o\beta_o\theta^2$ can be neglected. Substituting the above value for $k\rho$ in (3-42) and integrating we get

$$F(\theta,\theta_m) = +\left[2k_o\rho_o\left\{\theta_m\left(1 + \frac{\eta_o}{2}\theta_m\right) - \theta\left(1 + \frac{\eta_o}{2}\theta\right)\right\}\right]^{1/2} \quad . \tag{3-63}$$

If the integration is carried out from S_1 to S_2 where $T = T_o$, or $\theta = 0$, we have, from (3-63) and (3-51),

$$F = \left[2k_o\rho_o\theta_m\left(1 + \frac{\eta_o}{2}\theta_m\right)\right]^{1/2} \tag{3-64}$$

and

$$V^2 = 8k_o\rho_o\theta_m\left(1 + \frac{\eta_o}{2}\theta_m\right) \quad . \tag{3-65}$$

Substituting F from (3-64) into (3-59) and performing the indicated integration we have for $\theta = 0$,

$$\frac{R_o}{R} = \frac{\beta_o}{\eta_o} + \frac{\alpha_o}{\eta_o}\frac{1}{G}\arctan G \quad , \tag{3-66}$$

where

$$G^2 = 2\eta_o\theta_m\left(1 + \frac{\eta_o}{2}\theta_m\right) \quad . \tag{3-67}$$

Equation (3-66) gives θ_m implicitly in terms of known and measured parameters, and its value can be determined by iteration. This value can then be plugged into (3-65) to solve for k_o.

CHAPTER IV

CALCULATION PROCEDURES

Indirect Method:

We have shown in Chapter III that, in the indirect method, if the resistance of the neck and the voltage drop across it are measured with a current passing through the specimen, the thermal conductivity can be determined from these measured parameters using equations (3-65), (3-66) and (3-67). Greater precision can be achieved, however, if measurements are made at a number of different current levels. In the present investigation measurements were made at four or five current levels, and the way in which the data have been analyzed is presented in this section.

For each current level we can write

$$V^2 = 8\, k_o\, \rho_o\, \theta_m \left(1 + \frac{\eta_o}{2}\, \theta_m \right) \qquad (3\text{-}65)$$

It was impractical in our experimental set-up to hold T_o at exactly the same value for different current settings. If we let T_r be an arbitrary constant reference temperature then we can write:

$$\rho_o = \rho_r \left[1 + \alpha_r \left(T_o - T_r \right) \right], \qquad (4\text{-}1)$$

$$k_o = k_r \left[1 + \beta_r \left(T_o - T_r \right) \right], \qquad (4\text{-}2)$$

and

$$k_o \rho_o = k_r \rho_r \left[1 + \eta_r \left(T_o - T_r \right) \right] \qquad (4\text{-}3)$$

where k_r and ρ_r are evaluated at $T = T_r$, and $\eta_r = \alpha_r + \beta_r$. The higher order term in $\alpha_r \beta_r$ is neglected. Substituting this expression for $k_o \rho_o$ in (3-65) we get

$$V^2 = 8\, k_r\, \rho_r\, \theta_m \left(1 + \frac{\eta_o}{2}\, \theta_m \right) \left\{ 1 + \eta_r \left(T_o - T_r \right) \right\}. \qquad (4\text{-}4)$$

We do not measure θ_m directly but, rather, use the neck as a resistance thermometer, the relation between the electrical resistance of the neck, R, and the temperature rise, θ_m, being given by (3-66) and (3-67). In the limit of small $\alpha_o \theta_m$, (3-66) reduces to

$$\frac{R - R_o}{\alpha_o R_o} = \frac{2}{3} \theta_m \tag{4-5}$$

where R_o is the resistance the neck would have if it were uniformly at temperature T_o. We define an adjusted resistance, R', for the general case where $\alpha_o \theta_m$ is not sufficiently small for (4-5) to be valid and where T_o may differ from T_r:

$$R' = R_r \left(1 + \frac{2}{3} \alpha_r \theta_m\right) . \tag{4-6}$$

In the limiting case where $T_o = T_r$ and $\alpha_o \theta_m << 1$, (4-6) reduces to (4-5) and $R' = R$.

We also define an adjusted voltage, V', given by

$$V'^2 = \frac{V^2}{\left[1 + \frac{\eta_o}{2} \theta_m\right] \left[1 + \eta_r (T_o - T_r)\right]} . \tag{4-7}$$

Substituting (4-6) and (4-7) into (4-4), we obtain

$$V'^2 = 12 k_r \rho_r \frac{R' - R_r}{\alpha_r R_r} \tag{4-8}$$

Differentiating (4-8) and rearranging, we obtain

$$k_r = \frac{\alpha_r R_r}{12 \rho_r} \frac{d V'^2}{d R'} . \tag{4-9}$$

The thermal conductivity is thus determined from the slope of the V'^2 vs. R' curve. From (4-6) and (4-7) we see that

$$\frac{d V'^2}{d R'} = \lim_{\substack{\alpha_o \theta_m \to 0 \\ T_o \to T_r}} \frac{d V^2}{d R} . \tag{4-10}$$

In the analysis given in Chapter III and also that given just above, we explicitly assumed that there was no loss or gain of either electric current or heat across the surface C of the conductor. In the present investigation a necked-down sample is employed, the neck and the specimen as a whole being surrounded by an insulating powder. Since this insulating powder has an electrical conductivity many orders of magnitude lower than that of the specimen material, the assumption of no flow of electric current across the boundaries is completely valid. The powder surrounding the neck prevents heat loss by convection, and radiation through the powder is negligible. However, the powder conducts heat away from the neck and it is necessary to analyze this heat loss and develop an appropriate correction for it.

Since most of the temperature rise in the necked-down region is in the neck itself, we will consider only heat losses from the neck and will neglect other heat exchanges. We idealize the neck and its environment as shown in the sketch below and as described in the following discussion.

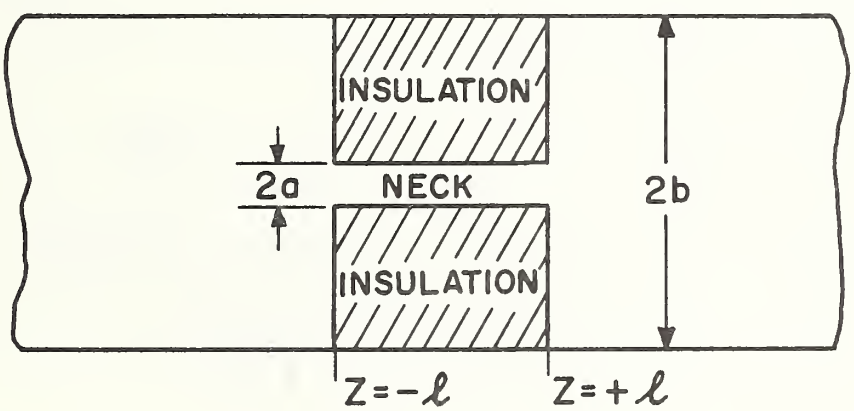

Figure 18. The neck surrounded by powder insulation.

The region $-\ell < z < \ell$, $a < r < b$ contains thermal insulation of thermal conductivity k_0. The surfaces $r = b$ and $z = \pm\ell$ are maintained at zero temperature. The neck region, $r < a$, has thermal conductivity k_o, and is heated by electric current, I. We assume the neck to be isothermal across any given cross section, and that there is continuity of temperature and heat flux at the interface between the neck and the insulation.

The solution to this problem is given by Carslaw and Jaeger [25, p. 221, eq. (25)], and, in our nomenclature, is

$$u^* = \sum_{n=1,3,5,}^{\infty} C_n F_o[R_n;B_n] \cos Z_n \quad , \tag{4-11}$$

where the notation n = 1,3,5, indicates that the summation is to be taken only over odd values of n, and where

$$C_n \equiv \frac{4(-1)^{\frac{n-1}{2}} \rho_o I^2}{n\pi\left\{[\pi^2 a^2 A_n^2 k_o - \alpha_o \rho_o I^2]\, F_o\,[A_n;B_n] - 2\pi^2 a^2 A_n k_o F_1[A_n;B_n]\right\}} \quad , \tag{4-12}$$

$$F_o[x;y] \equiv I_o(x)K_o(y) - K_o(x)I_o(y) \quad , \tag{4-13}$$

$$F_1[x;y] \equiv I_1(x)K_o(y) + K_1(x)I_o(y) \quad , \tag{4-14}$$

$$A_n \equiv \frac{n\pi a}{2\ell} \quad , \quad B_n \equiv \frac{n\pi b}{2\ell} \quad , \quad R_n \equiv \frac{n\pi r}{2\ell} \quad , \quad Z_n \equiv \frac{n\pi z}{2\ell} \quad ,$$

$\rho = \rho_o(1 + \alpha_o u^*)$ is the electrical resistivity of the neck material,

I_m = modified Bessel function of first kind and order m,

K_m = modified Bessel function of second kind and order m,

u^* = excess temperature above that at the boundaries r = b and $z = \pm\ell$.

The temperature in the neck itself is given by

$$u^* = \sum_{n=1,3,5,}^{\infty} C_n F_o[A_n;B_n]\cos Z_n \quad . \tag{4-15}$$

Since the Thomson effect is small, we can assume a symmetrical temperature distribution with the maximum temperature, u_m^*, occurring at the center of the neck, z = 0. Evaluation of (4-15) at z = 0 yields, after some rearrangement,

$$u_m^* = \frac{16\ell^2\rho_o I^2}{\pi^5 a^4 k_o} \sum_{n=1,3,5,}^{\infty} \frac{(-1)^{\frac{n-1}{2}}}{n^3\left[1 - \frac{4\ell^2\alpha_o\rho_o I^2}{n^2\pi^4 a^4 k_o} - \frac{4\ell}{n\pi a}\frac{\hbar_o}{k_o}\frac{F_1[A_n;B_n]}{F_o[A_n;B_n]}\right]} \tag{4-16}$$

as the maximum temperature in the presence of heat losses.

For the parameter values appropriate to our experiment, the term in $\alpha_o I^2$ and the term in $\hbar_o/k_o$ in the denominator of the right-hand side of (4-16) are small compared to unity and, as shown in Appendix E, (4-16) reduces to the form

$$u_m^* = u_m\left[1 - \frac{\hbar_o}{k_o} \cdot \frac{128\ell}{\pi^4 a}\frac{K_1(\pi a/2\ell)}{K_o(\pi a/2\ell)}\right] \quad , \tag{4-17}$$

where u_m is the maximum temperature rise the neck would have if there were no heat losses, i.e., if $\hbar_o = 0$.

The temperature distribution along the center-line of the specimen (not to scale) is shown schematically in Figure 19.

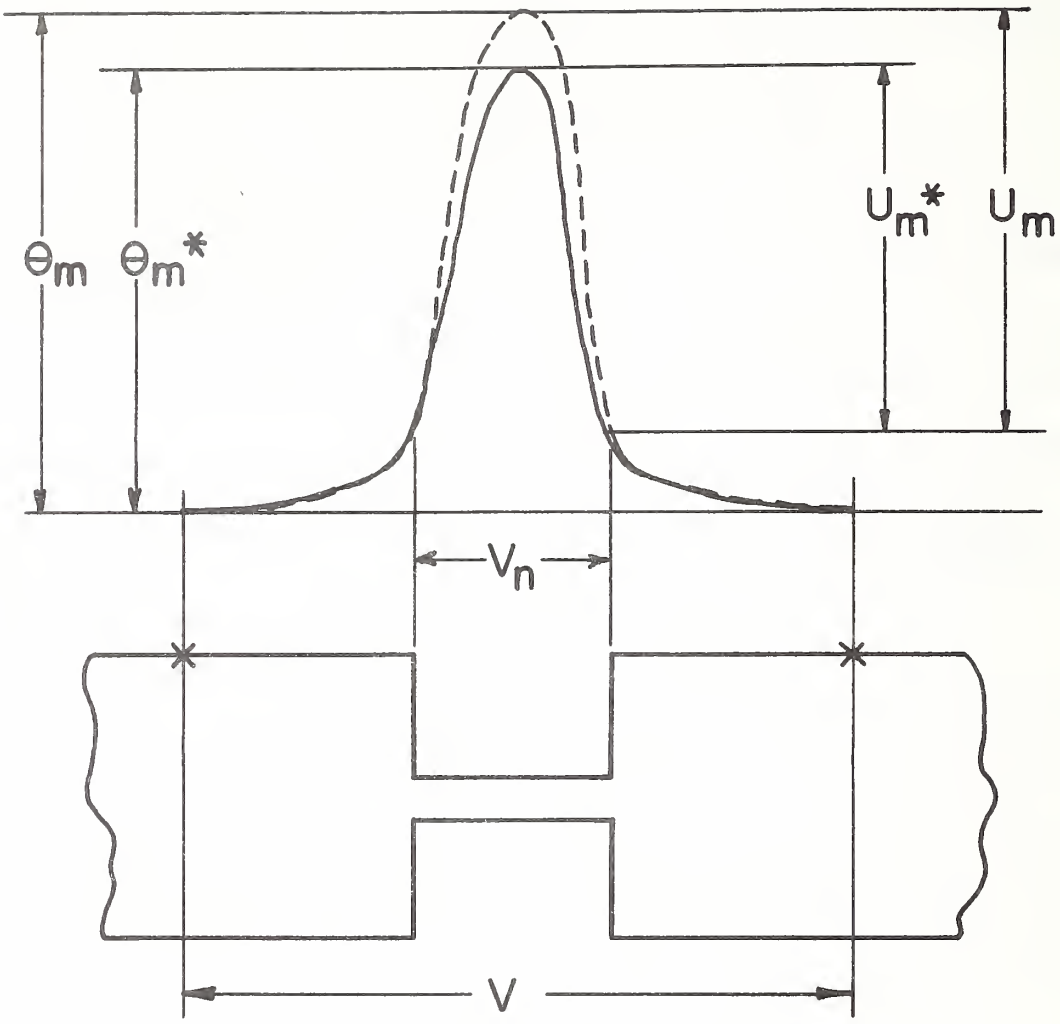

Figure 19. Temperature distributions in the necked-down region.

The quantities θ_m^* and θ_m refer to the maximum temperature rises between potential taps in the presence and absence, respectively, of heat losses from the neck. The quantities u_m^* and u_m refer to the temperature rises only in the neck itself. The solid curve indicates the actual temperature distribution; the dotted curve indicates the temperature distribution that would exist in the absence of heat losses.

For the purpose of evaluating heat losses from the neck we can neglect the temperature-dependence of $k\rho$ and write an expression, analogous to (3-65), for the temperature rise in the neck in the absence of heat losses

$$u_m = \frac{V_n^2}{8k_o\rho_o} \quad , \tag{4-18}$$

where V_n is the voltage drop in the neck itself. For $\alpha\theta_m << 1$, V_n is given by:

$$V_n = \frac{2\ell}{\pi a^2} \frac{\rho_o}{R_o} V \quad , \tag{4-19}$$

where V is the total voltage drop between the potential taps. Thus from (4-18) and (4-19)

$$u_m = \frac{\ell^2}{2\pi^2 a^4} \frac{\rho_o}{k_o} \frac{V^2}{R_o^2} \quad . \tag{4-20}$$

From (4-17) we can write

$$\theta_m - \theta_m^* = u_m - u_m^* = \frac{\hbar_o}{k_o} \frac{128\ell}{\pi^4 a} \frac{K_1(\pi a/2\ell)}{K_o(\pi a/2\ell)} u_m \quad , \tag{4-21}$$

which, after substitution from (4-20) and (3-65), becomes

$$\theta_m = \theta_m^*[1 + C] \quad , \tag{4-22}$$

where C is a constant given by

$$C = \frac{\hbar_o}{k_o} \Omega \tag{4-23}$$

and the geometrical factor, Ω, is given by

$$\Omega = \frac{64}{\pi^3 a^2} \left(\frac{2\ell}{\pi a}\right)^3 \frac{K_1(\pi a/2\ell)}{K_o(\pi a/2\ell)} \frac{\rho_o^2}{R_o^2} \quad , \tag{4-24}$$

with the term in $\eta_o\theta_m$ from (3-65) neglected.

We define an adjusted resistance, R* (analogous to R'), as

$$R^* = R_r\left(1 + \frac{2}{3}\alpha_r\theta_m^*\right) \tag{4-25}$$

In the absence of heat losses $\theta_m^* = \theta_m$ and $R^* = R'$. From (4-6), (4-22) and (4-25) we get, in the case of small $\alpha_r\theta_m$

$$R' = R^*\left(1 + \frac{2}{3}\alpha_r C\theta_m^*\right) \tag{4-26}$$

For small $\alpha_r\theta_m$ voltage drops are proportional to resistances and we can write

$$V' = V^*\left(1 + \frac{2}{3}\alpha_r C\theta_m^*\right) \tag{4-27}$$

where V' is the value V* would have in the absence of heat losses. The thermal conductivity in the absence of heat losses is given by (4-9) and is proportional to dV'^2/dR'. When heat losses are present the measured resistances and voltage drops are too low and must be corrected to correspond to the values they would have in the absence of heat losses. We can write for small $\alpha_r\theta_m$

$$\frac{dV'^2}{dR'} = \frac{dV'^2}{dR^*}\frac{dR^*}{dR'} = \frac{dR^*}{dR'}\frac{d}{dR^*}\left[V^{*2}\left(1 + \frac{4}{3}\alpha_r C\theta_m^*\right)\right] \tag{4-28}$$

Using the definitions of R' and R* and carrying through the algebra (4-28) reduces to

$$\frac{dV'^2}{dR'} = \frac{1 + \frac{8}{3}\alpha_r C\theta_m}{1 + C\left(1 + \frac{4}{3}\alpha_r\theta_m\right)}\frac{dV^{*2}}{dR^*} \quad . \tag{4-29}$$

If $C << 1$ and also $\alpha_r\theta_m << 1$, the terms involving products of these quantities can be neglected and (4-29) becomes simply

$$\frac{dV'^2}{dR'} = \frac{1}{1 + C} \frac{dV^{*2}}{dR^*} \qquad (4\text{-}30)$$

Thus in the presence of small heat losses from the neck, the apparent value of k_r obtained by assuming $dV'^2/dR' = dV^{*2}/dR^*$ must be multiplied by the factor $1/(1 + C)$ to get the true value

$$k_r = \frac{1}{1 + C} \frac{\alpha_r R_r}{12\rho_r} \frac{dV^{*2}}{dR^*} \quad , \qquad (4\text{-}31)$$

where C is given by (4-23); if C goes to zero (4-31) reduces to (4-9).

The calculation procedure used is as follows: let us assume that, at any given nominal temperature, measurements are made at n current levels. Let $(T_o)_1$, $(T_o)_2$, . . . $(T_o)_n$ be the end temperatures at each of the n current settings, and let $(R_o)_1$, $(R_o)_2$, . . . $(R_o)_n$ be the resistances the neck would have if it were uniformly at these temperatures. Further, let $(R)_1$, $(R)_2$, . . . $(R)_n$ be the actual measured resistances of the neck at the different current settings. Then, the reference temperature T_r is taken as the average value of the end temperatures:

$$T_r = \frac{1}{n} \sum_{i=1}^{n} (T_o)_i \quad . \qquad (4\text{-}32)$$

An approximate value for the resistance R_r is computed from the resistance $(R)_1$ corresponding to the lowest current level for which Joule heating is minimal, and the neck is nearly isothermal at temperature $(T_o)_1$ so that $(R)_1 \approx (R_o)_1$:

$$R_r \approx (R)_1[1 + \alpha_1(T_r - (T_o)_1)] \quad , \qquad (4\text{-}33)$$

where α_1 is evaluated at temperature $(T_o)_1$. Values of α were computed from the data obtained in the resistivity measurements [see Chapter VII].

For each experimentally determined resistance $(R)_i$ we compute a

corresponding approximate value of θ_m^* using (4-5) and a value for $(R_o)_i$ given by

$$(R_o)_i = R_r[1 + \alpha_r((T_o)_i - T_r)] , \qquad (4\text{-}34)$$

where α_r is evaluated at $T = T_r$. Using this value of θ_m^* as the first trial value, Newton-Raphson iteration is used to compute the value of θ_m^* which satisfies (3-66).[6/] Values for R^* and V^{*3} are then computed from (4-6) and (4-7) respectively. A least-squares straight line through these values of R^* and V^{*3} gives R_r as the ordinate intercept and dV^{*3}/dR^* as the slope. This value for R_r is a more accurate value than the initial value used, as it is based on an extrapolation to $I = 0$. Improved values for $(R_o)_i$ are now computed from the new R_r using (4-35). The calculation is then repeated using these values of $(R_o)_i$. This in turn leads to improved values for R_r and dV^{*3}/dR^*. The iteration converges in a few passes and the final values for R_r and dV^{*3}/dR^* are used in (4-31) to compute the apparent thermal conductivity.

The above calculation procedure was effected using a high-speed digital computer. It would not be practical for hand calculations since iterative solution of (3-66) for θ_m^* would be too tedious. An alternative calculation procedure, suitable for use with a desk calculator, is given in Appendix D.

Using the apparent value of k_r, as computed above, and equation (4-23) and (4-24) the correction factor for heat losses from the neck is computed and plugged into (4-32) to give the true value for the thermal conductivity.

6/ Values for β_o, computed from the thermal conductivity data obtained in the NBS Metals Apparatus on the same specimen [76], were used as first trial values, and these values were also iterated on.

Direct Method

In the direct method of measuring the thermal conductivity each datum point is computed by simultaneous solution of three tests:

1. an "isothermal" test with no power input to the specimen heater and with the temperature distribution on the guard adjusted to closely match that on the specimen.

2. a "matched"gradient test with sufficient power input to the specimen heater to maintain the desired longitudinal temperature gradient in the specimen and with a matched temperature distribution on the guard.

3. an "unmatched"gradient test with the power input to the specimen heater and the temperature at the center of the measuring span the same as in the "matched"gradient test, and with the temperature distribution on the guard parallel to that on the specimen but 10° below it.

For each of these tests, assuming one-dimensional steady-state heat flow in the specimen (an assumption justified in Appendix H), the total heat flow, Q, through the specimen is

$$Q = -k\,A\,\frac{dT}{dz} \qquad (4\text{-}36)$$

where k is the thermal conductivity, A is the cross-sectional area of the specimen, T is temperature and z is the longitudinal coordinate. For moderate temperature ranges, the thermal conductivity of the specimen can be assumed to vary linearly with temperature; then (4-36) becomes

$$Q = -k_r A \left\{1 + \beta_r (T-T_r)\right\} \frac{dT}{dz} \qquad (4\text{-}37)$$

where k_r is the thermal conductivity of the specimen at a reference temperature, T_r, and β_r is its corresponding temperature coefficient. The difference between the heat flows in two tests is given by

$$Q-Q' = -k_r A\left[\left(\frac{dT}{dz}\right) - \left(\frac{dT}{dz}\right)'\right]$$

$$-k_r A\beta_r\left[(T-T_r)\left(\frac{dT}{dz}\right) - (T'-T_r)\left(\frac{dT}{dz}\right)'\right] \qquad (4\text{-}38)$$

where quantities of one test are distinquished from those of the other by use of primes. If we define the reference temperature as

$$T_r = \frac{T\,(dT/dz) - T'\,(dT/dz)'}{(dT/dz) - (dT/dz)'} \qquad (4\text{-}39)$$

the second term on the right-hand side of (4-38) vanishes, and the thermal conductivity at the reference temperature, T_r, is given by

$$k_r = \frac{-(Q-Q')}{A\left[\left(dT/dz\right) - \left(dT/dz\right)'\right]} \qquad (4\text{-}40)$$

Inspection of (4-40) reveals that systematic errors in the measured heat flow, and in the measured temperature gradient, which are not dependent on these quantities, are eliminated by simultaneous solution of two tests having different heat flows. The most obvious errors of this type are thermocouple errors. In a simultaneous solution each thermocouple in effect measures a temperature difference so that errors in calibration of the thermocouples cancel out to first order. Further possible sources of error will become evident below. Determination of k_r involves measurement of the cross-sectional area of the specimen, the total heat flow in the specimen and the longitudinal temperature gradient in the specimen for each of two tests. These quantities are evaluated at the position of the middle thermocouple in the measuring span.

Cross-sectional area

The effective diameter of the specimen at 25°C was computed from the measured diameter and surface roughness as described in the section on density measurements in Chapter V. The diameter at temperature T was computed from that at 25°C using the equation

$$D_T = D_{25} \, (0.99978 + 8.876\times10^{-6}T + 1.311\times10^{-9}T^2) \qquad (4\text{-}41)$$

This equation was fitted to smoothed thermal expansion data for platinum [77]. The cross-sectional area was then computed from the diameter.

Heat Flow

The total heat-flow through the specimen at the position of the center thermocouple was calculated using the expression

$$Q = P - q_a - q_b - q_n - q_i - q_c \qquad (4\text{-}42)$$

where P is the measured electrical power input to the specimen heater;

q_a and q_b are the heat losses along the two leads carrying current to the specimen heater;

q_n is the heat loss across the necked-down portion of the specimen;

q_i is the heat loss into the insulation surrounding the specimen; and

q_c is the heat loss down the thermocouple wires and ceramic tubes next to the specimen.

Each of the quantities in (4-42) is considered separately below.

Power input to Specimen Heater (P): The electrical circuit for the specimen heater is illustrated diagrammatically in Figure 20 below.

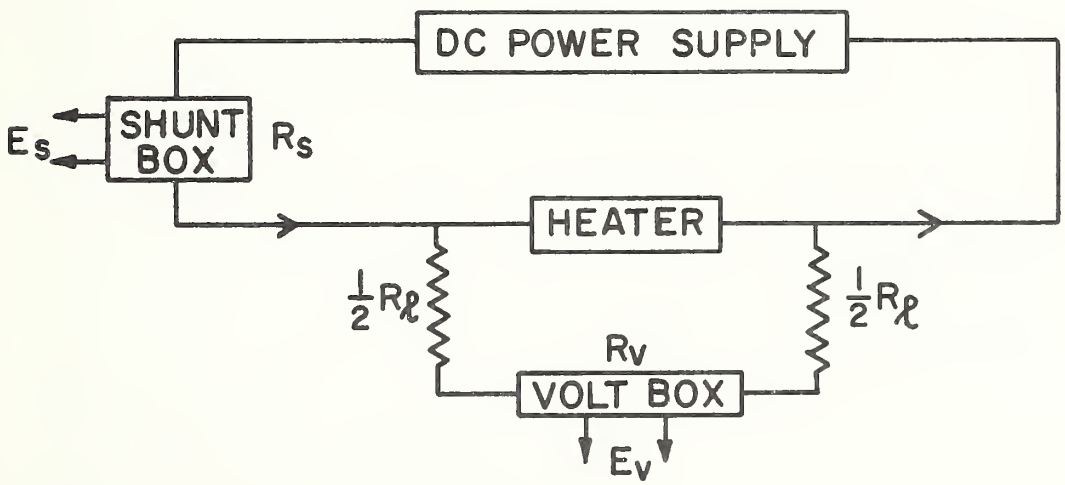

Figure 20. Circuit diagram for the specimen heater.

The power input to the heater is measured in terms of the current flowing through it and the potential drop across it, and is given by

$$P = nE_V (1 + R_\ell/R_V)(E_S/R_S - n E_V/R_V) \qquad (4\text{-}43)$$

where E_V is the voltage drop across the output of the volt box as measured with a potentiometer, n is the resistance ratio of the volt box, E_S is the voltage drop across the standard resistor, R_S, in the shunt box, as measured with a potentiometer, R_ℓ is the total resistance of the potential leads and R_V is the total resistance of the volt box.

Heat Flow in Current Leads (q_a,q_b): The circuit diagram in Figure 20 shows only one set of potential leads coming from the heater. In fact there were two sets as shown in Figure 21, but only the inner set, i.e. the potential taps closer to the heater, was used in measuring the power input to the heater. The two sets of potential leads were required in measuring heat conduction along the current leads.

Figure 21. Arrangement of potential leads for the specimen heater.

The current leads were platinum and the potential leads Pt 10 % Rh. Consequently, each current lead could be used along with its two potential leads as a differential thermocouple to measure the temperature drop, ΔT, between the potential taps. With current flowing to the heater the voltage drop measured between 1-2 or 3-4 is the algebraic sum of the IR drop between adjacent potential taps (where I is the current and R the resistance

of the current lead between the potential taps) and the Seebeck emf due to the temperature drop, ΔT, between the potential taps. Assuming no heat losses from the current leads, it can be shown (Appendix F) that the heat conducted along the leads is given by

$$q_{a,b} = \frac{\rho k}{R} \Delta T - \frac{I^2 R}{2} , \qquad (4\text{-}44)$$

where ρ is the electrical resistivity of the current lead and k its thermal conductivity. By taking measurements with the current flowing forward and reverse, R and ΔT can be determined for each lead, and consequently q_a and q_b.

The derivation of (4-44) is based on the assumption that there is no heat flow across the surface of a current lead. In fact, however, heat lost from the current leads into the surrounding powder insulation is not necessarily negligible, but a significant portion of it flows back to the specimen and so in effect is not lost. The rest of the heat lost into the powder either flows to the guard or flows longitudinally in the powder insulation. It is very difficult to analytically derive a correction for the effective heat loss from the current leads into the insulation and no such correction has been applied to the data presented in this paper. The heat conducted along the leads, as determined from (4-44), was less than 0.05% of the heat flowing in the specimen and the error due to neglecting heat loss from the surfaces of the current leads into the insulation is discussed in Chapters VII and VIII.

Heat Flow across Neck (q_n): Referring to Figure 18, it is seen that heat can be conducted across the necked-down region of the specimen by the neck itself and by the powder insulation surrounding it. The conductance of the powder is $\pi(b^2 - a^2)/2\ell$ where λ is its thermal conductivity and the

other parameters are defined in Figure 18. The conductance of the specimen between the two thermocouples (marked by x in Figure 18) is kF where k is the thermal conductivity of the specimen and F is the geometric factor. The factor, F, can be determined from the corresponding equation for electrical conductance, $I = \sigma FV$ where I is the current, σ the electrical conductivity and V is the voltage drop between the thermocouples. This data is available from measurements by the indirect method.

The heat flow across the neck is then given by

$$q_n = \left[kF + \hbar \frac{\pi(b^2 - a^2)}{2\ell} \right] \Delta T \qquad (4\text{-}45)$$

where it is assumed that the temperature differential across the insulation is the same as that measured between the thermocouples.

Heat Loss into the Insulation (q_i): In order to determine q_i, the heat exchange between the specimen and the surrounding insulation, it was necessary to perform an extensive mathematical analysis. If the temperature distribution along the guard exactly matched that along the specimen there would be no radial heat exchange between the specimen and the guard. However, there would still be an exchange of heat between the specimen and the surrounding insulation in order to provide the longitudinal heat flow in the insulation adjacent to the specimen.

The heat flow from an elemental length of the surface of the specimen is

$$dq_i = 2\pi a \hbar \left(\frac{\partial \theta}{\partial r} \right)_{r = a} dz \qquad , \quad (4\text{-}46)$$

where a is the radius of the specimen, $\hbar$ the thermal conductivity of the insulation, θ the temperature in the insulation relative to an arbitrary fixed temperature, r the radial coordinate and z the longitudinal coordinate.

The net heat flowing across the surface r = a between z_1 and z_2 is

$$q_i(z_1, z_2) = 2\pi a \int_{z_1}^{z_2} \hbar \left(\frac{\partial \theta}{\partial r}\right)_{r = a} dz \quad , \qquad (4\text{-}47)$$

where $\hbar$ is, in general, temperature dependent. Let us define a new potential, ξ, that satisfies the relation

$$\hbar_r \nabla \xi = \hbar(\theta) \nabla \theta \quad , \qquad (4\text{-}48)$$

where $\hbar_r = \hbar(0)$

Integrating (4-48) ,

$$\xi = \frac{1}{\hbar_r} \int_0^{\theta} \hbar(\theta)\, d\theta \quad , \qquad (4\text{-}49)$$

where we have selected the integration constant so that $\xi = 0$ when $\theta = 0$. Writing (4-47) in terms of ξ we get

$$q_i(z_1, z_2) = \hbar_r D(z_1, z_2) \quad , \qquad (4\text{-}50)$$

where

$$D(z_1, z_2) = 2\pi a \int_{z_1}^{z_2} \left(\frac{\partial \xi}{\partial r}\right)_{r = a} dz \qquad (4\text{-}51)$$

In order to evaluate $D(z_1, z_2)$ one must know the temperature dependence of the thermal conductivity of the powder insulation as well as the radial temperature gradient at the surface of the specimen. The thermal conductivity of the insulation was assumed to be a linear function of temperature;

$$\hbar = \hbar_r(1 + \gamma_r \theta) \quad , \qquad (4\text{-}52)$$

where $\hbar_r$ and γ_r are evaluated at $\theta = 0$, γ being the temperature coefficient of the thermal conductivity of the insulation. Then, from (4-49)

$$\xi = \theta + \frac{\gamma_r}{2} \theta^2 \qquad (4\text{-}53)$$

The radial temperature gradient at the surface of the specimen was determined by Fourier analysis of the hollow cylinder of powder insulation between the specimen and the guard with known temperature distributions at its boundaries. At the surface of the specimen, r = a, the potential distribution was represented by

$$(\xi)_{r=a} = g_o + (g_\omega - g_o)\frac{z}{\omega} + \sum_{n=1}^{\infty} A_n \sin\frac{n\pi z}{\omega} \qquad (4\text{-}54)$$

and at the inner surface of the guard, r=b, the potential distribution was represented by

$$(\xi)_{r=b} = h_o + (h_\omega - h_o)\frac{z}{\omega} + \sum_{n=1}^{\infty} B_n \sin\frac{n\pi z}{\omega} \quad , \qquad (4\text{-}55)$$

where $\xi(r,z)$ has the values $\xi(a,0) = g_o$, $\xi(a,\omega) = g_\omega$, $\xi(b,0) = h_o$, $\xi(b,\omega) = h_\omega$, at the ends of the region, z=0 and z=ω, which correspond to the outermost thermocouples on the guard. At these ends the radial temperature distribution in the powder insulation was assumed to be logarithmic:

$$(\xi)_{z=0} = g_o + (h_o - g_o)\frac{\ell n\, r/a}{\ell n\, b/a} \qquad (4\text{-}56)$$

$$(\xi)_{z=\omega} = g_\omega + (h_\omega - g_\omega)\frac{\ell n\, r/a}{\ell n\, b/a} \quad . \qquad (4\text{-}57)$$

The Fourier coefficients A_n and B_n in (4-54) and (4-55) were determined from the measured temperature distributions along the specimen assembly and the guard cylinder. In the gradient region of the specimen, and in the upper and lower specimen extensions, the observed temperature and thermocouple locations (corrected for thermal expansion) were used to derive quadratic equations giving θ vs. z, where θ was measured relative to the temperature at the center of the gradient region of the specimen. In

the neck region, which is nearly isothermal at all times, a linear equation was used. The three quadratics in θ transform to quartics in ξ and the linear equation in θ transforms to a quadratic in ξ with application of (4-53). In the intervening heater regions, smoothing cubics [100] were used which provided continuity of temperature and longitudinal temperature gradients. Thus the ξ-distribution along the specimen was described by seven smoothly-joined polynomials: quartic (lower extension), smoothing cubic (lower extension heater), quartic (gradient region of specimen), smoothing cubic (specimen heater), quadratic (neck region of specimen), smoothing cubic (upper extension heater), quartic (upper extension). Equating this set of polynomials to the right-hand side of (4-54) and making use of orthogonality enabled calculation of the A_n's. A similar set of polynomials was used to represent the ξ-distribution along the guard, from which the B_n's were calculated. It would serve no useful purpose to explicitly display the expressions for A_n or B_n in this paper; they are quite lengthy and rather complex.

With the boundary conditions (4-54), (4-55), (4-56), and (4-57) the potential, ξ, at any point in the powder insulation is given by

$$\xi = \left[g_o + (h_o - g_o) \frac{\ell n\, r/a}{\ell n\, b/a} \left(1 - \frac{z}{\omega}\right) + \left[g_\omega + (h_\omega - g_\omega) \frac{\ell n\, r/a}{\ell n\, b/a} \right] \frac{z}{\omega} \right.$$

$$\left. + \sum_{n=1}^{\infty} \frac{A_n F_o(n\pi\, r/\omega;\ n\pi\, b/\omega) - B_n F_o(n\pi r/\omega;\ n\pi a/\omega)}{F_o(n\pi a/\omega;\ n\pi b/\omega)} \sin \frac{n\pi z}{\omega} \right. , \quad (4\text{-}58)$$

where

$$F_o(x,y) = I_o(x)\, K_o(y) - K_o(x)\, I_o(y)$$

I_m = modified Bessel function of first kind and order m,

K_m = modified Bessel function of second kind and order m.

Substitution of (4-58) into (4-51) finally yields $D(z_1, z_2)$:

$$D(z_1, z_2) = 2\pi a\left[\left\{(h_o - g_o)(z_2 - z_1) + (h_\omega - h_o - g_\omega + g_o)\frac{z_2^2 - z_1^2}{2\omega}\right\}\frac{1}{a \ell n\, b/a}\right.$$

$$\left. - \sum_{n=1}^{\infty} \frac{A_n F_1(n\pi a/\omega;\ n\pi b/\omega) - (\omega/n\pi a)B_n}{F_o(n\pi a/\omega;\ n\pi b/\omega)}\left(\cos\frac{n\pi z_2}{\omega} - \cos\frac{n\pi z_1}{\omega}\right)\right], \quad (4\text{-}59)$$

where $F_1(x,y) \equiv I_1(x)\ K_o(y) + K_1(x)\ I_o(y)$. (4-60)

Since the heat flow in the specimen is to be evaluated at the position of the center thermocouple in the gradient region all the heat loss to the insulation from the location of the heater down to the position of the center thermocouple must be considered. In addition, heat losses in the region between the specimen heater and the neck must be considered since these have to be provided by the specimen heater. The neck in effect, can be considered as the upper end of the specimen for purposes of this analysis, since any heat exchanges between the powder and the specimen above the neck do not affect that part of the specimen below the neck as long as zero temperature differential is maintained across the neck. Therefore, in evaluating q_i, the limits of integration for $D(z_1, z_2)$ are the position of the center thermocouple (z_1) and the position of the center of the neck (z_2).

Heat loss along thermocouple wires and insulator (q_c): The heat loss q_c, along the thermocouples and ceramic insulators next to the specimen was computed from the expression

$$q_c = \sum_{i=1}^{n} C_i\left(\frac{dT}{dz}\right), \quad (4\text{-}61)$$

where C_i is the longitudinal thermal conductance of the i^{th} wire and its insulator, n is the total number of wires crossing the plane where the thermal conductivity is evaluated, and dT/dz is the temperature gradient at that plane. Each C_i was computed from the thermal conductivities and dimensions of the wire and insulator.

Temperature Gradient

The temperature gradient in the specimen was computed from the measured temperatures at the five thermocouple positions in the gradient region. The separations between thermocouple grooves at room temperature were accurately measured before the thermocouples were installed; the separation at elevated temperature was computed using (4-41). Since temperature gradients in the specimen were rather small (less than 5°C/cm) it was essential that the conversion of thermocouple emfs to temperature not introduce any additional uncertainties. The equation

$$E = 15.83952\left(\frac{T}{1000}\right) - 9.18328\left(\frac{T}{1000}\right)^2 + 7.30572\left(\frac{T}{1000}\right)^3 - 1.92753\left(\frac{T}{1000}\right)^4 - 2.50480\,(1.0 - \exp[-4.18312(T/1000)]) , \qquad (4\text{-}62)$$

where T is temperature (°C) and E is emf (mV), was found to fit to within 1 μV the calibration data for the Pt/Pt 10%Rh thermocouple wire from which the specimen thermocouples were fabricated. This equation was used for converting the thermocouple voltages to temperatures.

The temperature gradient was computed by evaluating the slope, at the center thermocouple location, of the quadratic equation of least-squares fit to the five temperatures and thermocouple positions.

Appendix G gives a brief analysis of temperature measurement errors due to conduction of heat along the thermocouple wire.

In analysing the data the "isothermal" test is combined with the "matched gradient" test and with the "unmatched gradient" test to give two equations of the form (4-40). Inspection of equations (4-40), (4-42) and

(4-50) shows that k_r is a linear function of λ_r. The effective thermal conductivity of the insulation surrounding the specimen depends on the density of the powder and the pressure and type of gas present, and is best determined under experimental conditions. This is done by simultaneous solution of the two equations of the form (4-40) which yields values both for the thermal conductivity of the specimen, k_r, and the thermal conductivity of the insulation λ_r.

Electrical Resistivity:

The electrical resistivity of the gradient region of the specimen was determined by measuring the voltage drops between platinum legs of the thermocouples in that region with a 10A d-c current passing through the specimen. The specimen was held isothermal to better than 1°C during this measurement. In order to minimize thermoelectric effects, voltage drops were measured, with the current flowing forward and reversed. Resistivity values were computed from these voltages and from the measured current and geometry. The effective mean temperature was computed by Simpson's rule integration of the observed temperatures.

CHAPTER V

SPECIMEN CHARACTERIZATION

In order for a truly valid comparison to be made between the results of different investigators who measure on a particular kind of material it is necessary that their specimens be characterized as extensively as possible so that differences in specimens may be accounted for. For this reason a number of pertinent measurements have been made in an attempt to characterize the specimen used in the present investigation. These measurements and the results thereof are described below. Additional appropriate information is also provided.

Source: The platinum was provided by Engelhard Industries, Inc., and was classified as being of commercial purity or according to Engelhard classification as being E-2 grade. Spectrographic analyses are given below.

Three samples were provided, all three coming from the same casting as described below. The first sample was a bar 0.805 inch in diameter and 12.200 inches long from which the thermal conductivity specimen was later machined. The second sample was a rod 0.150 inch in diameter and 9.84 inches long to be used for resistivity measurements. The third sample consisted of 20-mil diameter wire to be used in resistivity measurements and in measurements of thermoelectric power versus Pt 27 [78].

Fabrication and Thermal History of Specimen: Commercial purity platinum sponge(approx. 200 ounces) was induction-melted in air in a zirconium silicate crucible. The metal was slightly over the melting point when it was poured into a clean graphite mold (casting 1 1/4 inches in diameter and 15 inches long).

The cast bar was swaged cold to a diameter of 1 inch. The bar was then machined to 0.90-inch diameter. Next, a piece 12 3/4 inches long was cut from the middle of the bar, acid-cleaned in hot aqua regia and annealed at 700°C for 1 hour. This piece was then machined to a solid cylindrical bar, 0.805 inch in diameter and 12.200 inches long with a 0.531-inch diameter by 2.156-inch deep flat-bottomed hole drilled coaxially in one end.

The bottom end of the original bar was then worked down to a diameter of 0.162 inch, and a piece 12 inches long was removed to supply the 0.150-inch specimen. This piece was cleaned in boiling aqua regia and approximately 5% (by weight) of the surface was removed. It was then drawn to 0.150 inch in diameter by 9.84 inches long through clean carbide dies.

A portion of the remaining material was cold swaged to 80-mil diameter, drawn through clean carbide dies to 50-mil diameter, and drawn through diamond dies to 25-mil diameter. This wire was acid cleaned in hot aqua regia to 22-mil diameter. It was then drawn through clean diamond dies to a diameter of 20 mils.

The three samples were cleaned at finished size in the following manner: Ultrasonically cleaned, then pickled for 10 minutes in 50% hot nitric acid. Washed and then pickled for 10 minutes in 50% hot hydrochloric acid, washed in distilled or demineralized water. The fabrication and cleaning described above were carried out at the Engelhard Plant.

The as-received 0.805-inch bar was annealed in air for 5 1/2 hours at 770°C in a horizontal tubular furnace and furnace cooled at a rate of approximately 120°C per hour. Shortly thereafter the bar was accidentally dropped causing it to deform slightly at one end. After correcting the damage the bar was reannealed for 1 1/2 hours at 680°C and furnace cooled at a rate of approximately 90°C per hour. Its thermal conductivity was

then measured in the NBS Metals Apparatus over the temperature range -160° to +810°C. Following these measurements the hollow end of the bar was cut off and the remainder of the bar machined and ground to a solid bar 10 inches long by 0.786 inch diameter. The electrical resistance of this bar was measured at ice and liquid helium temperatures (see below). The thermal conductivity specimen (7.25 inches long by 0.786 inch diameter) was then cut from one end of this bar. A length of 2.5 inches was cut from the other end for low temperature thermal conductivity measurements (see Discussion of Results). The remaining disc, approximately 0.4 inch long, was reserved for metallographic and spectrographic analyses. Two 1/4-20 holes were chased 1/4 inch deep in the specimen, one at each end, and the thermocouple slits, heater holes and neck were machined in the specimen.

Steel cutting tools were used in machining the neck, while a mixture of trichlorethylene and oil served as a cutting fluid. To cleanse the neck of oil and any contamination contracted from the cutting tools, the following cleaning procedure was followed. Degreasing was effected by immersion for half an hour in trichlorethylene vapor. The neck was then pickled for 10 minutes in hot 50% nitric acid. Following this the neck was washed in distilled water, pickled for 10 minutes in 50% hot hydrochloric acid, and again washed in distilled water. There was equal likelihood of the rest of the specimen having slight surface contamination as a result of machining but its effect on the bulk properties of the specimen would not be nearly as grave as the corresponding effect in the neck region. It was considered sufficient to clean the surface of the specimen with toluene and carbon tetrachloride.

Hardness: Hardness measurements were made on the platinum bar in the as-received condition as well as after each of the two anneals. Measurements were made with a Vickers Pyramidal Diamond Tester using a 10 Kg load and a 2/3-inch objective. The results are tabulated below.

Table 3. Hardness Values as Measured on the Platinum Bar

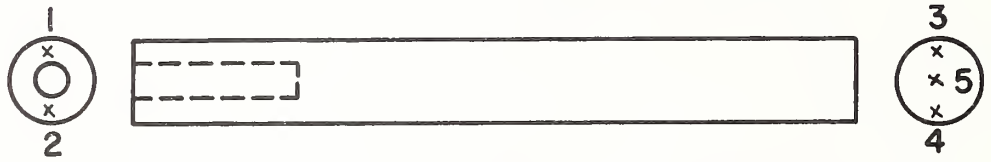

Location*	Vickers Hardness Number 1	2	3	4	5
As received	69.6	68.6	65.8	53.3	65.2
After first anneal	35.0	35.2	36.0	38.2	36.3
After second anneal	46.7	40.3	36.5	38.0	36.5

* The locations indicated above do not represent specific locations but merely general locations where the hardness measurements were made.

The higher values obtained at locations 1 and 2 after the second anneal, occurring as they do at the end that was deformed slightly when the bar fell, tend to indicate that not all of the hardening resulting from the fall was annealed out. However, no measurements were made on that end of the bar so that there was no need to worry about it.

Spectrographic Analysis: A quantitative spectrographic analysis on the 20-mil wire was made by Engelhard Industries, and the results of their analysis are tabulated below. A general qualitative spectrographic analysis was performed on the platinum disc at the National Bureau of Standards. The qualitative analysis, being less sensitive, detected only Ag (10-100 ppm), Mg (< 10 ppm), Pd (10-100 ppm), and Fe (< 10 ppm). The higher concentration of iron indicated for the wire may result from the extra fabrication.

Table 4. Spectrographic Analysis as Determined on Platinum Wire No. 175105

Quantitative Analysis No. 3312 By Engelhard Industries

Impurity	ppm	Impurity	ppm
Rh	3	Ca	0.4
Pd	73	Al	<1
Ir	<5	Ni	<1
Ru	ND	Cr	ND
Os	ND	Mn	<1
Au	<2	Sb	ND
Ag	3	B	ND
Pb	ND	Co	ND
Sn	ND	As	ND
Zn	ND	Bi	ND
Fe	39	Cd	ND
Cu	0.4	Mo	ND
Si	3	Te	ND
Mg	<1	Na	ND

Pt* 99.987+ %.

< less than ND - Not Detected

* This value, obtained by difference, represents only the metallic percent, no gas analysis having been done on the sample.

Metallography: Photomicrographs were made of the platinum disc cut from the bar sample. They showed grain size to be of the order of 0.01 inch. No evidence appeared of inclusions of foreign matter or of any irregularities in microstructure.

Density: The density was determined on the solid bar, when it was 10 inches long, by mass and dimensional measurements.

The diameter was measured at three angular orientations, approximately 120° apart, at each of six locations along the bar giving a total of 18 measurements. The value thus determined for the diameter of the bar at 21°C was

$$0.78643 \pm 0.00005 \text{ inches} \qquad (3\ \sigma \text{ limits}).$$

Five measurements were made on the length of the bar by comparison with a set of gage blocks using an electronic gage block comparator. The value

determined for the length of the bar at 21°C was

$$10.01300 \pm 0.00003 \text{ inches} \qquad (3\sigma \text{ limits}).$$

The surface roughness was measured on a Talysurf machine against an absolute datum with a 30 mg load and a stylus of radius less than 100 micro-inches. The value recorded was

29 micro-inches AA at 0.03-inch cutoff.

Assuming that the surface can be characterized by a sinusoidal profile, which is a fairly reasonable assumption, the amplitude of the sine wave is calculated as follows.

The arithmetic average deviation, automatically measured on the Talysurf machine, is defined as

$$AA = \frac{1}{L} \int_o^L |y| \, dx \qquad (5\text{-}1)$$

where y is the deviation of a point in the surface from a reference datum located such that the net area enclosed by it and the surface profile is zero, x is the position along the surface and L is the total distance traversed. In the case of a sine wave

$$AA = \frac{2}{\pi} \int_o^{\pi} h \sin x \, dx = \frac{2}{\pi} h \qquad (5\text{-}2)$$

$$h = \frac{\pi}{2} AA \qquad (5\text{-}3)$$

Assuming that peak to peak values were measured in measuring the diameter of the bar the correction to be applied in order to arrive at the effective diameter is

$$D = D_{measured} - 2 \left(\frac{\pi}{2} AA\right)$$

$$= 0.78643 - 0.00009$$

$$D = 0.78634 \text{ inch} = 1.9973 \text{ cm}$$

The bar was weighed on a balance (B-1) in the Mass Section of the National Bureau of Standards and the true mass computed to be

$$1703.975 \pm 0.010 \text{ gm.}$$

The density was computed from the above measurements to be

$$21.384 \pm 0.002 \text{ gm/cm}^3 \text{ at } 21°C.$$

The density just quoted is an average value for the whole bar and there is no guarantee that the density is uniform to that degree throughout the bar.

R273.15°K/R4.2°K: The ratio of the resistance at the ice-point temperature to that at the boiling point of helium at atmospheric pressure is a measure of the extent and condition of impurities in a material and of the crystallographic state of the material. This ratio was determined on each of the three samples provided by Engelhard. The 0.786-inch diameter bar was 10 inches long and had been annealed as described in the section on Fabrication and Thermal History above. The other two samples were also annealed prior to these measurements. The 0.150-inch diameter rod was annealed in air for one hour at 850°C and allowed to slowly furnace-cool. The 20-mil diameter wire was annealed in air by passing a dc current through it using its change in resistance as a measure of its mean temperature.

The ice-point resistances were measured both before and after the helium point measurements. The current was supplied from a regulated dc power supply and was measured using a shunt box and precision potentiometer. The voltage drops in the specimens were measured on a high precision 6-dial potentiometer. In each case the resistance was measured at three or four different current levels and the value corresponding to zero current obtained by plotting resistance as a function of current squared and extrapolating to zero current. The measured values of the resistances are

presented in Table 5, each value representing the average of four measurements, two with the current flowing forward and two with the current reversed. The values for the resistance ratios are also given, these values being good to within better than 1% for the two smaller samples and probably good to within 1% for the large bar.

Table 5. Resistance Values for Three Samples of Platinum at Ice-Point and Helium-Point Temperatures, and the Computed Resistance Ratios at Zero Current.

	Temperature 273.15°K			Temperature 4.2°K		
Sample	Nominal Current Amps	Resistance Before μΩ	Resistance After μΩ	Nominal Current Amps	Resistance μΩ	Resistance Ratio
0.786 in. diam. bar	0*	58.96		0*	0.150	393
	10	58.96	58.97	30	0.151	
	20	58.99	58.99	60	0.150	
	30	59.01	59.01	80	0.150	
	40	59.04	59.06	95	0.150	
0.150 in. diam. rod	0*	1545.		0*	3.612	428
	1	1545.	1545.	10	3.618	
	2	1546.	1545.	20	3.615	
	3	1546.	1545.	30	3.612	
				40	3.612	
0.020 in. diam. wire	0*	90280.		0*	233.5	387
	0.2	90320.		0.8	233.5	
	0.5	90430.	90450.	1.5	233.5	
	0.8	90560.	90550.	3.0	233.6	
	1.0	90650.	90620.			

* The values tabulated at zero current are extrapolated values.

Ice-Point Resistivity: A set of knife edges of known separation was fastened to the 0.786-inch bar during the first set of ice-point resistance measurements. The knife edges acted as potential taps. Since the separation of the knife edges and the cross sectional area of the bar were known it was

possible to compute the ice-point resistivity. The value obtained, corrected to 0°C dimensions, was

$$\rho o = 9.847 \pm 0.010 \ \mu\Omega \text{ cm.}$$

E. M. F. vs Pt 27: The following table gives the values of the electromotive force of the 20-mil platinum wire versus the platinum standard Pt-27 corresponding to the temperature of the measuring junction when the reference junctions are at 0°C as determined at the National Bureau of Standards.

Table 6. E. M. F. vs Pt 27 as determined on 20-mil Platinum Wire. National Bureau of Standards Test No. 3.1d/8404A.

Degrees C (Int. 1948)	Absolute Microvolts	Degrees C (Int. 1948)	Absolute Microvolts
0	0	600	+6
100	+1	700	+8
200	+2	800	+10
300	+3	900	+13
400	+4	1000	+14
500	+5	1100	+15

The platinum wire was electrically annealed in air for one hour at about 1450°C before testing.

CHAPTER VI

TEST PROCEDURES

Preliminaries

The furnace was heated to 150°C and the system evacuated to 3×10^{-4} torr Initial pump-down was through a needle valve to give a sufficiently slow rate so as not to disturb the very light power insulation. When the pressure had fallen below 100 microns the diffusion pump was turned on, pumping initially through the needle valve, and, when the pressure was below 10^{-2} torr, through the 4 inch port. After pumping for 24 hours the pumps were turned off and the system back-filled with high purity (99.99%) argon. The argon was bled in slowly through a needle valve to avoid disturbing the powder. The pressure was allowed to build up to almost one atmosphere before the valves were shut off and the cycle of evacuating and backfilling repeated. The final argon pressure after the second backfilling was about three-quarters of an atmosphere.

The cooling-water flows to the system were adjusted to the desired level as indicated on flow-meters. The water was pressure-regulated to maintain constant flow rate. A control thermocouple on the specimen was wired to shut all the heaters off if its temperature exceeded a pre-determined level. This was a safety precaution in the event of an interruption in the cooling-water flow.

The test procedures are described in detail below. To facilitate the discussion let us refer to Figure 12. The region of the specimen below the specimen heater, Q_2, will be referred to as the lower part of the specimen, and the region above Q_2 as the upper part of the specimen.

Direct Method

"Matched" Gradient Test: The furnace temperature was raised by means of heater Q_7. The power to the specimen heater, Q_2, was adjusted to give a temperature gradient of 5°C/cm in the lower part of the specimen. This heater was fed from a constant voltage dc power supply with regulation of ±0.005% or better. The output voltage ranged from 10 to 15 V with a current of about 1 A. Power to Q_3 was automatically controlled, using a proportional controller, to maintain minimum temperature drop across the neck. The Pt10%Rh legs of thermocouples 9 and 12 were used in conjunction with the necked-down portion of the specimen as a differential thermocouple activating the proportional controller. The temperature drop across the neck never exceeded 0.1°C. The specimen was maintained at the required mean temperature by thermostatting the power high-low to the lower heater Q_1.

The temperature distribution along the guard was forced to match that along the specimen by controlling the power to heaters Q_4, Q_5 and Q_6. Temperatures at corresponding locations on the specimen and the guard generally agreed to within 1°C.

After allowing time for the system to come to equilibrium readings were taken and recorded. The readings were made in the following sequence:

(a) The emfs of the guard thermocouples were read to 0.1μV.

(b) The emfs of thermocouples 1 through 3 and 9 through 15 on the specimen assembly were to read to 0.1μV (thermocouples 1, 2, 14 and 15 are not shown in Figure 12 but refer to the thermocouples on the molybdenum extensions).

(c) The emfs of thermocouples 4 through 8 on the specimen were read to 0.01μV.

(d) The differential temperature $T_{11} - T_{10}$ across the neck was read to 0.01μV using the Pt10%Rh legs of thermocouples 11 and 10 and the necked-down region of the specimen as a differential thermocouple.

(e) The current to the specimen heater, Q_2, and the voltage drop across the inner taps were read to five significant figures.

The above sequence of readings was taken three times to check the equilibrium, each set of readings taking about three-quarters of an hour. The temperatures never drifted more than a few hundredths of a degree from one set of readings to the next and the three sets of data were averaged. When the drift between the first and second sets of readings was less than 0.01°C the third set of readings was not taken. On completion of the last set of readings the following additional readings were made :

(f) The voltage drop across the outer taps of the specimen heater was measured to 0.1mV.

(g) The potential drops in the current leads, E_{12} and E_{34} (see Figure 21), were measured to 1μV.

The current through the specimen heater was then reversed and readings (e), (f) and (g) repeated.

"Unmatched" Gradient Test: Upon completion of the "matched" gradient test the guard heaters Q_4, Q_5 and Q_6 were adjusted to lower the temperatures on the guard by 10°C while maintaining the temperature distribution parallel to that on the specimen. With the guard at the lower temperature heat losses from the specimen to the surrounding insulation were significantly increased and the heat flow in the specimen reduced. As a result, the temperature gradient in the specimen and its mean temperature were decreased.

The power to heater Q_1 was adjusted to restore the specimen to the initial mean temperature. The system was then allowed to equilibrate and the same series of readings were taken as for the "matched" gradient test.

"Isothermal" Test: For the "isothermal" test heater Q_2 was shut off and heater Q_1 adjusted until the specimen was approximately isothermal. No adjustments had to be made to Q_3 as the controller automatically adjusted to maintain $T_{11} - T_{10} = 0$. The guard heaters were likewise adjusted until the temperature distribution on the guard once again matched that on the specimen. When the system was in equilibrium the readings listed above for the gradient tests, with the exception of items (e) and (f), were taken.

At 1100°C an additional "matched" gradient test was run after the three regular tests were completed. The extra data obtained in this test served as a check on drifts in thermocouple calibrations during the testing period.

Resistivity

After completion of the thermal conductivity measurements by the direct method, with the specimen still isothermal (to within 1°C), a 10A dc current was passed through the specimen. The current was supplied from a dc power supply with current regulation of better than 0.01%. The resistance of the lower part of the specimen was determined by simultaneous measurement of the current and of the voltage drops between the platinum legs of the thermocouples. Readings were taken in the following sequence:

(a) The emfs of thermocouples 4 through 8 were read to 0.01μV.

(b) The voltage drops between the platinum legs of the thermocouple

combinations 4-8, 4-6, and 6-8 were read to 0.01μV while the current was read simultaneously to 0.1mA.

(c) All of readings (a) and (b) were taken in the reverse sequence.

(d) The current was reversed and readings (a), (b) and (c) repeated.

With current flowing through the specimen differential temperature control at the neck could not be employed and Q_3 was controlled absolutely, as described in Chapter II, to maintain T_{11} as close to T_{10} as possible.

Indirect Method

Measurements by the indirect method were made immediately following the resistivity measurements. Power to heaters Q_1 and Q_3 was controlled to maintain T_{10} and T_{11} constant with $|T_{11} - T_{10}|$ less than 0.2°C. Temperatures along the guard in the region opposite the neck were maintained at the same value as T_{10}. The current through the neck and the voltage drop across it were measured with a dc current passing through the specimen. The current was supplied by a 100A dc power supply with current regulation of 0.05% or better. With 10A passing through the specimen the following readings were taken

(a) The emfs of the guard couples in the neck region were read to 0.1μV.

(b) The emfs of thermocouples 9, 12, 10 and 11 on the specimen were read in that sequence to 0.01μV.

(c) The voltage drops between the platinum legs of thermocouples 10 and 11, and 9 and 12, were measured to five significant figures with the current measured simultaneously to five significant figures.

(d) All of readings (b) and (c) were taken in reverse sequence.

(e) Steps (b), (c) and (d) were repeated and finally

(f) Readings (a) were repeated.

In this way each quantity, with the exception of the guard temperatures, was measured four times with the averages all corresponding to the same mean time. The temperatures never drifted more than a few hundredths of a degree during a test (approximately three-quarters of an hour), and although the current showed drifts of 0.05% the measured resistances remained constant to 0.01% with current and voltage being read simultaneously.

To compensate for thermoelectric effects and IR drops in the thermocouples the current was reversed, the above sequence of measurements repeated and data from the two tests averaged. During tests at 300°C a quick check was made on the magnitude of IR drops in thermocouples 9 through 12. The emfs of these thermocouples were read with a current of 50A flowing forward. The current was reversed and the emfs read immediately again. The emfs changed by amounts ranging from 2.5 to 13 μV.

With current flowing through the specimen the Peltier effect gives rise to heat generation at one of the platinum-molybdenum interfaces and heat absorbtion at the other depending on the direction of the current flow. For example, at 1000°K with 100A flowing through the specimen the Peltier heat generated or absorbed at a platinum-molybdenum interface is approximately 4 watts. When the current is reversed the processes are reversed, and, at the interface where heat was generated, it is now absorbed and vice versa. Consequently when the current was reversed heaters Q_1 and Q_3 had to be adjusted to compensate for the Peltier effect, and time had to be allowed for the system to reach a new equilibrium.

The measurements made at 10 amps were repeated at 58, 82, and 100 amps giving four sets of data at approximately even increments of I^2.

All of the measurements described above were made at a number of temperatures. Tests were first run in air at 100°C, then in argon at 100, 300, 500, 700, 600, 400, and 200°C in that order. One of the guard heaters would short out at about 750°C and consequently the upper limit on the first run was 700°C. After completing that run in argon the system was evacuated and backfilled with helium (99.99% pure) to a pressure of about three-quarters of an atmosphere. The helium, having a much higher thermal conductivity than argon, changed the effective thermal conductivity of the insulation surrounding the specimen. Tests were run in helium at 200 and 400°C to experimentally evaluate heat losses from the specimen to the insulation. The system was then opened up and the trouble with the guard heater rectified. The furnace was filled with fresh powder insulation, the powder being packed lightly around the neck to ensure that the necked-down region was uniformly filled with insulation. The system was refilled with argon as described at the beginning of this section and tests were run at 300, 500, 700, 900, and 1100°C. Heater Q_3 burned out during the indirect test at 1100°C and that test was incomplete. The thermocouples started drifting at 1100°C and losing their calibration due to contamination. Consequently it was decided to terminate the tests at that point.

CHAPTER VII

RESULTS

Electrical Resistivity

The ice-point resistivity was determined on the platinum bar before the neck was machined in it (see Chapter V). The value obtained was

$$\rho_o = 9.849 \pm 0.010 \ \mu\Omega \text{ cm} \qquad (7\text{-}1)$$

corresponding to room temperature (25 °C) dimensions.

In the indirect method of measuring thermal conductivity the resistance of the necked-down region of the specimen at each temperature was determined at a number of current levels. The resistance, R_T, at temperature, T, was evaluated by extrapolation to zero current as described in Chapter IV. In the first series of tests, or the first run as it will be referred to, measurements were made at 40 and 100 °C in air, at 100, 300, 500, 700, 600, 400, and 200 °C in argon and at 200 and 400 °C in helium in that order. The apparatus was then opened up for repair of the guard heater as described in Chapter VI. In the second series of tests, or the second run as it will be referred to, measurements were made at 300, 700, 900, and 1100 °C in argon.

The values for the resistance of the neck obtained during the second run were about 1½% higher than the values obtained at corresponding temperatures in the first run. This increase in resistance was observed both for measurements at the inner potential taps (10-11) and for measurements at the outer potential taps (9-12) indicating that the increase in values were due to a change in the geometric factor of the neck. What happened is not known but, apparently, the neck suffered some slight geometric change when repairs were being made to the guard heater. In determining the electrical resistivity, data from the first run and that from the second run had to be treated separately in view of the change in the geometric factor.

A least-squares quadratic equation fits the data from the first run with a standard deviation of 0.03%. The equation, extrapolated to 0 °C and normalized to the ice-point resistivity, (7-1), gives

$$\rho = 9.849(1 + 3.953 \times 10^{-3}T - 0.5744 \times 10^{-6}T^2) \qquad (7\text{-}2)$$

as the electrical resistivity of the neck from 0 to 700 °C where T is in °C. Departures of the data points from this equation are plotted in Figure 22 where the overall scatter is seen to be ±0.05%. All but two of the points fall within 0.025% of the curve and there is no significant difference between the values obtained on heating and cooling.

A second quadratic equation was fitted to the data points at 300, 700, and 900 °C obtained in the second run. The equation, normalized to the value given by (7-2) at 700 °C is

$$\rho = 9.797(1 + 4.001 \times 10^{-2}T - 0.6043 \times 10^{-6}T^2) \qquad (7\text{-}3)$$

While the geometric factor of the neck changed between the first and second runs there is no reason to believe the resistivity would have changed. Any strains introduced when the geometric factor changed would have annealed out at 700 °C. Thus normalizing the data from the second run to that from the first run at 700 °C is felt to be justified. The departures of the normalized data points at 300, 700, 900, and 1100 °C from the values given by equation (7-2) are indicated by triangles in Figure 22. The 1100 °C data point was not used in deriving (7-3). The thermocouples started to drift at 1100 °C due to contamination so that greater uncertainty had to be assigned to data obtained at that temperature. The 1100 °C data point agrees with the extrapolated value given by equation (7-3) to within 0.02%. The deviations from the quadratic equation (7-2) at the higher temperatures as shown in Fig. 22 are in line with what one would expect. Recent measurements at NBS [80] in conjunction with work toward extending platinum resistance thermometry to the gold point showed that the measured resistance of a certain high purity platinum

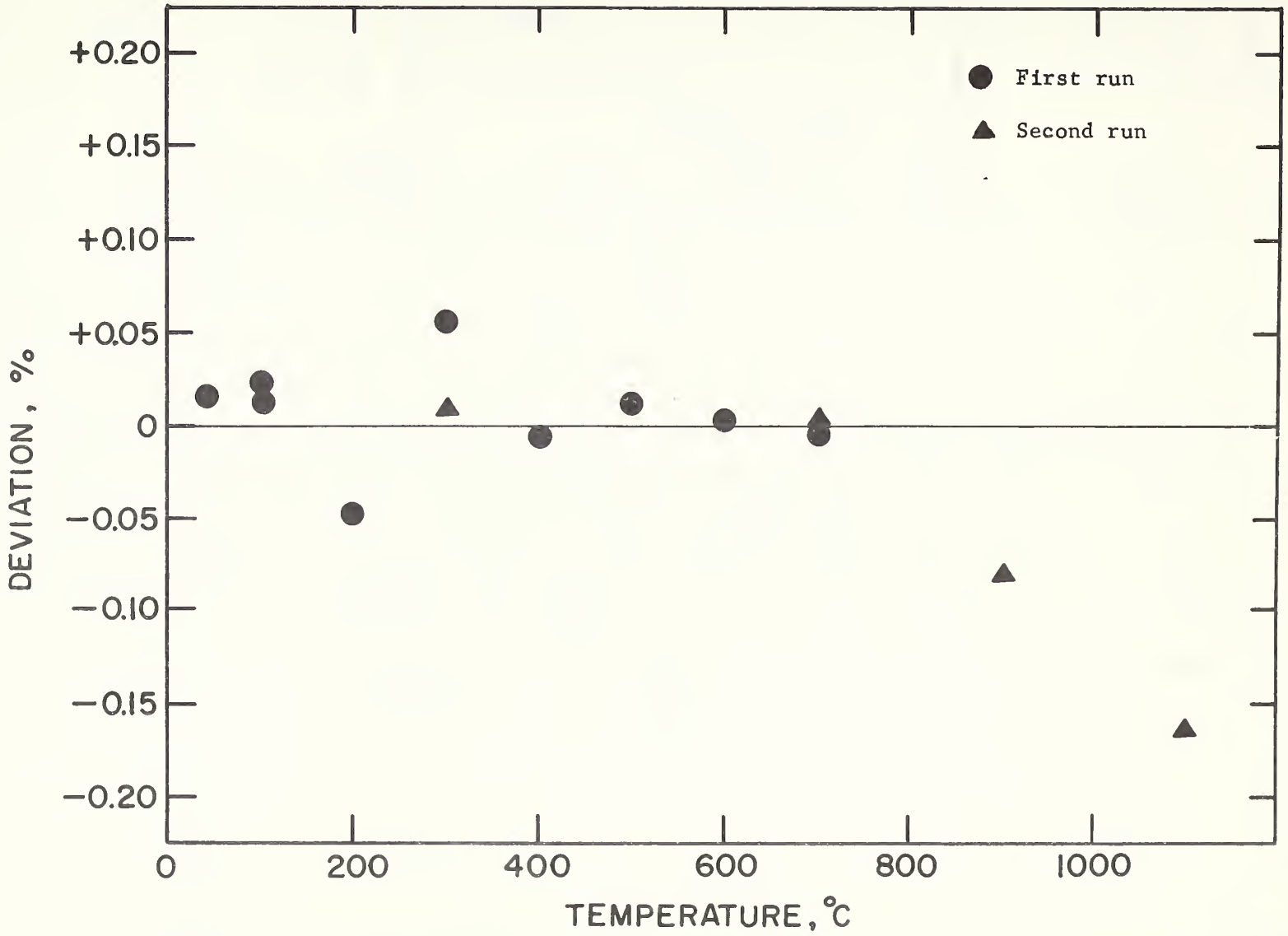

Figure 22. Percentage deviations from equation (7-2) of electrical resistivity data points obtained in the necked-down region of the platinum specimen.

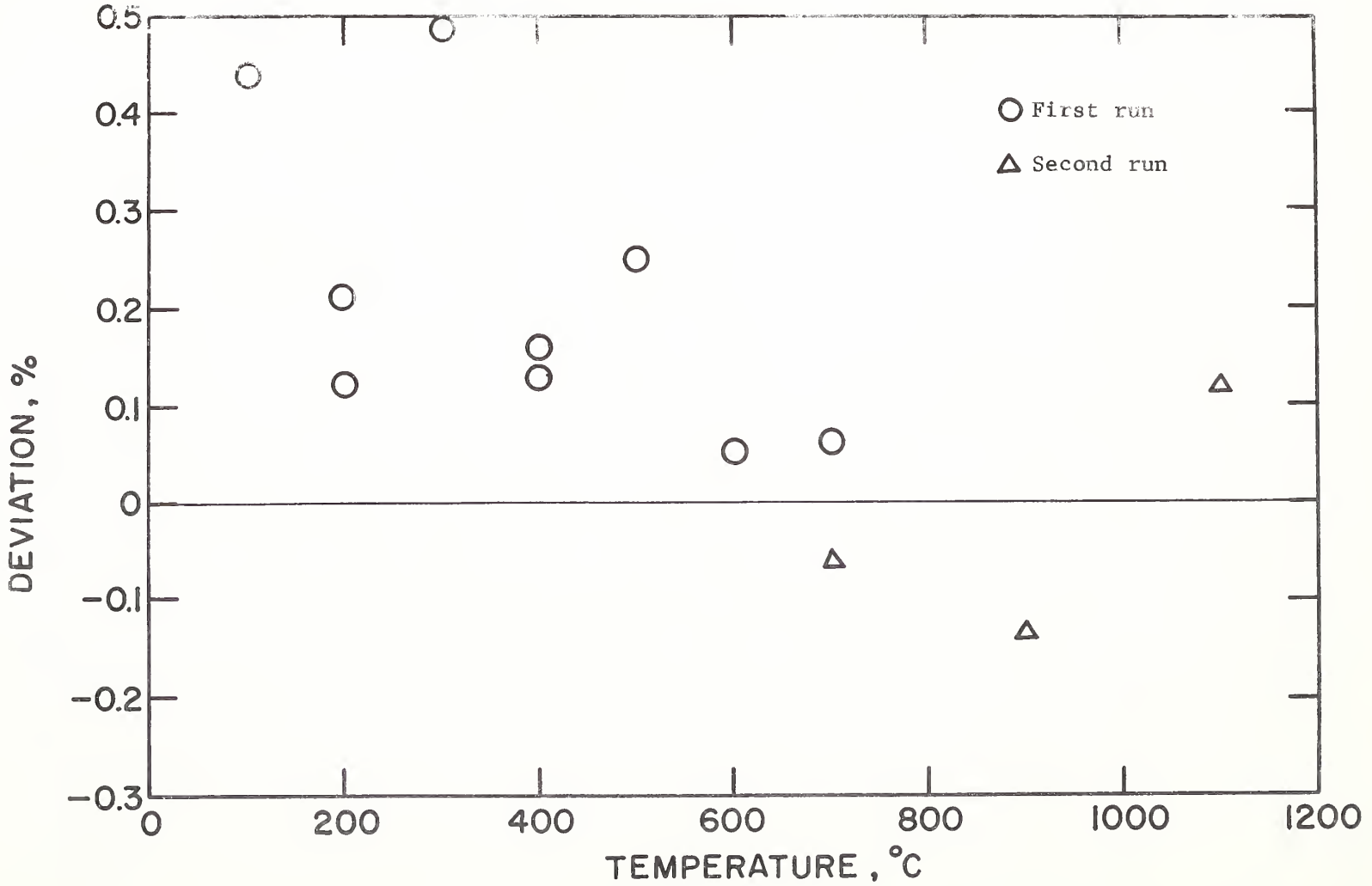

Figure 23. Percentage deviations of electrical resistivity data points obtained in the lower part of the platinum specimen from equation (7-2).

resistance thermometer at the gold point (1063 °C) was about 0.07% below the value obtained by extrapolating the Callendar equation [7] for that thermometer to the gold point. Laubitz [81] in measuring the electrical resistivity of high purity (99.999% pure) platinum found that between 800 and 1200 °C his experimental results fell consistently below the values extrapolated from an equation similar to (7-2) by an average amount of 0.10%.

Values for the electrical resistivity, ρ, and its temperature coefficient $\alpha = \frac{1}{\rho} \cdot \frac{d\rho}{dT}$ used in computing the thermal conductivity by the indirect method were calculated from (7-2) for the first run and from (7-3) for the second run.

Electrical resistivity data were also obtained from measured resistances and dimensions in the lower part of the specimen using the defining equation $\rho = RA/L$, where R is the resistance of a length L of specimen of cross-sectional area A. Measurements of the cross-sectional area are described in Chapter V. The length, L, was the spacing between the potential taps. The Pt legs of the thermocouples were used as potential taps. The thermocouple wires were pressed into slits machined in the specimen. The slits were 8mils wide and the spacing between slits was measured optically prior to installing the thermocouples. Resistances were determined by simultaneous measurements of the current and the voltage drops between locations 4-8, 4-6, and 6-8. (see Figure 12). The average value of the three resistances was used giving the first one twice as much weight as each of the other two. The mean temperature was computed from the five temperatures T_4 through T_8 by Simpson's Rule integration. Values obtained with the current flowing forward and reverse were averaged.

A least-squares parabola fits the resistivity data obtained in the lower part of the specimen with a standard deviation of 0.14%, and the value given by extrapolation of the equation to 0 °C is 9.88 as compared with 9.85

for the measured ice-point resistivity. The values obtained on cooling are consistently lower than those obtained on heating in the first run, and the overall scatter is much greater than that obtained from measurements in the necked-down region. The resistance of the neck was 15 times larger than that of the lower part of the apecimen so that its value could be more accurately determined. Moreover the resistance values determined for the neck represent an extrapolation to zero current whereas the values determined in the lower part of the specimen are based solely on the data for 10A. In view of the above factors the resistivity values determined from the measured resistances in the neck and from the ice point resistivity are considered to be more accurate. A discussion of the accuracy of the resistivity data will ensue in the next Chapter. Departures from the values given by (7-2) of the data obtained in the lower part of the specimen are plotted in Figure 23.

Thermal Conductivity

Direct Method: The experimental values obtained for the thermal conductivity of platinum by the direct method are shown in Table 7. Thermal conductivity values are given both corrected for and uncorrected for thermal expansion (the values discussed below refer to values uncorrected for thermal expansion; corrections can easily be made with the use of equation (4-41)). Values are also given for the effective thermal conductivity of the insulation, these values having been determined by simultaneous solution of the "matched" and "unmatched" gradient tests as described in Chapter IV. A typical set of data is shown in Table 8. In all but the tests at 100°C the temperature gradient was nominally 5°C/cm. In the tests at 100°C the gradient was nominally 2°C/cm. The temperature drop across the necked-down region was always less than 0.1°C and q_n while temperature dependent was always less than 7mW. The heat flow in the current leads, q_a and q_b were

TABLE 7: Experimental values for the thermal conductivity of platinum as determined by the direct method: values both corrected for (k_w) and uncorrected for (k) thermal expansion are given along with values for the thermal conductivity (k_p) of the powder insulation and the temperature gradient (grad.) in the specimen.

T	grad.1/	k_p	k_w	k	Conditions
°C	°C/cm	mW/cm °C	mW/cm °C	mW/cm °C	
99.63	1.85		0.715	0.715	Argon, first run
99.82	1.91		0.715	0.716	Argon, first run
201.72	4.84	0.504	0.721	0.722	Argon, first run
301.01	5.08		0.729	0.730	Argon, first run
400.19	4.96	0.838	0.740	0.743	Argon, first run
501.47	4.94		0.753	0.756	Argon, first run
601.32	5.27	1.256	0.769	0.773	Argon, first run
701.19	4.91		0.784	0.790	Argon, first run
300.03	5.04	0.667	0.729	0.731	Argon, second run
701.32	4.84	1.553	0.786	0.791	Argon, second run
900.04	5.10	2.070	0.822	0.829	Argon, second run
1100.80	5.47		0.857	0.867	Argon, second run
199.64	5.01	1.655	0.721	0.722	Helium, first run
400.61	5.09	2.156	0.740	0.742	Helium, first run

1/ grad. = $\left(\frac{dT}{dz}\right) - \left(\frac{dT}{dz}\right)$

TABLE 8: Typical set of data from measurements of the thermal conductivity by the direct method. The data are from the second test run in argon at 700 °C.

Test:		"Matched" gradient	"Isothermal"	"Unmatched" gradient
Temperature distribution along the specimen - deg C	T_4	682.2	700.1	683.5
	T_5	691.8	700.0	692.3
	T_6	701.3	699.7	701.1
	T_7	710.9	699.6	710.2
	T_8	720.4	699.4	719.3
Temperature gradient at the center of the specimen - deg C/cm	$\frac{dT}{dz}$	4.75	-0.09	4.42
Power generated in the specimen heater - W	P	12.137	0.0	12.133
Heat flow across the necked-down region - W	q_u	-0.005	-0.006	-0.005
Heat flow along the current leads - W	q_a	0.007	0.001	0.009
	q_b	0.0002	0.001	0.008
Heat flow to the insulation - W	q_i	+0.013	+0.038	+0.739
Heat flow along thermocouple wires and insulators - W	q_c	0.045	-0.001	0.042

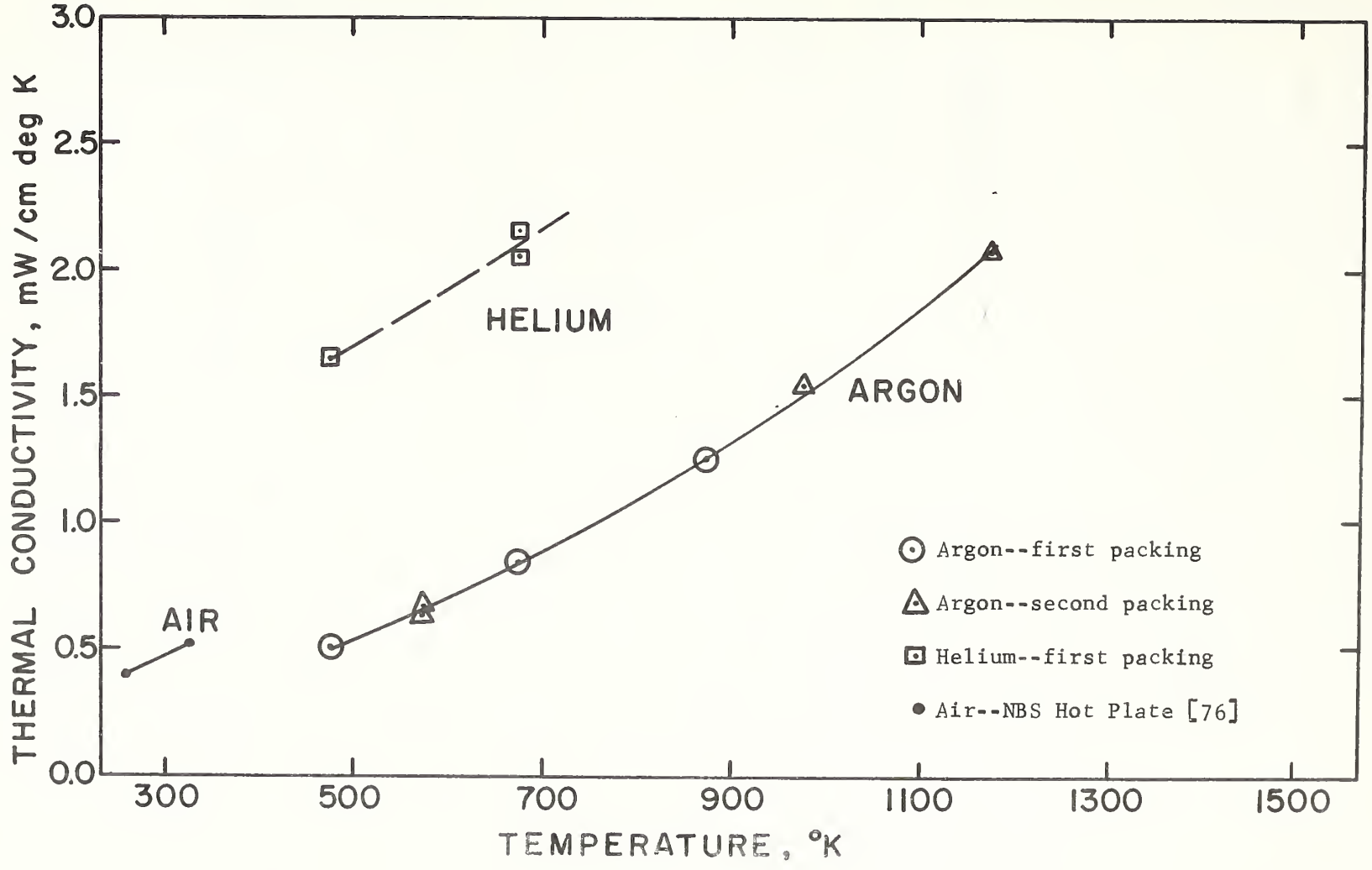

Figure 24. Effective thermal conductivity in argon, helium and air of the powder insulation surrounding the specimen.

always of the same order of magnitude being essentially independent of temperature. The heat flow to the insulation, q_i, being directly proportional to the thermal conductivity of the insulation, had approximately the same temperature dependence as it. The values obtained for the thermal conductivity of the powder insulation in air, in argon and in helium are plotted in Figure 24. The heat flow along the thermocouple wires and the ceramic tubing insulating them should have decreased with increasing temperature as a result of the decrease in the conductance of the ceramic tubing.

A least squares cubic equation was found to fit the thermal conductivity data from the direct method with a standard deviation of 0.08%. This was significantly less than the standard deviation from a parabola. The equation is

$$k = 0.713 + 0.130\times10^{-4}T + 0.175\times10^{-6}T^2 - 0.505\times10^{-10}T^3 \qquad (7\text{-}4)$$

where T is temperature in °C. The corresponding equation in °K is

$$k = 0.723 - 0.936\times10^{-4}T + 0.216\times10^{-6}T^2 - 0.504\times10^{-10}T^3 \qquad (7\text{-}5)$$

Departures of the data points from (7-4) are plotted in Figure 25. With the exception of the point at 1100°C all the data points, including the two obtained in helium fall within ±0.10% of the curve. There are no significant differences between the values obtained on heating and cooling in the first run and none between the values from the first run and those from the second run. At 1100°C the thermocouples started drifting giving rise to significant uncertainties in temperature measurement. After completing the "matched" gradient, "unmatched" gradient and "isothermal" tests at 1100°C a second "matched" gradient test was run. Two values for the thermal conductivity were obtained by simultaneous solution of each of the two "matched" gradient tests with the "isothermal" test. The first value (0.833) was below the value predicted by (7-4) and the second value (0.896) was above it.

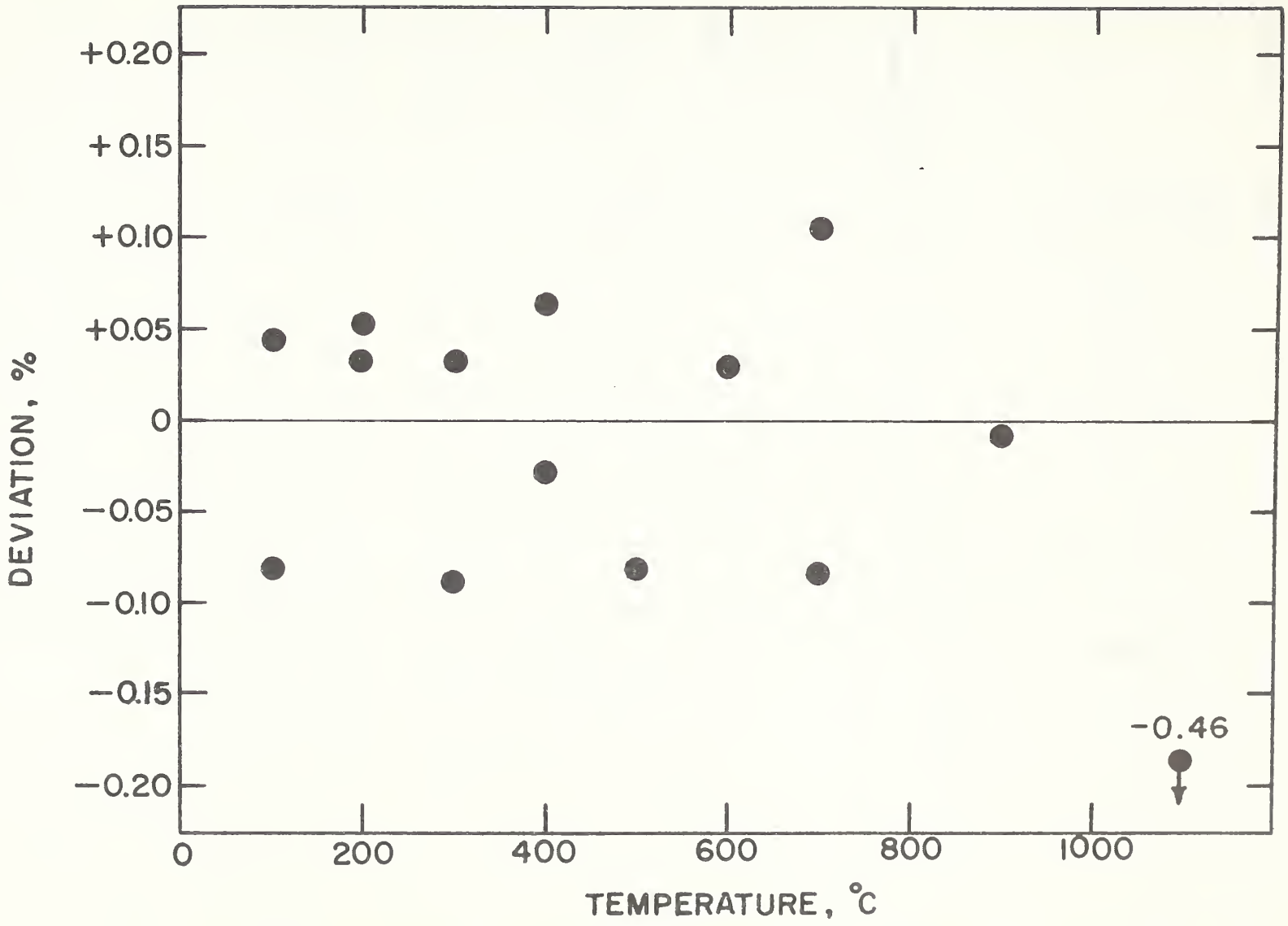

Figure 25. Percentage deviations from equation (7-4) of thermal conductivity data points obtained by the direct method.

Assuming that the temperature drifts were linear with time, interpolation to the time of the "isothermal" test gives a value of 0.867 for the thermal conductivity of the specimen at 1100°C. This value is 0.46% below the value given by extrapolation of (7-4) to 1100°C. The 1100°C point, due to the larger uncertainty associated with its value, was not used in deriving (7-4).

Indirect Method: The experimental values obtained for the thermal conductivity of platinum by the indirect method are given in Table 9 along with some other pertinent data. The values for ρ and α were computed from equations (7-2) in the first run and from (7-3) in the second run. The values given for the maximum temperature rise in the neck are the actual values. The values that would exist in the absence of heat losses are given by (4-22). The values for S show that thermal conductivity values computed on the assumption that the resistance of the neck is related to the maximum temperature in it by $R + R_o(1 + \frac{2}{3}\alpha_o\theta_m)$ would be too high by amounts ranging from 0.36% at 100°C to 2.85% at 900°C. The heat loss correction is seen to vary from 0.24% at 100°C to 1.15% at 900°C, and the Lorenz number varies from 2.63 to 2.78.

A least-squares cubic equation was found to fit the thermal conductivity data obtained in argon from the indirect method with a standard deviation of 0.31 percent, the equation being

$$k = 0.717 - 0.205\times10^{-5}T + 0.193\times10^{-8}T^2 - 0.832\times10^{-10}T^3 \qquad (7\text{-}6)$$

where T is temperature in °C. The 1100°C data point was not used in deriving (7-6) as the indirect test at that temperature was incomplete. The value shown in Table 9 for k at 1100°C is based only on measurements at 10A forward and reverse and 58A forward, and consequently the uncertainty associated with this value is greater. Deviations of the data points from

Table 9. Experimental values for the thermal conductivity of platinum as determined by the indirect method: values both corrected for (k_w) and uncorrected for (k) thermal expansion are given as well as values for the electrical resistivity, ρ, the Lorenz number, L, the heat loss correction factor, C, the maximum temperature rise, θ_m, in the neck with 100A flowing through it and the percentage departure, S, of k from the value that would be obtained on the basis of the assumption that $R = R_o(1 + \frac{2}{3}\alpha_o\theta_m)$.

T	α	β	ρ	θ_m	S	C	k_w	k	ρk	L	Conditions
^oC	deg C^{-1}	deg C^{-1}	$\mu\Omega$-cm	^oC	%	%	W/cm ^oC	W/cm ^oC	$\mu\Omega W/^oC$	$(V/^oC)^2$	air, first run
98.8	0.002764	0.000064	13.68	27.05*	-0.36	0.24	0.720	0.721	9.86	2.643	argon, first run
99.7	0.002765	0.000064	13.68	35.18	-0.52	0.24	0.716	0.716	9.80	2.628	argon, first run
202.0	0.002096	0.000109	17.48	49.30	-0.74	0.33	0.720	0.721	12.61	2.653	argon, first run
299.9	0.001691	0.000151	21.02	59.70	-1.01	0.42	0.732	0.734	15.42	2.691	argon, first run
400.3	0.001403	0.000193	24.53	66.30	-1.26	0.53	0.738	0.740	18.16	2.697	argon, first run
500.1	0.001193	0.000231	27.90	74.34	-1.57	0.65	0.749	0.752	20.98	2.714	argon, first run
599.6	0.001032	0.000267	31.16	80.21	-1.85	0.77	0.763	0.768	23.92	2.741	argon, first run
700.1	0.000903	0.000300	34.33	85.81	-2.15	0.90	0.779	0.784	26.92	2.766	argon, first run
199.9	0.002107	0.000108	17.40	48.64	-0.74	1.05	0.722	0.723	12.73	2.659	helium, first run
400.2	0.001403	0.000193	24.53	65.79	-1.25	1.33	0.745	0.748	18.49	2.724	helium, first run
300.1	0.001695	0.000151	21.03	60.31	-1.02	0.41	0.731	0.733	15.40	2.687	argon, second run
699.9	0.000900	0.000300	34.33	89.15	-2.24	0.88	0.774	0.780	26.76	2.750	argon, second run
900.0	0.000709	0.000357	40.28	100.01	-2.85	1.15	0.804	0.811	32.65	2.783	argon, second run
1098.5	0.000573	0.000401	45.76	- - -	- - -	0.222	- - -	0.869	- - -	- - -	argon, second run

* Corresponding to a current of 85A.

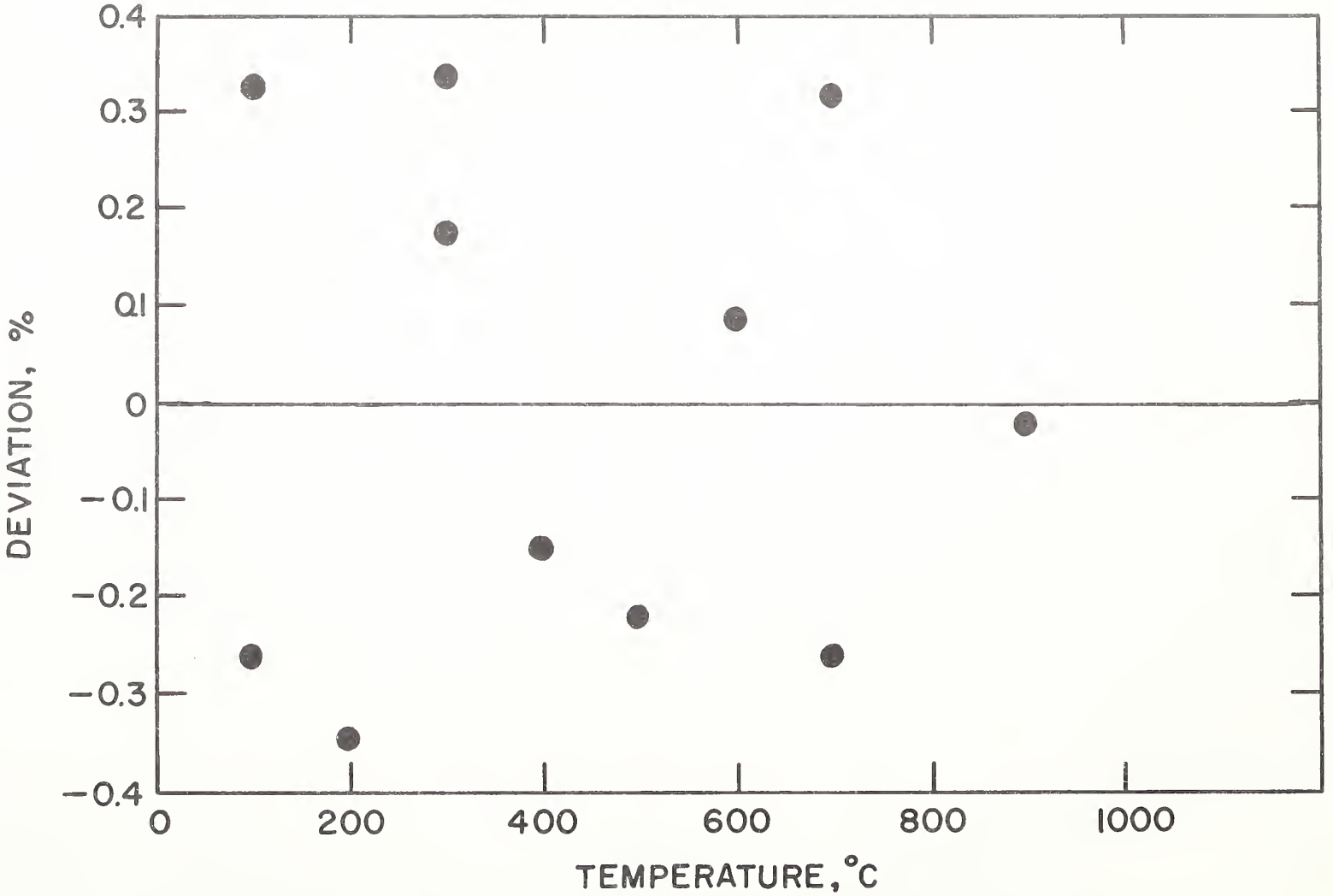

Figure 26. Percentage deviations from equation (7-6) of thermal conductivity data points obtained by the indirect method.

equation (7-6) are plotted in Figure 26 where the scatter in the data is seen to be within ±0.4 percent. The scatter is random and there are no significant differences between values obtained on heating and cooling or between the first run and the second run. The value obtained in helium at 200°C agrees within 0.01% of the value given by (7-6) but the helium point at 400°C shows a deviation of +0.94 percent. The measurements in helium were made during the first run and there is a possibility that the powder insulation did not uniformly and completely fill the necked-down region. If the powder did not completely fill the space the boundary conditions assumed in deriving the heat loss corrections (see Chapter IV, p. 65) would not have been met. Any errors in the heat loss correction would be amplified in helium particularly at the higher temperature due to the high thermal conductivity of this gas. In the second run the powder was carefully packed around the neck so that the necked-down region was completely and uniformly filled with insulation.

CHAPTER VIII

DISCUSSION OF RESULTS

Accuracy

Electrical Resistivity

The electrical resistivity values were computed from

$$\rho = \rho_o \frac{R_r}{(R_r)_o} \tag{8-1}$$

where ρ_o is the independently-measured ice-point resistivity, R_r is the resistance of the necked-down region at zero current, and $(R_r)_o$ is the value of R_r extrapolated to the ice point. The fractional total uncertainty in ρ is given by

$$\left|\frac{\Delta\rho}{\rho}\right| = \left|\frac{\Delta\rho_o}{\rho_o}\right| + \left|\frac{\Delta R_r}{R_r} - \frac{\Delta(R_r)_o}{(R_r)_o}\right| , \tag{8-2}$$

where $|\Delta\rho_o/\rho_o|$ is the fractional uncertainty in the ice-point resistivity. The quantities ΔR_r and $\Delta(R_r)_o$ appear inside the same absolute value sign since they are correlated quantities rather than being independent.

The uncertainty in ρ_o was not more than 0.1%. The uncertainties in the measured values of R_r did not exceed 0.05%. However, an additional uncertainty must be assigned to the values of R_r due to the uncertainty in the temperature to which these values correspond. Quite conservatively, temperatures were known to within 0.5°C, corresponding to 0.14% of R_r at 100°C and 0.04% at 900°C. The uncertainty in $(R_r)_o$, which is based on an extrapolation, is estimated to be less than 0.25%. Values of ΔR_r corresponding to the lower temperatures are correlated with $\Delta(R_r)_o$ so that these quantities tend to cancel at lower temperatures but not necessarily at higher temperatures. The overall uncertainty in electrical resistivity is estimated as $\left|\frac{\Delta\rho}{\rho}\right| < 0.10\%$ at 0°C and $\left|\frac{\Delta\rho}{\rho}\right| < 0.44\%$ at 900°C.

Thermal Conductivity

Direct Method: The thermal conductivity values were computed from the relation

$$k_r = \frac{-(Q - Q')}{A[(dT/dz) - (dT/dz)']} \quad , \tag{4-40}$$

as discussed in Chapter IV. The fractional total uncertainty in k_r is given by

$$\left|\frac{\Delta k_r}{k_r}\right| = \left|\frac{\Delta(Q - Q')}{(Q - Q')}\right| + \left|\frac{\Delta A}{A}\right| + \left|\frac{\Delta[(dT/dz) - (dT/dz)']}{[(dT/dz) - (dT/dz)']}\right| \tag{8-3}$$

where $|\Delta A/A|$ is the fractional uncertainty in area, etc. We now consider each of the terms in (8-3) individually.

Heat Flow: From (4-42) we write

$$\frac{\Delta(Q-Q')}{(Q-Q')} = \frac{\Delta(P-P')-\Delta(q_a-q_a')-\Delta(q_b-q_b')-\Delta(q_n-q_n')-\Delta(q_i-q_i')-\Delta(q_c-q_c')}{(P-P')-(q_a-q_a')-(q_b-q_b')-(q_n-q_n')-(q_i-q_i')-(q_c-q_c')} \cdot \tag{8-4}$$

For purposes of error analysis, we can neglect the correction terms in the denominator of (8-4); furthermore, for our tests P'=0 ("isothermal" test) and we can write

$$\left|\frac{\Delta(Q-Q')}{(Q-Q')}\right| \approx \left|\frac{\Delta P}{P}\right| + \frac{|\Delta(q_a-q_a')| + |\Delta(q_b-q_b')| + |\Delta(q_n-q_n')| + |\Delta(q_i-q_i')| + |\Delta(q_c-q_c')|}{P} \tag{8-5}$$

The following error estimates are based on the value of P necessary to maintain a temperature gradient of 5°C/cm in the specimen.

The potentiometer, voltbox, and shunt box were each calibrated to 0.01 percent or better. The emf of the standard cell was known to 0.01 percent or better. The correction terms in (4-43) for the voltage drop in the potential leads and for the current through the voltbox were small (a few tenths

of a percent) and uncertainties in these corrections could not have introduced more than 0.01 percent additional error in P. Thus the percentage uncertainity in the measured power input was $|\Delta P/P| < 0.05\%$.

The corrections $(q_a - q_a')$ and $(q_b - q_b')$ for heat flow along the current leads were each about 0.05 percent or less of P. The derivation of (4-44), the equation used to compute q_a and q_b was based on the assumption that there was no heat flow from the leads into the powder insulation. If the leads were at the same temperature as the specimen at the point where they enter the specimen, the assumption of no heat loss from the leads would be a good assumption. Preliminary tests with the same style of heater as the specimen heater had shown that the mean temperature of the heater winding would be significantly higher than that of the adjacent specimen material. In order to minimize the corresponding temperature rise in the current leads, swaged elements of relatively low electrical resistance were installed (see Chapter II, p. 39) for the purpose of tempering, or thermally grounding, the leads.

In Appendix I it is shown that the tempering attained by these elements was sufficiently good to limit heat losses out the current leads to 0.05% of P. The corrections q_a and q_b probably compensate for much of this, but to cover the case where they don't an uncertainty of 0.05% due to heat flow out each current lead is adopted. This uncertainty, it should be noted, would always be a heat loss and not a gain and hence must be added to the root-mean-square of the other uncertainties which have approximately equal probability of being either positive or negative.

The correction $(q_n - q_n')$ for heat flow across the necked-down region of the specimen was always less than 0.05% of P. Errors in the temperature drop across the neck due to possible inhomogenieties in the thermocouple

leads or to stray thermal emfs would, for the most part, cancel since they were common to q_n and q_n'. At 300°C a series of tests were run in which the temperature drop across the neck was held in turn at about -5°C, 0°C, and +5°C, a range 20 times larger than that which occurred during normal measurements. The corresponding values for (q_n-q_n') were about +1%, 0%, and -1%, respectively, of P. The three thermal conductivity values obtained using (4-45) to effect the correction for heat flow across the neck, fell within a range of less than ±0.02%. For normal tests, in which the temperature difference across the necked-down region was maintained quite small, it is felt that $|\Delta(q_n-q_n')/P| < 0.02\%$.

The correction (q_c-q_c') for shunting of heat by the thermocouples and ceramic tubing was rather large, falling from about 0.8% at 100°C to 0.3% at 1100°C, this falloff being due to the rapidly decreasing thermal conductivity of the ceramic tubing. Although the thermal conductivity of the thermocouple wires were known fairly accurately (5%) the thermal conductivity of the ceramic tubing was known only approximately (15%). Furthermore, the cross-sectional areas of the wires and tubing were not accurately known (5%). Thus the total conductance of the wires and the ceramic tubing was only known to about 25%. This implies $|\Delta(q_c-q_c')/P| < 0.20\%$ at 100°C and $<0.08\%$ at 1100°C.

The correction (q_i-q_i') for heat exchange with the powder insulation was potentially a large source of error and considerable effort was expended to, first, keep this correction small and, second, evaluate it accurately. Evaluation of this correction as seen from (4-50) requires a knowledge of the integral, $D(z_1, z_2)$, and of the thermal conductivity, k_r, of the insulation.

Numerous factors could adversely effect the determination of $D(z_1, z_2)$. The use of logarithmic functions to define the radial temperature distribution across the ends of the hollow cylinder of insulation is an approximation. However, an argument similar to that developed in Appendix B shows that the potential distribution near the specimen is not affected by the boundary conditions at the remote ends of the extensions. The details of the actual temperature distributions in the heater regions where smoothing cubics are used could conceivably influence $D(z_1, z_2)$ (see Chapter IV, pp. 79-82). Any such effects should be small, involving as they do only second and higher order derivatives. Furthermore, except for the regions of Q_2 and Q_5 such effects should be about the same in the gradient and in the isothermal tests. In the mathematical analysis it is assumed that the temperatures on the inner surface of the guard are the same as the temperatures measured on the outer surface. The molybdenum guard has high thermal conductivity so that any radial temperature gradients in the guard would be small and the associated errors would tend to cancel on simultaneous solution. Angular variations in the temperature distribution on the guard could arise if the specimen and guard were not concentric or if the insulation between the specimen and the guard was not packed uniformly. Great care was taken to avoid both of these conditions. Any angular variations would be approximately the same for two tests at the same mean temperature and so the associated errors would in large part cancel under simultaneous solution. Such would not be the case for errors arising from uncertainties in the longitudinal positions of the thermocouples since the temperature distribution along the guard cylinder in the gradient test differs from that in the isothermal test. The necessary steps were taken to ensure that the longitudinal position of the guard was accurately known relative to that of the specimen, and the location of thermocouple slits both on the guard and

on the specimen assembly were measured accurately prior to installation of the thermocouples.

As discussed in Chapter IV, the effective thermal conductivity of the powder insulation was determined in place by making measurements with the guard unmatched. The values thus obtained are shown in Fig. 24 . The precision of the data is quite good, especially considering that they were obtained essentially as a by-product. The data labeled "air" were obtained [82] on the NBS guarded hot plate apparatus on a sample of alumina powder from the same lot and packed to about the same density.

If there was a significant heat exchange between the specimen and the insulation that was not being adequately corrected for, one would expect a systematic difference between the values obtained for the thermal conductivity of the specimen in helium and those obtained in argon, due to the large difference between the thermal conductivity of the powder in the different atmospheres. In fact, however, the values measured in helium fell within the scatter band of those measured in argon indicating that any uncorrected heat exchanges were certainly less than 0.2%, the width of the scatter band.

For all sets of tests $| q_i - q_i' | < 0.1\%$ of P. It is felt that $D(z_1, z_2)$ and $\hbar_r$ were each known to better than 10%, and hence $| \Delta(q_i - q_i') | / P < 0.02\%$. However, in view of all the factors which conceivably could influence this correction, an uncertainty of $| \Delta(q_i - q_i') | / P < 0.10\%$ is assigned.

The ratio of heat absorbed (or released) to that conducted in the specimen is given approximately by

$$\frac{wcAL(dT/dt)}{kA(dT/dz)} = \frac{L}{\kappa} \frac{(dT/dt)}{(dT/dz)} \qquad (8\text{-}6)$$

where w is density, c is specific heat, A is area, L is total length of specimen below necked-down region, dT/dt is time rate of temperature change, k is thermal conductivity, dT/dz is temperature gradient, and $\varkappa = k/wC$ is thermal diffusivity. Temperatures in the system did not drift at a rate greater than 0.03°C/hr (i.e., 10^{-5}°C/sec); the length, L, was about 14cm; the temperature gradient was 5°C/cm; and the thermal diffusivity of platinum in the temperature range 0-1100°C is always greater than 0.2cm²/sec [83]. Hence the ratio of heat absorbed (or released) to that conducted was less than ±0.02%.

The above uncertainties in heat flow sum to an estimated maximum uncertainity in (Q-Q') of 0.49 percent at 100°C and 0.37 percent at 1100°C, with an estimated probable uncertainty (i.e., root-mean-square) of 0.33 percent at 100°C and 0.24 percent at 1100°C.

Area: The cross sectional area of the specimen at room temperature is believed to have been known to within ±0.02% (see Chapter V, pp. 89-90)

Temperature Gradient: The separations between the slits in which the thermocouples were located were measured with an uncertainty much less than the half-width of the slits so that the effective position of a thermocouple in a slit was the controlling factor in the uncertainty of thermocouple separations. In determining the temperature gradient at the center of the specimen a least-squares parabola was fitted to the five temperatures. However, the temperature distribution was almost linear, and for the purpose of error analysis, it can be assumed that it was. For five thermocouples evenly spaced at points a distance ℓ apart, each with an uncertainty $|\Delta\ell|$ in position, the maximum error in the slope of a straight line through these points due to the uncertainties in their positions is $\frac{2}{3}\frac{|\Delta\ell|}{\ell}$.

The thermocouples were spaced 2cm apart and $|\Delta\ell| < 0.01$ cm so that the maximum possible uncertainty in the slope is 0.33 percent. A value of 0.01cm is considered to be an extremely conservative estimate of $|\Delta\ell|$ since it implies that the effective position of a thermocouple coincides with the edge of the groove in which it is located. A more probable uncertainty in the gradient due to uncertainties in effective thermocouple positions is 0.2 percent.

As mentioned in Chapter IV, the simultaneous solution of a gradient and an isothermal test largely eliminates the effects of variations between the calibrations of individual thermocouples. All that is required is that the slope of the temperature versus emf curve be the same for the different thermocouples. Evidence indicating the fulfillment of this requirement is provided by the fact that during an "isothermal" test the thermocouple readings all agreed quite closely. For example, at 900°C the temperatures indicated by the five thermocouples in the lower part of the specimen were within 0.1°C of each other or within 0.01% of the temperature. These differences of 0.1°C or less should have been compensated for to better than 0.01°C by the simultaneous solution of the two tests. It is estimated that the conversion of thermocouple emfs to temperatures introduced uncertainties of less than 0.2% of the 40°C temperature drop in the specimen. The errors in reading the emf differences did not introduce an uncertainty of more than 0.05% (for a 40°C drop). As discussed in Appendix G, errors due to heat conduction along thermocouple leads should have been negligible and were certainly less than 0.05%.

The estimated maximum uncertainty in the temperature gradient is 0.59% and the estimated probable uncertainty is 0.29%.

In addition to the above uncertainties, all of which are associated with (4-40), there is the uncertainty in the temperatures to which the thermal conductivity values correspond. For a 0.5°C uncertainty in temperature, the associated uncertainty in thermal conductivity is less than 0.001% at 100°C and less than 0.02% at 900°C.

Summarizing all of the above uncertainty, the estimated maximum uncertainty in the thermal conductivity values from the direct method is $|\Delta k_r/k_r| < 1.10\%$ at 100°C and $< 1.00\%$ at 900°C. The estimated probable uncertainties (i.e., r.m.s. value) are 0.44% at 100°C and 0.38% at 900°C.

Indirect Method: In the indirect method, the thermal conductivity values were computed from

$$k_r = \frac{1}{1+C} \frac{\alpha_r R_r}{12\rho_r} \frac{dV^{*2}}{dR^*} \quad . \tag{4-32}$$

as discussed in Chapter IV. The fractional total uncertainty in k_r is given by

$$\left|\frac{\Delta k_r}{k_r}\right| = \left|\frac{\Delta C}{1+C}\right| + \left|\frac{\Delta \alpha_r}{\alpha_r}\right| + \left|\frac{\Delta (R_r/\rho_r)}{R_r/\rho_r}\right| + \left|\frac{\Delta (dV^{*2}/dR^*)}{(dV^{*2}/dR^*)}\right| \quad . \tag{8-7}$$

The uncertainty in the sensitivity, α_r, of the specimen as a resistance thermometer is essentially the uncertainty in the sensitivity of the thermocouples used plus a small uncertainty in the resistance measurements and the thermocouple emf measurements. That this is so is seen by considering that we measure R_r as a function, say $R_r = f(E)$, of the thermocouple emf, E. Then

$$\alpha_r = \frac{1}{R_r}\frac{dR_r}{dT} = \frac{1}{f(E)} \frac{df(E)}{dE}\frac{dE}{dT} \equiv g(E)\frac{dE}{dT} \quad , \tag{8-8}$$

and $$\left|\frac{\Delta\alpha_r}{\alpha_r}\right| = \left|\frac{\Delta(dE/dT)}{dE/dT}\right| + \left|\frac{\Delta(g(E))}{g(E)}\right| \quad . \tag{8-9}$$

The uncertainty in dE/dT is estimated to be less than 0.20% while the uncertainty in the resistance and voltage measurements is less than 0.05%, so that $|\Delta\alpha_r/\alpha_r| < 0.25\%$.

The quantity R_r/ρ_r is uncertain only by the scatter in the individual R_r points around a smoothed curve, since ρ_r was derived by smoothing the R_r values. Therefore $|\Delta(R_r/\rho_r)/(R_r/\rho_r)| < 0.05\%$.

The voltage drop across the neck and the resistance of the neck were each measured with an uncertainty of about 0.02%. The change in the resistance of the neck for the different current levels was small compared to the resistance itself, so that any error in measuring resistance would be greatly magnified in computing the rate of change of resistance as a function of the voltage drop. For all of the data taken, the departures of the R* values from the least-squares straight line fitted to the R* and V^{*3} values were less than 0.01% and for a majority of the tests they were less than 0.005%. However, since $(R-R_r) \ll R$, the small scatter in R is highly magnified in calculating dV^{*3}/dR^*. What departures did exist tended to be systematic rather than random and tended to indicate that the plot of R* vs V^{*2} was very slightly concave downward rather than linear, as assumed. Such an effect could possibly be due to neglecting higher order terms in the temperature dependence of the thermal conductivity and the electrical resistivity. As a result of these departures there was an uncertainty in dV^{*2}/dR^* that is estimated to be $|\Delta(dV^{*2}/dR^*)/(dV^{*2}/dR^*)| < 1.50\%$.

In evaluating the correction, C, for heat loss from the neck it was assumed that the boundaries $z = \pm\ell$ and $r = b$ (see Figure 18) were isothermal whereas in fact they were not. Moreover, while the correction accounts for

the cooling of the neck by heat losses through the powder insulation, it does not account for the fact that some of the heat lost from the neck goes back to the specimen through the surfaces $z = \pm\ell$ thereby heating the specimen at $|z| > \ell$. The replacement of (4-16) by (4-17) does not introduce an error of more than 10% in C. The thermal conductivity of the powder insulation surrounding the neck was assumed to be the same as that determined from the tests by the direct method. However, the packing of the powder insulation around the necked-down region, especially during the first run, may have led to a different density, and therefore a somewhat different thermal conductivity, than that in the region between the specimen and the guard. All in all, the uncertainty in C may have been as large as 50% of C. For the tests in argon this corresponds to $|\Delta C/(1+C)| < 0.12\%$ at 100°C and $< 0.55\%$ at 900°C. For the tests in helium $|\Delta C/(1+C)| < 0.53\%$ at 200°C and $< 0.66\%$ at 900°C

The above-mentioned uncertainties, associated with (4-32), lead to an estimated maximum uncertainty in k_r due to systematic errors of $|\Delta k_r/k_r| <$ 1.92% at 100°C and $< 2.35\%$ at 900°C, in argon, and estimated probable uncertainties of $< 1.78\%$ at 100°C and $< 2.11\%$ at 900°C.

In the derivation of the mathematical expressions used to compute thermal conductivity in the indirect method, there were a number of explicit or implicit assumptions made which could lead to erroneous results if these assumptions were not valid.

It was shown in Chapter III (pp. 57-58) and in Appendix C that the Thomson effect cancels out to first order provided the temperatures at the two potential taps (used to measure V) are approximately the same. The requirement that the potential taps be at the same temperature is also necessary for the Fermi energy and Seebeck emf terms in (3-50) to drop out.

In all of our measurements, the temperatures at the inner potential taps (10-11) agreed within 0.2°C or better, as compared to values of θ_m (for 100A current) ranging from 35°C at 100°C to 100°C at the highest temperatures. The integral term involving the Seebeck emf in (3-50) reduces to $(T_2 - T_1)S^{abs}$, provided $(T_2 - T_1)$ is much less than the absolute temperature. For $(T_2 - T_1) < 0.2°C$, $(T_2 - T_1)S^{abs}$ is less than $2\mu V$ at 100°C and less than $5\mu V$ at 1100°C as compared with an IR drop in the necked-down region of $5 \times 10^3 \mu V$ at 100°C and $2 \times 10^3 \mu V$ at 1100°C for a current of 10A, the worst case. Thus, neglecting the Seebeck term in (3-50) involved an error of less than 0.05%.

We can make an order of magnitude estimate of the term in (3-50) involving the Fermi energy by considering a metal with free electrons obeying Fermi-Dirac statistics, for which [84, p. 16]

$$\zeta = \zeta_o - \frac{\pi^2 k^2 T^e}{12\zeta_o} \quad . \quad . \quad . \quad , \tag{8-10}$$

where ζ_o is the value of the Fermi energy (chemical potential) at absolute zero and k is the Boltzmann constant. Thus

$$\frac{1}{e}(\zeta_2 - \zeta_1) = \frac{\pi^2 k^2}{12e\zeta_o}(T_1^2 - T_2^2)$$

$$= \frac{\pi^2 k^2 T}{6e\zeta_o}(T_1 - T_2) \quad , \tag{8-11}$$

for small values of $(T_1 - T_2)$. For platinum ζ_o/k is probably greater than 10,000°K [84, p. 277] so that $\frac{1}{e}(\zeta_2 - \zeta_1) < 2\mu V$ at 100°C and $< 4\mu V$ at 1100°C. Thus this term is comparable with the Seebeck terms and involves an error of less than 0.05%.

It is explicitly assumed in Chapter III that we are dealing with a homogeneous and isotropic medium; this should be a valid assumption for pure

platinum.

As stated on p. 51, we are considering the electron current to be the only mass current. In principle it would be possible for platinum, or any impurities which might be present, to migrate under the influence of the electric potential gradient (electromigration) or under the influence of the temperature gradient (Soret effect). If such mass motion existed there would be an associated entropy flow and equation (3-4) and all following equations in Chapter III would have to be modified to include a term involving the mass current density and its associated entropy transport. A rigorous analysis including mass migration would be quite complex and was felt to be beyond the scope of the present investigation. We can, however, give a qualitative discussion of the probable effect of such mass motion if it were to occur.

In electromigration, the energy flow is proportional to the electric field [71]. Similarly, the energy flow due to the Thomson effect is essentially proportional to the electric field. Thus if one were to introduce an electromigration term into (3-4) and rigorously go through the analysis, the equivalent expression to (3-31) would include an electromigration term of a form analogous to (i.e., proportional to the electric field) the term in (3-31) involving the Thomson coefficient. Provided this term were small compared with the first two terms in (3-35) it would, to first order, cancel in a similar manner to the way the Thomson term cancelled, provided the temperature at the two potential taps were the same and the medium was homogeneous and isotropic. Physically what happens is that the energy transport due to electromigration adds to the energy transport by conduction on one side of the surface of maximum temperature (S_m in Figure 17) and subtracts on the other side, with no net effect on the maximum temperature

rise in the conductor or on the voltage drop between the potential taps, at least to first order. To reemphasize, the temperatures at the taps must be the same for this cancellation to occur and also the medium must be homogeneous and isotropic.

In the Soret effect, the energy transport is proportional to the temperature gradient. Thus the ratio of energy transport due to the Soret effect to that due to heat conduction by other mechanisms is independent of the temperature gradient. The Soret effect is a diffusion process, similar to heat conduction. For a homogeneous medium, therefore, the Soret effect simply behaves as an additional mechanism for "heat conduction" and thus is a legitimate augmentation (or depletion, depending on the sign of the heat of transport) of the thermal conductivity and should be included in the total thermal conductivity value.

For the conditions of our experiments, there would be no errors involved due to electromigration or Soret effect provided the medium remained homogeneous and isotropic. Both of these effects can change the distribution of impurities and vacancies in a solid. In our experiments the current was in one direction through the specimen about one-half of the time and in the other direction about one-half of the time. Thus, it is doubtful if there was significant inhomogenity introduced due to electromigration effects, even if they were occurring in our temperature range. The Soret effect, if large enough, could cause a redistribution of impurities in the specimen.

For platinum of the purity we used, the thermal conductivity at high temperatures would not be expected to be significantly affected by changes in the impurity and vacancy distribution. All of the data at low temperatures, where impurity concentration could affect the thermal conductivity, were taken before the specimen was heated to temperatures where significant

mass migration was likely to occur. In view of the above discussion it is felt that neither electromigration nor Soret effect had any adverse effect on the results.

Comparison with Other Investigations

Electrical Resistivity

Smoothed values for the electrical resistivity of platinum based on equations (7-2) and (7-3) are compared with the values of Roeser [85] and Laubitz [81] in Table 10.

Table 10. Comparison of smoothed resistivity values for platinum with those of Roeser [85] and Laubitz [81].

Investigation	Roeser	Laubitz	Present		
T, °C	ρ_R	ρ_L	ρ	$\rho-\rho_R$	$\rho-\rho_L$
0	9.83	9.82	9.85	0.02	0.03
100	13.68	13.67	13.69	0.01	0.02
200	17.43	17.41	17.41	-0.02	0.00
300	21.06	21.04	21.02	-0.04	-0.02
400	24.57	24.54	24.52	-0.05	-0.02
500	27.96	27.94	27.90	-0.06	-0.04
600	31.24	31.22	31.17	-0.07	-0.05
700	34.40	34.38	34.33	-0.07	-0.05
800	37.44	37.43	37.38	-0.06	-0.05
900	40.38	40.36	40.28	-0.10	-0.08
1000	43.21	43.18	43.07	-0.14	-0.11
1100	45.93	45.98	45.78	-0.15	-0.20

Roeser probably used resistance thermometry grade (99.999) platinum and Laubitz used platinum that was 99.999% pure. The platinum used in the present investigation was only 99.98% pure and its resistivity would be expected to be higher than the values reported by Roeser and Laubitz. The resistance ratio $R_{273.2°K}/R_{4°K}$ of Laubitz's platinum was 1890 so that the residual resistivity was 9.82/1890 = 0.005μΩcm. The resistance ratio of the platinum used in the present investigation was 390 so that the residual resistivity was 9.85/390 = 0.025μΩcm. Thus on the basis of Matthiessen's rule, according to which the ideal and residual resistivities are additive, one would expect the values obtained in the present investigation to be higher than those of Laubitz by the constant amount of 0.02μΩcm. As can be seen in Table 10 the converse is true with the present investigation giving values lower than those of Laubitz. Laubitz reports an estimated error of ±0.3% and the estimated uncertainties in the present work range from 0.1% at 0°C to 0.44% at 900°C so that differences between the two sets of data fall well within the estimated limits of experimental error.

Thermal Conductivity

Values for the thermal conductivity of platinum based on equations (7-4) and (7-6) are compared with the smoothed values of Watson and Flynn [76] and Halpern and Flynn [86,A] in Table 11. The measurements by Watson and Flynn were made on the bar from which the specimen for the present investigation was machined. The measurements by Halpern and Flynn were made on a sample cut from the same bar. Watson and Flynn made their measurements in air in the NBS Metals Apparatus [87] which is a longitudinal heat flow apparatus. Halpern and Flynn conducted their measurements in vacuum in the NBS Low Temperature Apparatus [88] which is also a longitudinal apparatus.

While these two methods are in principal the same as the direct method of the present investigation the experimental variations and differences in analysis make each of the methods unique. Thus the values in Table 11 for the thermal conductivity of platinum represent values obtained by four different methods.

Table 11. Thermal conductivity of platinum: values are given for the thermal conductivity as determined by the direct method and the indirect method; the values of Watson and Flynn determined on the bar from which the specimen was machined, and those of Halpern and Flynn, determined on a sample cut from the same bar, are also shown.

T °C	Watson & Flynn	Halpern & Flynn	Present Investigation Direct Method	Indirect Method
-150	0.712	0.729		
-100	0.711	0.719		
- 50	0.710	0.714		
0	0.711	0.712	0.713*	0.717*
50	0.712	0.714	0.714*	0.717*
100	0.714		0.716	0.718
200	0.720		0.722	0.723
300	0.729		0.731	0.731
400	0.742		0.743	0.741
500	0.758		0.756	0.754
600	0.777		0.772	0.767
700	0.799		0.790	0.781
800	0.825		0.809	0.796
900			0.829	0.811
1000			0.850	0.825
1100			0.871*	0.838*

* Extrapolated values.

The values from the present investigation extrapolated to 50°C agree with each other and with the results of the other two investigations to within 0.7%. The values given by the indirect method are slightly higher (0.3%) than those given by the direct method at 100°C and are lower by 2.2% at 900°C. As shown above the estimated probable uncertainty in the direct method ranges from 0.44% at 100°C to 0.38% at 900°C while the estimated probable uncertainty in the indirect method ranges from 1.42% at 100°C to 1.85% at 900°C. The results of the two methods are thus seen to agree within the combined estimated uncertainties of the two methods.

The results of the indirect method agree with those obtained in the NBS Metals Apparatus to within 0.3% from 100 to 500°C. Above 500°C the results of Watson and Flynn shown a greater increase of thermal conductivity with temperature, the value at 800°C being higher by 1.7% than that given by the direct method. This value is still well within the combined estimated uncertainties of the two methods.

Values for the thermal conductivity of platinum given by the direct method are compared with those of other investigators in Figures 27 and 28. At the higher temperatures the results of the present investigation show the same slope as those of Martin, Sidles and Danielson [83] and Holm and Störmer [14]. The value at 1100°K is 3% higher than that of Martin, Sidles and Danielson. Values reported by Laubitz [101] for the thermal conductivity of platinum are not shown in Figure 27 but they agree within experimental error with those of present investigation.

The values given by the direct method at lower temperatures are confirmed by the results of Watson and Flynn and those of Halpern and Flynn [86, A]. They are also in good agreement with the results of Bode [41],

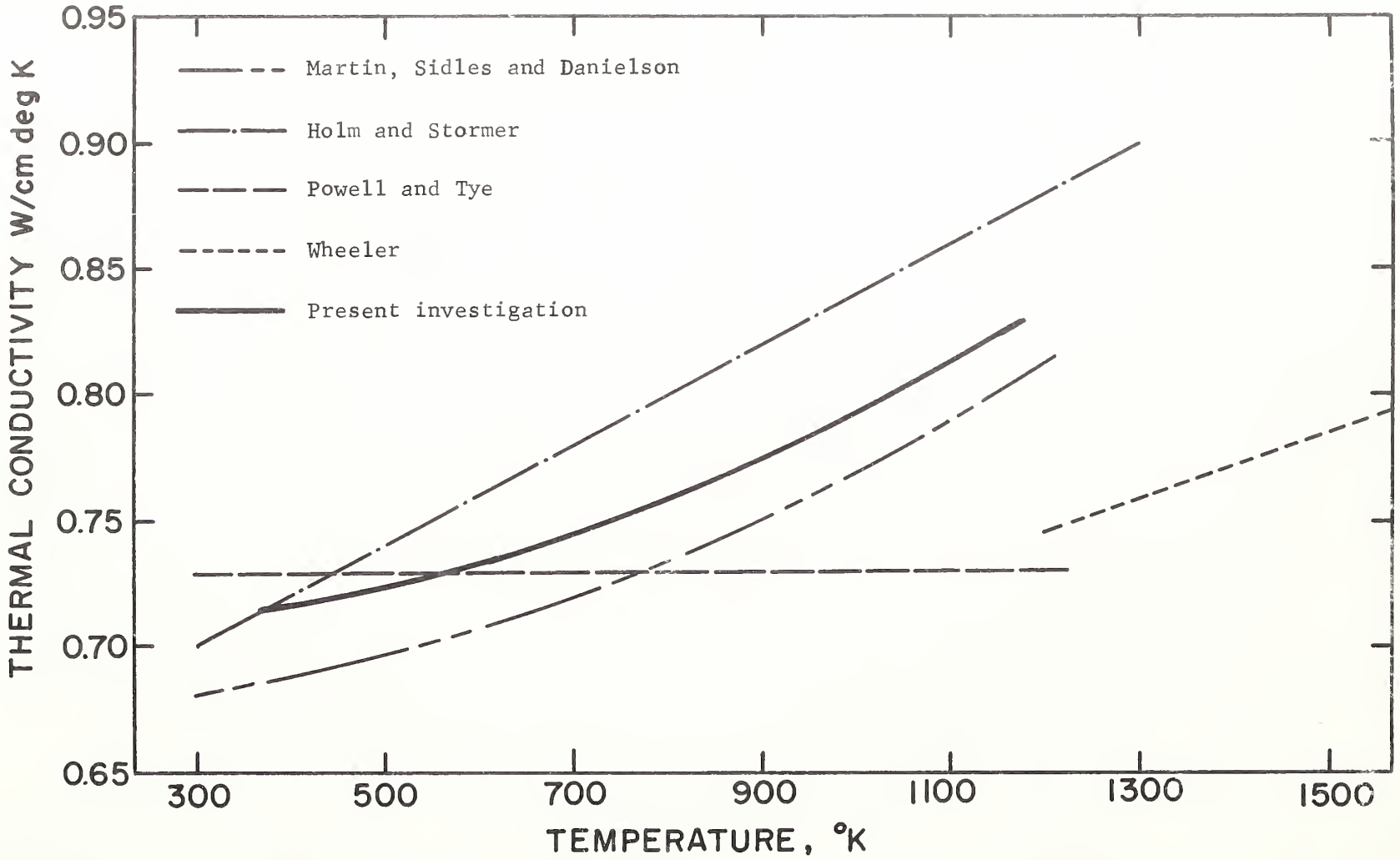

Figure 27. Thermal conductivity of platinum: comparison between existing high temperature data and those of the present investigation.

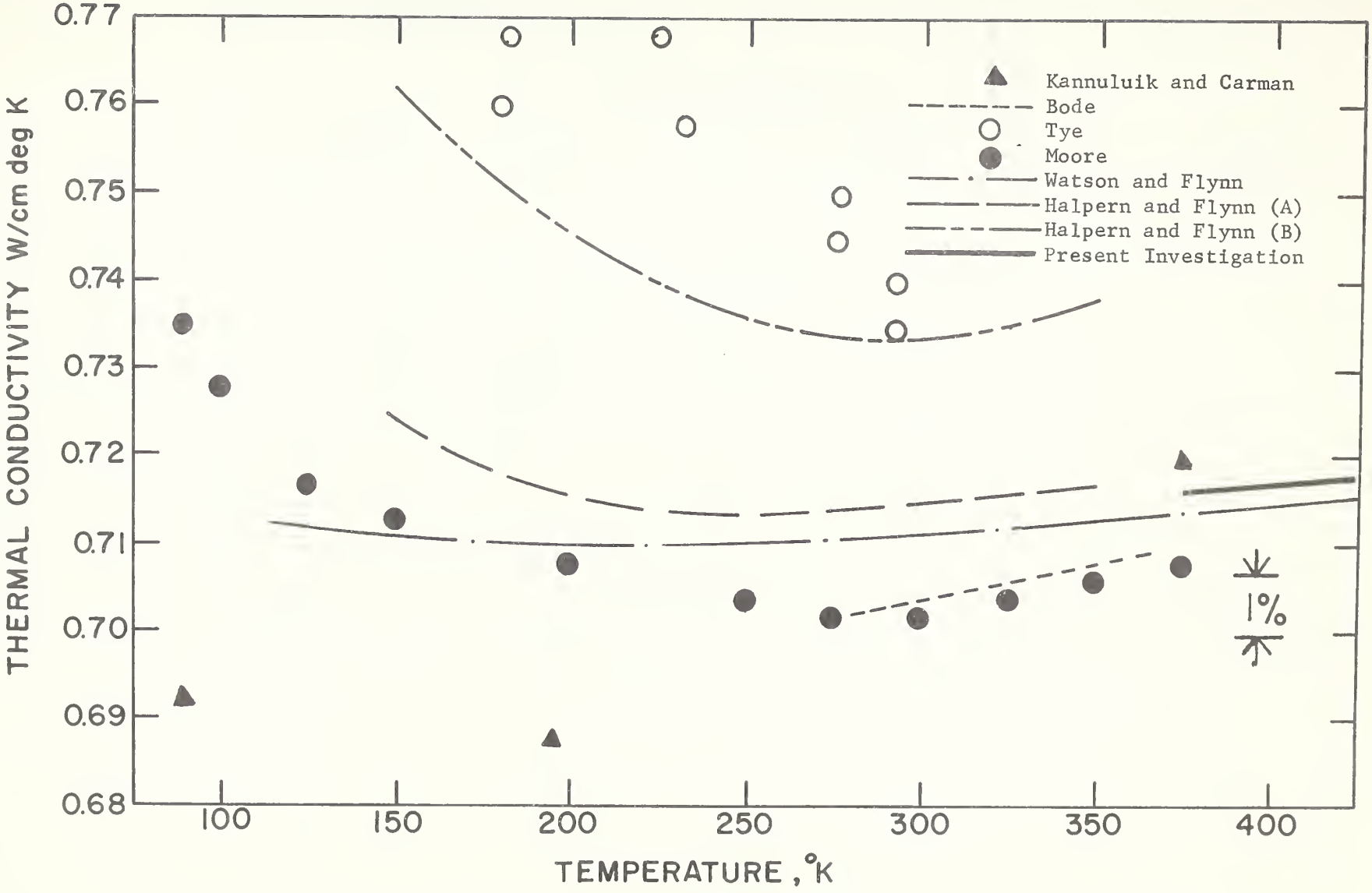

Figure 28. Thermal conductivity of Platinum: comparison between existing low temperature data and those of the present investigation.

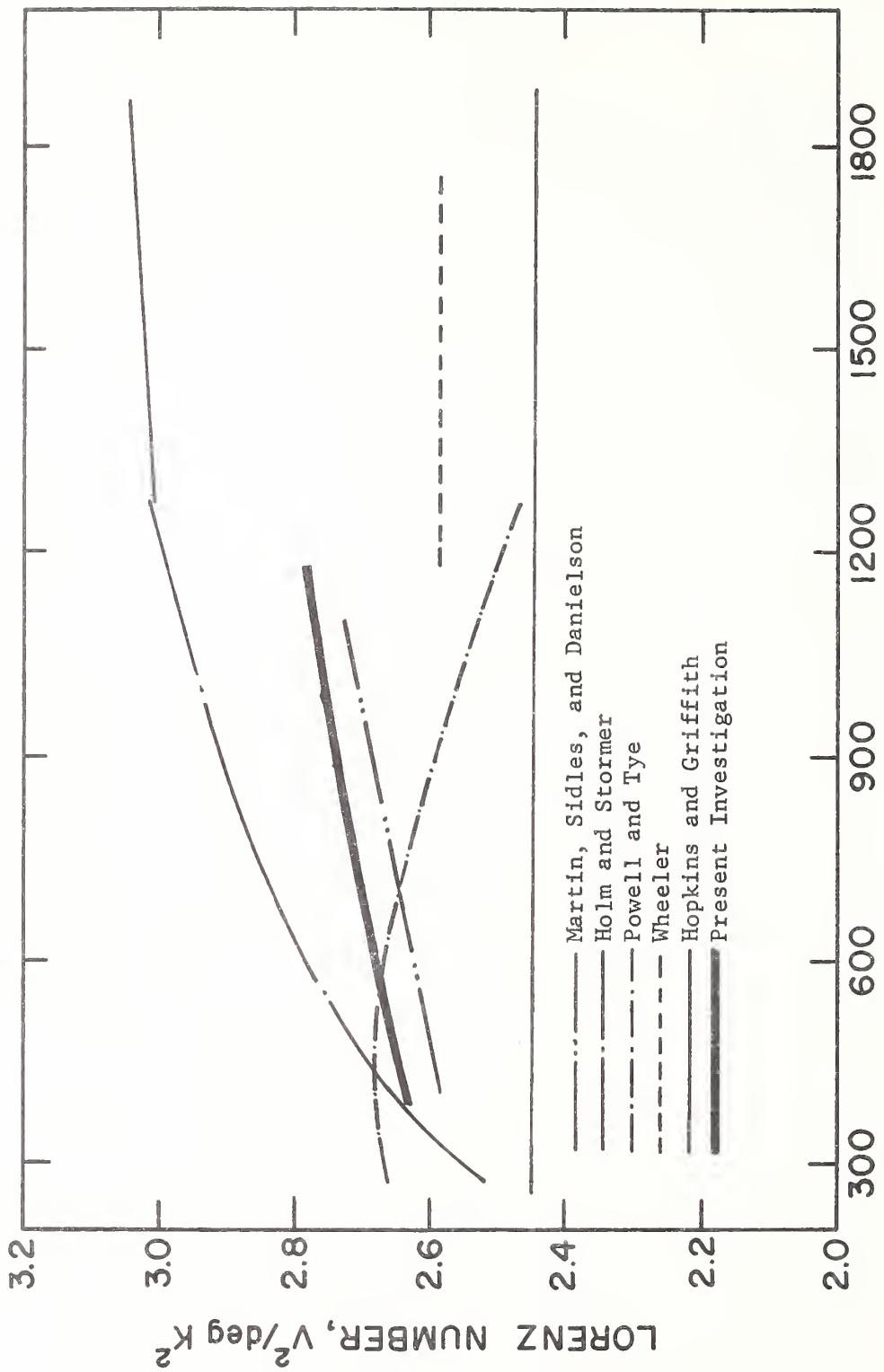

Figure 29. Lorenz number for platinum: comparison between existing data and those of the present investigation.

Kannuluik and Carman [27], Meissner [13] and Moore [89] although the results of Moore would be expected to be higher due to the higher purity of his platinum. At the lower temperatures one must consider the purity of the samples since impurities have a significant effect on thermal conductivity values. At the higher temperatures no significant effects are to be expected due to small amounts of impurities. The purity of the specimen used in the present investigation and in those of Watson and Flynn and Halpern and Flynn [86, A] was 99.98%. Bode's specimen was of the same purity. The measurements by Moore were made on the same specimen as used by Tye [90], the platinum being 99.999% pure. The purity of the second sample measured by Flynn and Halpern [86, B] was almost 99.999% , and the difference in values from their first sample are considered to be due in large part to the differences in purities.

Values obtained for the Lorenz number are compared with those of other investigators in Figure 29. The Lorenz number was found to increase with temperature contrary to theoretical predictions. However, this increase with temperature is considered to be real in view of the high precision with which the Lorenz number was measured. Consequently it would seem that the theory requires modification to account for this effect in a transition metal such as platinum.

APPENDIX A

Machining the Neck and Wiring the Specimen

Due to the structural weakness of a small neck in a large bar a special technique, described below, had to be developed for machining the neck in the specimen.

The platinum bar was held in a precision-bored jig that consisted essentially of two clamps--one clamping the bar on either side of the neck--rigidly coupled together by four ribs which bridged the neck region (see Figure 30). With the jig mounted between centers and one of the ribs removed a passing cut was made with a 0.125-inch diameter end-mill (Figure 31). The jig was then rotated through an angle of six degrees and another passing cut made. This process was repeated sixty times as the jig was rotated through 360° replacing and removing ribs as needed but always having at least three ribs in place. Successively deeper series of cuts were made until the desired neck size was reached. The cross-sectional configuration of the neck was that of a sixty-sided polygon. Several prototype specimens were fabricated out of lead to test this technique on a weak material. One of the prototype specimens had a neck as small as 20 mils in diameter.

The jig described above extended the whole length of the specimen and had to be removed in order to install the heater and thermocouples. It was necessary to design a second fixture to support the neck while the specimen was being wired and installed. A split brass collar was clamped to the bar on the lower side of the neck. A split aluminum collar was precision bored so that it clamped on the upper part of the bar and on the brass collar simultaneously. Dowel pins projecting from the brass

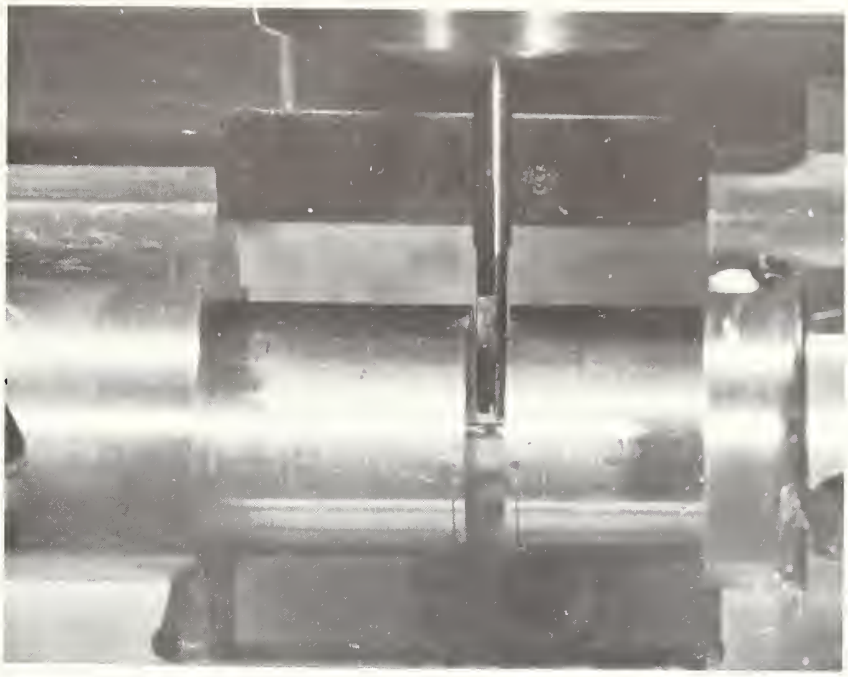

Figure 30. The specimen being machined. One of the four ribs connecting the two halves of the jig has been removed and the end mill is being positioned for a final passing cut.

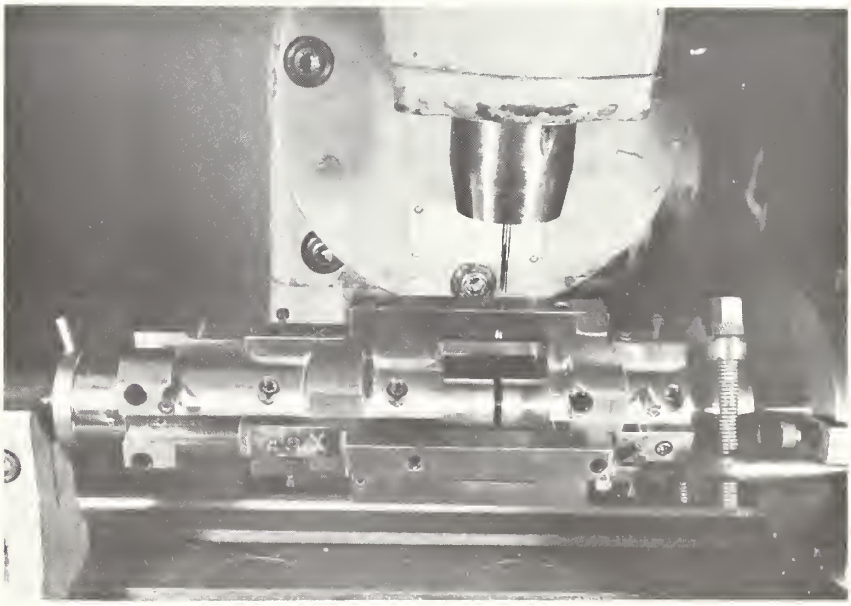

Figure 31. The machining set-up for machining the neck in the specimen. The specimen is held in the machining jig with the latter mounted between centers. Three of the ribs connecting the two halves of the jig can be seen. The milling head is centered over the neck which has just been machined.

collar guided the aluminum collar into place fixing the relative vertical position of the two. This clamp was attached to the specimen before removing it from the machining jig. When the specimen was mounted in the apparatus and ready for testing, the clamp was then removed carefully.

The two thermocouples adjacent to the neck were installed while the specimen was still in the machining jig but before the support clamp was attached. The support clamp had slots machined in it to accomodate the thermocouple wires. With the support clamp in place the specimen was removed from the machining jig and mounted on vee blocks. The molybdenum extensions were screwed into the ends of the specimen. The remainder of the thermocouples and the heater were installed with the specimen assembly resting on the vee blocks. The thermocouples were pressed into the slits using a small screw driver with head-width approximately that of the slit. All the heater welds were made with an oxygen-gas torch using a very fine tip.

APPENDIX B

Potential Perturbations

The procedures used for calculating the electrical resistivity and the thermal conductivity (direct method) assume that the equipotential surfaces along the specimen are parallel and also that the isothermal surfaces along the specimen are parallel. The discrete nature of the specimen heater introduces perturbations in the heat and electric current flow which cause the isothermal and equipotential surfaces to be distorted in the vicinity of the heater. Also, at the cold end of the specimen nonuniform contact with the molybdenum extension may give rise to distortions. It is the purpose of this Appendix to show that these distortions decay to negligible proportions in the region where temperatures are measured.

We can approximate the discrete heater problem by considering a semi-infinite solid with heat or electric current flowing through uniformly spaced strips on the surface (Figure 32).

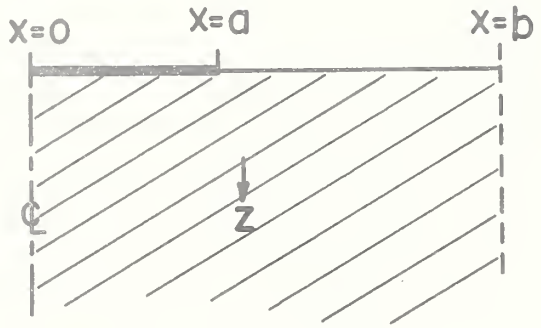

Figure 32. Semi-infinite solid.

The boundary conditions are:

$$\frac{\partial \theta}{\partial z} = \frac{J}{\sigma} \quad , \quad 0<x<a \quad , \quad z = 0 \qquad \text{(B-1)}$$

$$\frac{\partial \theta}{\partial z} = 0 \quad , \quad a<x<b \quad , \quad z = 0 \qquad \text{(B-2)}$$

$$\frac{\partial\theta}{\partial x} = 0 \quad , \quad x=0 \text{ and } x=b, \; 0 \leq z < \infty \tag{B-3}$$

where θ is electric potential or temperature, J is flux of current or heat, σ is electrical or thermal conductivity, 2a is the width of the region through which flux passes, and 2b is the center-to-center distance between the regions passing flux.

The potential or temperature distribution satisfies $\nabla^2\theta = 0$ and the solution is easily shown to be

$$\theta = -\frac{a}{b}\frac{J}{\sigma}\left[z - \frac{2b^2}{\pi^2 a}\sum_{n=1}^{\infty}\frac{1}{n^2}\sin\frac{n\pi a}{b}\cos\frac{n\pi x}{b}\,e^{-n\pi z/b}\right]. \tag{B-4}$$

The gradient in the z-direction at any point is given by

$$\frac{\partial\theta}{\partial z} = -\frac{a}{b}\frac{J}{\sigma}\left[1 + \frac{2b}{\pi a}\sum_{n=1}^{\infty}\frac{1}{n}\sin\frac{n\pi a}{b}\cos\frac{n\pi x}{b}\,e^{-n\pi z/b}\right]. \tag{B-5}$$

The average value of the gradient in the z-direction is given by

$$\left\langle\frac{\partial\theta}{\partial z}\right\rangle = \frac{1}{b}\int_0^b\left(\frac{\partial\theta}{\partial z}\right)dx = -\frac{a}{b}\frac{J}{\sigma}\,. \tag{B-6}$$

The fractional difference between the local value of the gradient and its average value is given by

$$f = \frac{\dfrac{\partial v}{\partial z} - \left\langle\dfrac{\partial v}{\partial z}\right\rangle}{\left\langle\dfrac{\partial v}{\partial z}\right\rangle} \tag{B-7}$$

$$= +\frac{2b}{\pi a}\sum_{n=1}^{\infty}\frac{1}{n}\sin\frac{n\pi a}{b}\cos\frac{n\pi x}{b}\,e^{-n\pi z/b} \tag{B-8}$$

Values of the percentage difference, 100f, for different values of a/b, are plotted in Figure 33 for x/b = 0.0 and in Figure 34 for x/b = 1.0. It is

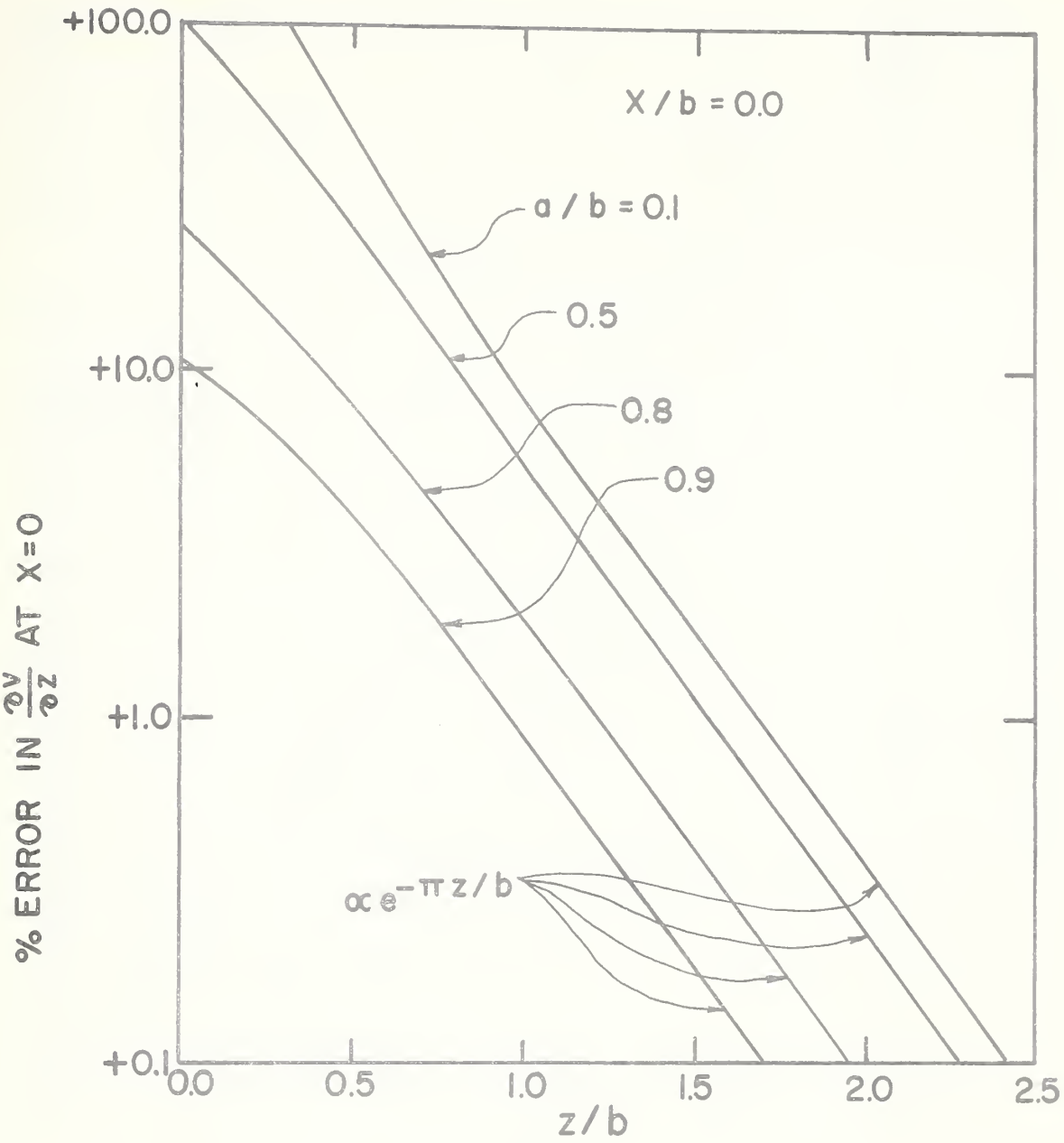

Figure 33. Local departures from the average value of the potential gradient caused by the presence of strip sources at z = 0. (x/b = 0.0)

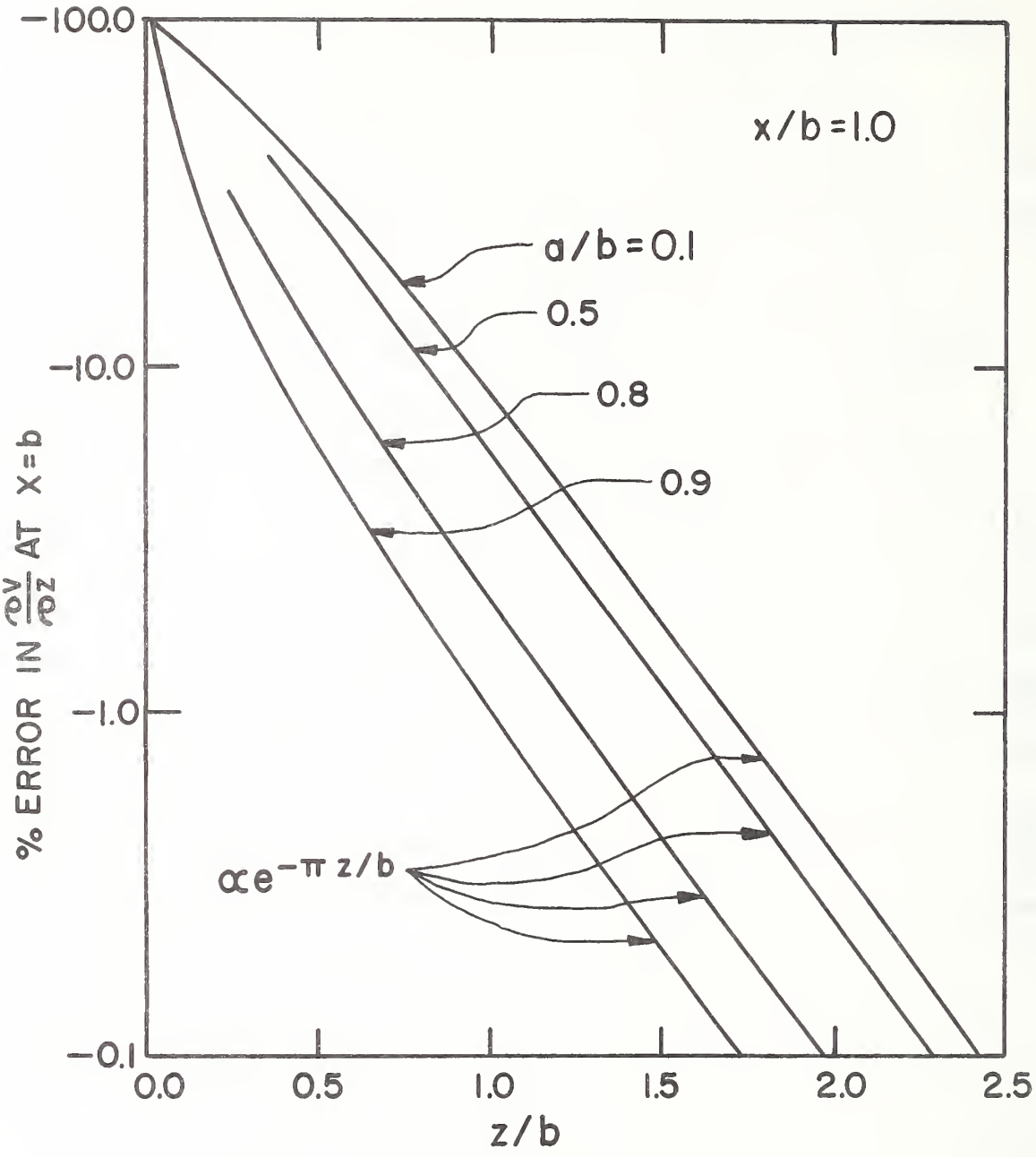

Figure 34. Local departures from the average value of the potential gradient caused by the presence of strip sources at z = 0. (x/b = 1.0)

seen that, regardless of the magnitude of the original disturbance, the error in the gradient has decayed to the order of 0.1 percent at positions only 2b away from the heater. In the present experiment the nearest thermocouple was about 4b away from the heater.

At the cold end of the specimen a molybdenum stud joins the specimen to the lower extension and this stud might cause preferential flow of heat or electrical current through the central region. We approximate this problem by considering a semi-infinite cylinder, of radius b, which is perfectly insulated except for a circle of radius a at z = 0 (Figure 35).

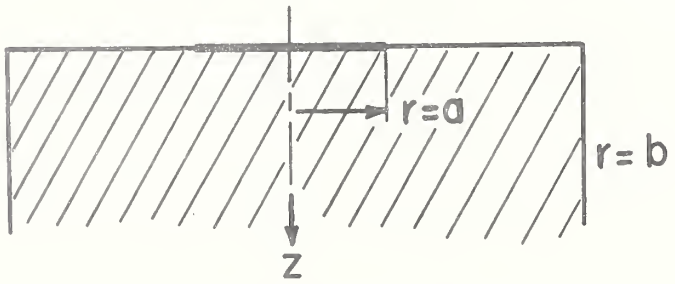

Figure 35. Semi-infinite cylinder.

The boundary conditions are

$$\frac{\partial\theta}{\partial z} = -\frac{J}{\sigma} \quad , \quad 0<r<a \quad , \quad z = 0 \qquad \text{(B-9)}$$

$$\frac{\partial\theta}{\partial z} = 0 \quad , \quad a<r<b \quad , \quad z = 0 \qquad \text{(B-10)}$$

$$\frac{\partial\theta}{\partial r} = 0 \quad , \quad r = b \quad , \quad 0 \leq z<\infty \qquad \text{(B-11)}$$

The solution is easily shown to be

$$\theta = -\frac{J}{\sigma}\frac{a^2}{b^2}\left[z - \frac{2b^2}{a}\sum_{n=1}^{\infty}\frac{J_1(\alpha_n\, a/b)\; J_o(\alpha_n r/b)}{\alpha_n^2\; J_o^2(\alpha_n)}\; e^{-\alpha_n z/b}\right], \qquad \text{(B-12)}$$

where J_o and J_1 are Bessel functions of the first kind of zero and first order, respectively, and α_n is the n^{th} root of $J_1(\alpha_n) = 0$. Differentiating,

$$\frac{\partial \theta}{\partial z} = - \frac{J}{\sigma} \frac{a^2}{b^2} \left[1 + \frac{2b}{a} \sum_{n=1}^{\infty} \frac{J_1(\alpha_n a/b)\ J_o(\alpha_n r/b)}{\alpha_n\ J_o^2(\alpha_n)} e^{-\alpha_n z/b} \right] \quad \text{(B-13)}$$

As before,

$$\left\langle \frac{\partial \theta}{\partial z} \right\rangle = \frac{2}{b^2} \int_o^b r \left(\frac{\partial \theta}{\partial z} \right) dr = - \frac{J}{\sigma} \frac{a^2}{b^2} \quad \text{(B-14)}$$

and

$$f = \frac{2b}{a} \sum_{n=1}^{\infty} \frac{J_1(\alpha_n a/b)\ J_o(\alpha_n r/b)}{\alpha_n\ J_o^2(\alpha_n)} e^{-\alpha_n z/b} \quad \text{(B-15)}$$

Values of the percentage difference, 100f, for different values of a/b, are plotted in Figure 36 for r/b = 1 (temperatures were measured at r = b). It is seen that, regardless of the magnitude of the original disturbance, the error in the gradient has decayed to the order of 0.1 percent at positions only one diameter (i.e. 2b) away from the disturbance. In the present investigation the disturbance was probably small to begin with (certainly nowhere nearly as drastic as assumed in the statement of the problem above) and the nearest thermocouple was one specimen diameter away from end of the specimen.

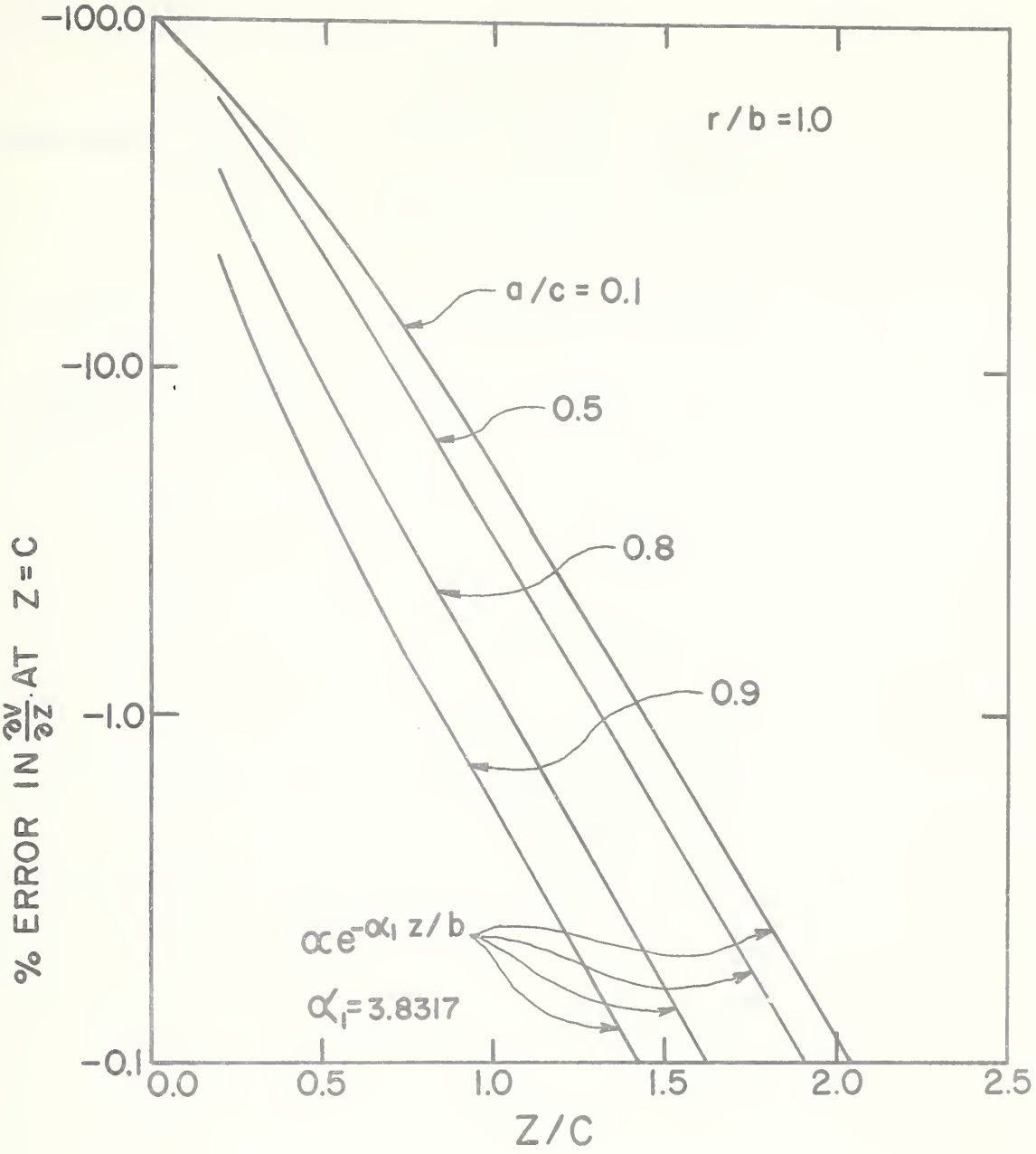

Figure 36. Local departures from the average value of the potential gradient caused by a circular source of radius, a, at the end, z = 0, of a semi-infinite cylinder of radius, b. (r/b = 1.0)

APPENDIX C

The Thomson Effect

We wish here to evaluate the magnitude of the Thomson effect represented by the second term on the right-hand side of (3-40):

$$\int_0^{\psi} \psi \, d\psi = \int_T^{T_m} k\rho \, dT + \int_0^{\psi} d\psi \int_T^{T_m} \tau \, dT \quad . \tag{3-40}$$

The Thomson coefficient τ is to a good approximation a linear function of the absolute temperature T [91]

$$\tau = \gamma T \quad , \tag{C-1}$$

where γ is a constant. Consequently

$$\int_T^{T_m} \tau \, dT = \frac{\gamma}{2} \left(T_m^2 - T^2 \right) \quad . \tag{C-2}$$

Since T is a function of ψ we must express (C-2) in terms of ψ before the Thomson term in (3-40) can be integrated.

Since the Thomson effect is in general a second-order effect, we can to a first approximation write

$$\int_0^{\psi} \psi \, d\psi = \int_T^{T_m} k\rho \, dT \quad . \tag{C-3}$$

Moreover in the case of a pure metal such as platinum we can write

$$k\rho = LT \quad , \tag{C-4}$$

where L is the Lorenz number. This is a good approximation if instead of using the theoretical value of the Lorenz number we use the value of L at temperature $\frac{T + T_m}{2}$ as determined experimentally, and assume that L is constant over the temperature interval $(T_m - T)$, that temperature interval being small in comparison with the absolute temperature T. Substituting (C-4) into

(C-3) and integrating we get

$$\psi^2 = L(T_m^2 - T^2) \quad . \tag{C-5}$$

Using (C-2) and (C-5) in (3-40) and integrating

$$\int_T^{T_m} k\rho\, dT = \frac{\psi^2}{2}\left[1 - \frac{\gamma\psi}{3L}\right] \quad . \tag{C-6}$$

The relative magnitude of the Thomson term is thus given by $\gamma\psi/3L$. Some representative values are shown below. The values shown for ψ correspond to the maximum current (100A) passed through the specimen, the variations in ψ reflecting the variation in resistance of the specimen with temperature.

Table 12. Values for the relative magnitude of the Thomson term in equation (3-40).

T	γ	L	$\psi \simeq V/2$	$\gamma\psi/3L$
°K	$(V/°C^2)\times10^8$	$(V/°C)^2\times10^8$	V	
300	-1.08	2.62	.02	.003
600	-1.08	2.69	.04	.004
900	-1.08	2.74	.06	.008
1200	-1.08	2.79	.08	.010
1500	-1.08	2.82	.10	.013

For the purpose of evaluating the Thomson effect it was assumed that $\psi = V/2$ where V is the measured voltage drop across the neck. The relative magnitude of the Thomson term is seen to be less than one percent over the entire temperature range. Moreover, in a conductor with the ends held at the same temperature the Thomson effect in one half of the conductor cancels that in the other half to first order so that the net Thomson effect is of the order of only 0.02 percent.

APPENDIX D

Alternative Calculation Procedure for the Indirect Method

Let us rewrite (3-66) in the form

$$\frac{R_o}{R} = 1 - \frac{2}{3}\alpha_o\theta_m U \quad , \tag{D-1}$$

where

$$U = U(\eta_o\theta_m) \equiv \frac{3}{2\eta_o\theta_m}\left[1 - \frac{1}{G}\arctan G\right] \quad , \tag{D-2}$$

and

$$G^2 = 2\eta_o\theta_m\left(1 + \frac{1}{2}\eta_o\theta_m\right) \quad . \tag{3-67}$$

Our definition of R' is

$$R' = R_r\left(1 + \frac{2}{3}\alpha_r\theta_m\right) \quad . \tag{D-3}$$

Eliminating θ_m between (D-1) and (D-3) yields, after some manipulation,

$$R' = R\left[1 + \frac{(\alpha_r/\alpha_o)R_r(R - R_o) - UR(R - R_r)}{UR^2}\right] \quad . \tag{D-4}$$

For $T_o = T_r$, $\alpha_o = \alpha_r$, $R_o = R_r$, and

$$R' = R\left[1 - \frac{(1 - R_r/R)(U - R_r/R)}{U}\right] \quad . \tag{D-5}$$

In the present investigation U was approximately constant with a value of 0.935, and R_r/R ranged from 0.936 to 1.000. The maximum temperature rise was 100°C and $|T_o - T_r|$ was generally less than 0.1°C. Thus for $\theta_m < 100$ the second term in brackets in (D-4) is quite small so that in order to calculate a value for U it is sufficient to use the value for θ_m given by $\theta_m = \frac{(R - R_o)}{2/3\ \alpha_o R_o}$. Likewise θ_m need be known only approximately for calculation

of V'^2 from (4-7) provided θ_m is not too large. Table 13 gives values of $U(\eta_o\theta_m)$ for arguments from 0.0 to 0.5.

Table 13. Values of $U(\eta_o\theta_m)$ for arguments from 0.0 to 0.5.

$\eta_o\theta_m$	0.00	0.01	0.02	0.03	0.04	0.05	0.06	0.07	0.08	0.09
0.00	1.000	0.993	0.986	0.979	0.973	0.966	0.960	0.953	0.947	0.941
0.10	0.935	0.929	0.923	0.917	0.911	0.905	0.900	0.894	0.889	0.883
0.20	0.878	0.873	0.867	0.862	0.857	0.852	0.847	0.842	0.837	0.832
0.30	0.828	0.823	0.818	0.814	0.809	0.805	0.800	0.796	0.792	0.787
0.40	0.783	0.779	0.775	0.771	0.767	0.763	0.759	0.755	0.751	0.747

APPENDIX E

A Simplified Expression for the Maximum Temperature Rise in the Neck in the Presence of Heat Losses

In Chapter IV we derived the expression

$$u_m^* = \frac{16\ell^2 \rho_o I^2}{\pi^5 a^4 k_o} \sum_{n=1,3,5,} \frac{(-1)^{\frac{n-1}{2}}}{n^3 \left[1 - \frac{4\ell^2 \alpha_o I^2}{n^2 \pi^4 a^4 k_o} - \frac{4\ell}{n\pi a} \frac{h_o}{k_o} \frac{F_1 [A_n; B_n]}{F_o [A_n; B_n]} \right]} \tag{4-16}$$

as the maximum temperature in the presence of heat losses. For the parameter values appropriate to the present experiment, the term in $\alpha_o I^2$ and the term in h_o/k_o in (4-16) are small compared to unity. Using the relation $(1 - x)^{-1} \approx 1 + x$ for small x, and the identities [92 ,p 64]

$$1 - \frac{1}{3^3} + \frac{1}{5^3} - \frac{1}{7^3} + \cdots\cdots\cdots\cdots\cdots\cdots \infty = \frac{\pi^3}{32} \tag{E-1}$$

$$1 - \frac{1}{3^5} + \frac{1}{5^5} - \frac{1}{7^5} + \cdots\cdots\cdots\cdots\cdots\cdots \infty = \frac{5\pi^5}{1536} \quad , \tag{E-2}$$

we can write

$$u_m^* = \frac{\ell^2 \rho_o I^2}{2\pi^2 a^4 k_o} \left[1 + \frac{5\alpha_o}{6} \left(\frac{\ell^2 \rho_o I^2}{2\pi^2 a^4 k_o} \right) - \frac{128\ell}{\pi^4 a} \frac{h_o}{k_o} \sum_{n=1,3,5} \frac{(-1)^{\frac{n-1}{2}}}{n^4} \frac{F_1 [A_n; B_n]}{F_o [A_n; B_n]} \right] \tag{E-3}$$

In the geometry used in the present experiment $b >> a$, and (E-3) reduces to

$$u_m^* = \frac{\ell^2 \rho_o I^2}{2\pi^2 a^4 k_o} \left[1 + \frac{5\alpha_o}{6} \left(\frac{\ell^2 \rho_o I^2}{2\pi^2 a^4 k_o} \right) - \frac{128\ell}{\pi^4 a} \frac{h_o}{k_o} \sum_{n=1,3,5} \frac{(-1)^{\frac{n-1}{2}}}{n^4} \frac{K_1(n\pi a/2\ell)}{K_o(n\pi a/2\ell)} \right] \tag{E-4}$$

Owing to the very rapid convergence of the series in (E-4), we need retain only the leading term of the series. We can then write

$$u_m^* = u_m \left[1 - \frac{h_o}{k_o} \frac{128\ell}{\pi^4 a} \frac{K_1(\pi a/2\ell)}{K_o(\pi a/2\ell)}\right] , \qquad (4\text{-}17)$$

where u_m is the maximum temperature rise in the neck in the absence of heat losses, i.e. for $h_o = 0$;

$$u_m = \frac{\ell^2 \rho_o I^2}{2\pi^2 a^4 k_o} \left[1 + \frac{5\alpha_o}{6}\left(\frac{\ell^2 \rho_o I^2}{2\pi^2 a^4 k_o}\right)\right] . \qquad (E\text{-}6)$$

The second order term in $\alpha_o I^2$ is neglected in (4-17).

APPENDIX F

Derivation of the Equation for Heat Flow in the Current Leads of the Specimen Heater

In this appendix equation (4-44) is derived.

Several papers [93, 94, 95, 96, 97, 98, 99] in the recent literature discuss the problem of heat flow along current-carrying leads. With the assumption of constant thermal conductivity and electrical resistivity, (4-44) can be derived from various expressions given in these papers. However, an extension of the mathematical analysis already given in Chapter 3 for the indirect method leads quite naturally to a general expression for heat flow along a current-carrying conductor.

Consider a conductor through which an electric current is passing, and which has its surface perfectly insulated both thermally and electrically. The geometry may be arbitrary. The heat flux, $\vec{Q}$, at any point in the conductor is

$$\vec{Q} = -k\nabla T \qquad \text{(F-1)}$$

where k is the thermal conductivity of the conductor and T the temperature.

Neglecting thermoelectric effects, we can write from (3-35) and (3-49)

$$\phi \nabla \phi = -k\rho \nabla T \quad , \qquad \text{(F-2)}$$

and

$$\phi^2 = 2\int_T^{T^*} k\rho \, dT \quad , \qquad \text{(F-3)}$$

where ϕ is the electrical potential, ρ the electrical resistivity of the conductor, and T^* a fixed reference temperature.

From (F-1) and (F-2)

$$\vec{Q} = \frac{1}{\rho} \phi \nabla \phi = -\phi \vec{J} \quad , \qquad \text{(F-4)}$$

where $\vec{J}$ is the electric current density.

Integrating (F-4) over an equipotential surface, S, we get

$$\vec{q} = -\phi \vec{I} \quad , \tag{F-5}$$

where $\vec{q}$ is the total heat flow through S and $\vec{I}$ is the total electric current through S. Substituting for ϕ from (F-3), (F-5) becomes

$$\vec{q} = -\left[2\int_{T}^{T^*} k\rho \, dT\right]^{\frac{1}{2}} \vec{I} \, . \tag{F-6}$$

Consider two equipotential, and hence isothermal, surfaces at temperatures T_1 and T_2, with total heat flows $\vec{q}_1$ and $\vec{q}_2$. Since the surface of the conductor is perfectly insulated we can write

$$I^2 R = q_1 - q_2 \quad , \tag{F-7}$$

where R is the total electrical resistance between the two surfaces and q_1, q_2, and I are the magnitudes of $\vec{q}_1$, $\vec{q}_2$, and $\vec{I}$, respectively. Utilizing (F-6), (F-7) becomes

$$I R = \left[2\int_{T_2}^{T^*} k\rho \, dT\right]^{\frac{1}{2}} - \left[2\int_{T_1}^{T^*} k\rho \, dT\right]^{\frac{1}{2}} . \tag{F-8}$$

Rearranging (F-8) and squaring both sides

$$2\int_{T_2}^{T^*} k\rho \, dT = 2\int_{T_1}^{T^*} k\rho \, dT + 2IR\left[2\int_{T_1}^{T^*} k\rho \, dT\right]^{\frac{1}{2}} + I^2R^2 \, , \tag{F-9}$$

from which

$$-\left[2\int_{T_1}^{T^*} k\rho \, dT\right]^{\frac{1}{2}} = \frac{1}{IR}\int_{T_1}^{T_2} k\rho \, dT + \frac{IR}{2} \, . \tag{F-10}$$

Substitution of (F-10) into (F-6) yields

$$q_1 = \frac{1}{R}\int_{T_1}^{T_2} k\rho \, dT + \frac{I^2R}{2} \, . \tag{F-11}$$

From (F-7) and (F-11),

$$q_2 = \frac{1}{R}\int_{T_1}^{T_2} k\rho\, dT - \frac{I^2R}{2} . \qquad \text{(F-12)}$$

Equations (F-11) and (F-12) are identical to equations (8) and (9) in the paper by Neighbor [94]. For constant k and ρ they reduce to

$$q_1 = \frac{k\rho}{R}(T_2 - T_1) + \frac{I^2R}{2} \qquad \text{(F-13)}$$

and

$$q_2 = \frac{k\rho}{R}(T_2 - T_1) - \frac{I^2R}{2} , \qquad \text{(F-14)}$$

which is identical with (4-44).

APPENDIX G

Errors in Temperature Measurements Due To Heat Conduction Along Thermocouple Wires

The purpose of this Appendix is to estimate the error in temperature measurement due to heat conduction along the wires of the thermocouple making the measurement. The specimen can be considered as a semi-infinite solid of thermal conductivity k, perfectly insulated over the plane $z = 0$, except for a circular area of radius a (representing a thermocouple wire) through which heat flows at a constant rate, Q, per unit area, per unit time.

Assuming circular symmetry, the Laplacian of the temperature, θ, can be written as:

$$\frac{\partial^2\theta}{\partial r^2} + \frac{1}{r}\frac{\partial\theta}{\partial r} + \frac{\partial^2\theta}{\partial z^2} = 0 \quad . \tag{G-1}$$

A solution to (G-1) for $z \geq 0$ is

$$\theta = e^{-\lambda z} J_0(\lambda r) \tag{G-2}$$

for any value of λ, where J_0 is the Bessel function of the first kind and order zero.

$$\theta = \int_0^\infty e^{-\lambda z} J_0(\lambda r) f(\lambda) d\lambda \tag{G-3}$$

is also a solution to (G-1) for any λ. The function $f(\lambda)$ must be chosen to satisfy the boundary conditions:

$$\begin{aligned} k\frac{\partial\theta}{\partial z} &= +Q \quad , \; z = 0, \; 0 < r < a \\ &= 0 \quad , \; z = 0, \; r > a \end{aligned} \tag{G-4}$$

Using the relation [94, sec. 13.42]

$$\int_0^\infty J_0(\lambda r) J_1(\lambda a) d\lambda = \begin{cases} 0 & , \ r > a \\ 1/2a & , \ r = a \\ 1/a & , \ r < a \end{cases} \qquad \text{(G-5)}$$

where J_1 is the Bessel function of the first kind and order one, we find that $f(\lambda) = -\frac{Qa}{k\lambda} J_1(\lambda a)$ satisfies the boundary conditions and we can write

$$\theta = -\frac{aQ}{k} \int_0^\infty e^{-\lambda z} J_0(\lambda r) J_1(\lambda a) \frac{d\lambda}{\lambda} \quad . \qquad \text{(G-6)}$$

The average temperature, $< \theta >$ over $o < r < a$ at $z = o$ is

$$< \theta > = -\frac{2Q}{k} \int_0^\infty J_1^2(\lambda a) \frac{d\lambda}{\lambda} = \frac{-8aQ}{3\pi k} \quad . \qquad \text{(G-7)}$$

At regions remote from $o < r < a$, $z = o$, the temperature $v = o$. The total heat flow $q = \pi a^2 Q$, so that, from (G-7)

$$< \theta > = \frac{-8q}{3\pi^2 ak} \quad . \qquad \text{(G-8)}$$

The above development is from Carslaw and Jaeger [25, pp 214-217].

Let us assume that the thermocouple wire supports a temperature gradient G so that the heat flow in it is given by

$$q = -\pi a^2 k_w G \quad , \qquad \text{(G-9)}$$

where k_w is the thermal conductivity of the wire. Eliminating q between (G-8) and (G-9), we get

$$< \theta > = \frac{8a}{3\pi} \frac{k_w}{k} G \quad , \qquad \text{(G-10)}$$

where $< \theta >$ can be considered as the effective change in temperature of the junction due to heat conduction along a thermocouple wire. If G is negative the junction is cooled an amount $< \theta >$.

In the present investigation only the Pt 10% Rh wires affected the temperatures at the measuring junctions on the specimen, as discussed in Chapter II. In the gradient region these were 8-mil wires. Assuming that they had the same thermal conductivity as the platinum specimen, a conservative estimate, and that they supported the same temperature gradient as the specimen in the gradient tests, i.e. 5°C/cm, the error introduced in the measured temperature due to heat conduction along the thermocouple wire was 0.085°C or 0.2% of the temperature drop between thermocouples 4 and 8 (see fig. 12). Since the thermocouple wire was wrapped part-way around the specimen in the isothermal plane of its junction the temperature gradient in the wire was probably much less than 5°C/cm . Furthermore since all the thermocouples were installed in a similar manner they would all give rise to about the same error both in sign and magnitude, and, hence in taking temperature differences, the errors would in large part cancel. Consequently it is felt that a conservative estimate of the maximum error in the measured temperature gradient due to heat conduction along the Pt 10% Rh thermocouple wires is 0.05%.

APPENDIX H

Departures From One-Dimensional Heat Flow in the Direct Method

The purpose of this Appendix is to show that radial temperature gradients in the specimen were negligibly small for the guarding conditions used in the direct method. To accomplish this we consider a circular bar of radius b, length ℓ and thermal conductivity k, with a constant heat flux q through the cylindrical surface of the bar. The boundary conditions are:

$$\theta = 0 \quad , \quad z = 0 \quad , \quad 0 < r < b \quad ;$$

$$\theta = T \quad , \quad z = \ell \quad , \quad 0 < r < b \quad ;$$

$$k \frac{\partial \theta}{\partial r} = -q \quad , \quad 0 < z < \ell \quad , \quad r = b \quad .$$

The use of isothermal boundary conditions at each end of the bar does not affect the radial temperature distribution at positions near the center of the bar since, as shown in Appendix B, the effect of the end boundaries decays very rapidly and is negligibly small at positions one diameter away.

The solution to the above problem is

$$\theta = T\frac{z}{\ell} - \frac{4\ell q}{\pi^2 k} \sum_{n=1,3,5,}^{\infty} \frac{1}{n^2} \frac{I_o(n\pi r/\ell)}{I_1(n\pi b/\ell)} \sin \frac{n\pi z}{\ell} \quad , \qquad \text{(H-1)}$$

where I_o and I_1 are the modified Bessel functions of the first kind and of zero and first order, respectively; the notation n = 1, 3, 5, indicates that the summation is over odd values of n only. The longitudinal gradient is

$$\frac{\partial \theta}{\partial z} = \frac{T}{\ell} - \frac{4q}{\pi k} \sum_{n=1,3,5,}^{\infty} \frac{1}{n} \frac{I_o(n\pi r/\ell)}{I_1(n\pi b/\ell)} \cos \frac{n\pi z}{\ell} \quad . \qquad \text{(H-2)}$$

The average value of $\partial\theta/\partial z$ at any longitudinal position is

$$\left\langle \frac{\partial \theta}{\partial z} \right\rangle = \frac{2}{b^2} \int_0^b r \left(\frac{\partial \theta}{\partial z} \right) dr \qquad \text{(H-3)}$$

Substituting (H-2) into (H-3) and integrating yields

$$\left\langle \frac{\partial \theta}{\partial z} \right\rangle = \frac{T}{\ell} - \frac{8\ell q}{\pi^2 b k} \sum_{n=1,3,5,}^{\infty} \frac{1}{n^2} \cos \frac{n\pi z}{\ell} \quad , \tag{H-4}$$

which sums to

$$\left\langle \frac{\partial \theta}{\partial z} \right\rangle = \frac{T}{\ell} - \frac{q}{bk} (\ell - 2z) \quad . \tag{H-5}$$

The fractional difference between $(\partial\theta/\partial z)_{r = b}$ and $\langle \partial\theta/\partial z \rangle$ is

$$f = \frac{\dfrac{8q\ell}{\pi^2 b k} \displaystyle\sum_{n=1,3,5}^{\infty} \frac{1}{n^2} \left[1 - \frac{n\pi b}{2\ell} \frac{I_o(n\pi b/\ell)}{I_1(n\pi b/\ell)} \right] \cos \frac{n\pi z}{\ell}}{\dfrac{T}{\ell} - \dfrac{q}{bk} (\ell - 2z)} \quad . \tag{H-6}$$

Since, for our experiments, $q\ell/bk << T/\ell$, we can write

$$f = \frac{q\ell}{kT} F(b/\ell ;\ z/\ell) \quad , \tag{H-7}$$

where

$$F(b/\ell ;\ z/\ell) = \frac{8\ell}{\pi^2 b} \sum_{n=1,3,5,}^{\infty} \frac{1}{n^2} \left[1 - \frac{n\pi b}{\ell} \frac{I_o(n\pi b/\ell)}{I_1(n\pi b/\ell)} \right] \cos \frac{n\pi z}{\ell} \quad . \tag{H-8}$$

Evaluation of F and f for the conditions of our tests indicated that $f < 0.02\%$ for the "unmatched" gradient tests and was considerably smaller still for the "matched" gradient and the "isothermal" tests.

APPENDIX I

Tempering of the Heater Current Leads

Consider a current-carrying wire of radius, a, surrounded by insulation of radius, b, all imbedded in a semi-infinite medium of high thermal conductivity which is maintained at zero temperature. The differential equation describing the temperature distribution in the wire is

$$\frac{d^2\theta}{dz^2} - \mu^2\theta = -M \quad , \tag{I-1}$$

where θ is the excess temperature of the wire above its surroundings,

$$\mu^2 = \frac{2\mathfrak{K}}{a^2 k \ln b/a} \quad , \tag{I-2}$$

$$M = \frac{\rho I^2}{\pi^2 a^4 k} \quad , \tag{I-3}$$

$\mathfrak{K}$ is the thermal conductivity of the insulation, k is the thermal conductivity of the wire, ρ is the electrical resistivity of the wire, and I is the current passing through the wire. We assume the boundary condition

$$\theta = V \quad , \quad z = 0. \tag{I-4}$$

The solution to (I-1) which satisfies (I-4) for $z > 0$ is

$$\theta = \frac{M}{\mu^2} + \left(V - \frac{M}{\mu^2}\right) e^{-\mu z} \quad , \tag{I-5}$$

The temperature gradient in the wire is given by

$$\frac{d\theta}{dz} = -\mu\left(V - \frac{M}{\mu^2}\right) e^{-\mu z} \quad , \tag{I-6}$$

while the heat flow along the wire is given by

$$q = -\pi a^2 k \frac{d\theta}{dz} = \pi a^2 \mu\left(V - \frac{M}{\mu^2}\right) e^{-\mu z} . \tag{I-7}$$

The above analysis is based on an infinitely long tempering lead while we used tempering leads of finite length. An approximate analysis of the finite case indicated that the analysis for the infinite case is a good approximation for the conditions present in our measurements. For the swaged elements (described in Chapter II) which were used to temper the leads, $a \approx 0.025$ cm and $b \approx 0.050$ cm. so that $\ell n\, b/a \approx 0.7$. We estimate that $k \geq 0.004$ W/cm deg and $k \leq 0.8$ W/cm deg at all temperatures. Thus $\mu^2 > 20$ cm^{-2} at all temperatures. Also at all temperatures $\rho I^2 < 6 \times 10^{-5}$ W cm, so that $M < 20$ deg/cm^2 at all temperatures. The length of swaged element used to temper each lead was 1.3 cm. Plugging all of these numbers into (I-5), (I-6), and (I-7) we obtain for the colder end of the swaged element

$$\theta < 1 + 0.0033(V - 1) \text{ °C}$$

$$\left| \frac{d\theta}{dz} \right| < 0.015(V - 1) \text{ °C/cm}$$

$$q < 0.000011(V - 1) \text{ W}$$

The temperature rise in the heater winding was always less than 200 °C; therefore

$$q < 0.0025 \text{ W}$$

and the combined heat flow out both current leads was less than 0.05% of the power input to the heater. This estimate is in concordance with the small values found for q_a and q_b.

REFERENCES

1. Robinson, H. E., Thermal conductivity reference standards, Proceedings of the Second Conference on Thermal Conductivity (Ottawa), 311 (1962).
2. Powell, R. W. and Tye, R. P., The promise of platinum as a high temperature thermal conductivity reference material, Brit. J. Appl. Phys. 14, 662 (1963).
3. Slack, G. A., Platinum as a thermal conductivity standard, J. Appl. Phys. 35, 339 (1964).
4. Hill, J. S. and Albert, H. J., Loss of weight of platinum, rhodium, and palladium at high temperatures, Engelhard Industries, Inc., Technical Bulletin, Vol. IV, 59 (1963).
5. Galagali, R. J., Change of platinum resistance by hydrogen, Brit. J. Appl. Phys. 15, 208 (1964).
6. Stimson, H. F., The international temperature scale of 1948, J. Res. NBS 42, 209 (1949).
7. Stimson, H. F., International practical temperature scale of 1948, text revision of 1960, J. Res. NBS 65A, 139 (1961).
8. Evans, J. P. and Burns, G. W., A study of stability of high temperature platinum resistance thermometers, Temperature, Its Measurement and Control in Science and Industry, Vol. 3, Part 1, 313 (Reinhold Publishing Corp., New York, 1962).
9. Bradley, Derek and Entwistle, A. G., Anomalous electrical resistance effects in small diameter platinum and platinum-rhodium resistance elements at temperatures in excess of 1000 °C in a gaseous environment, ibid., 319.

10. Walker, B. E., Ewing, C. T. and Miller, R. R., Thermoelectric instability of some noble metal thermocouples at high temperatures, Rev. Sci. Instr. 33, 1029 (1962).

11. Walker, B. E., Ewing, C. T. and Miller, R. R., Study of the instability of noble metal thermocouples in vacuum, Rev. Sci. Instr 36, 601 (1965)

12. Jaeger, W. and Disselhorst, H., Wärmeleitung, Elektrizitätsleitung, Wärmekapazität und Thermokraft einiger Metalle, Wiss, Abh. Phys.-Techn. Reichsanst 3, 269 (1900).

13. Meissner, W., Thermische und elektrische Leitfähigkeit einiger Metalle zwischen 20° und 373° abs., Ann. Phys. 47, 1001 (1915).

14. Holm, R. and Störmer, R., Messund der Wärmeleitfähigkeit einer Platinprobe ein Temperaturgebeit 19 bis 1020° C, Wiss. Veroff. Siemens-Werk 9, 312 (1930). (An English translation for NBS was made by Joint Publications Research Service, Job No. R-5191-D.)

15. Hopkins, M. R., The thermal and electrical conductivities of metals at high temperatures, Z. Phys. 147, 148 (1957).

16. Hopkins, M. R., and Griffith, R. Ll., The determination of the Lorenz number at high temperatures, Z. Phys. 150, 325 (1958).

17. Cutler, M., Snodgrass, H. R., Cheney, G. T., Appel, J., Mallon, C. E. and Meyer, C. H., Jr., Thermal conductivity of reactor materials, Final Report GS-1939, General Atomic Division, General Dynamics Corporation, San Diego (30 January 1961).

18. Holm, R., Electric Contacts Handbook, 3rd ed. (Springer-Verlag, 1958).

19. Holm. R., Eine Methode zur Bestimmung der Wärmeleitfähigkeit von Metallen, besondera bei hohen Temperaturen, Wiss. Veröff. Seimens-Werk 9, 300 (1930). (An English translation for NBS was made by Joint Publications Research Service, Job No. R-5191-D.)

20. Cutler, M., Thermoelectric measurements at small-area contacts, J. Appl. Phys. 32, 1075 (1961).

21. Cutler, M., Small area contact methods, Advanced Energy Conversion 2, 29 (1962).

22. Cutler, M. and Cheney, G. T., Measurement of thermal conductivity of electrical conductors at high temperatures, J. Appl. Phys. 34, 1714 (1963).

23. Mallon, C. E. and Cutler, M., Thermal conductivity of liquid semiconductor thallium-tellurium solutions, Phil. Mag. 11, 667 (1965).

24. Mallon, C. E. and Cutler, M., Thermal conductivity of electrically conducting liquids, Rev. Sci. Instr. 36, 1036 (1965).

25. Carslaw, H. S. and Jaeger, J. C., The Conduction of Heat in Solids 2nd ed. (Clarendon Press, Oxford, 1959).

26. Kannuluik, W. G. and Carman, E. H., The temperature dependence of the thermal conductivity of air, Australian J. Sci. Res. 4A, 305 (1951).

27. Kannuluik, W. G. and Carman, E. H., The thermal conductivity of rare gases, Proc. Phys. Soc. 65B, 701 (1952).

28. Krishnan, K. S. and Jain, S. C., Determination of thermal conductivities at high temperatures, Brit. J. Appl. Phys. 5, 426 (1954).

29. Bode, K. H., Measurements of the thermal conductivity of metals at high temperatures, Progress in International Research on Thermodynamics and Transport Properties, 481 (Academic Press, New York, 1962).

30. Kannuluik, W. G. and Law, P. G., The thermal conductivity of carbon dioxide between -78.50° C and 100° C, Proc. Roy. Soc. Vict. 58, 142 (1957).

31. Jain, S. C. and Krishnan, K. S., The distribution of temperature along a thin rod electrically heated in vacuo, Part I, Proc. Roy. Soc. A222.

167 (1954); Part II, Proc. Roy. Soc. A225, 1 (1954); Part III, Proc. Roy. Soc. A225, 7 (1954).

32. Wheeler, M. J., Thermal diffusivity at incandescent temperatures by a modulated electron beam technique, Brit. J. Appl. Phys. 16, 365 (1965).

33. Martin, J. J. and Sidles, P. H., Thermal diffusivity of platinum from 300 to 1300°K, Report No. IS-1018, contribution No. 1614 of the Ames Laboratory of the U.S. Atomic Energy Commission (1964).

34. Zolotukhin, G. E., Issledovanie teploprovodnosti metallov i spelovov v usloviyakh teplovogo ravnovesiya s ispolbzovaniem dugovogo razryada, Fiz. Metal i Metalloved, Akad. Nauk. SSSR, Ural. Filial 3, 508 (1956).

35. Schulze, F. A., Die Wärmeleitfähigkeit einiger Reihen von Edelmetall-Legierungen, Physik. Z. 12, 1028 (1911).

36. Cowan, R. D., Proposed method of measuring thermal diffusivity at high temperatures, J. Appl. Phys. 32, 1363 (1961).

37. Sidles, P. H., Thermal diffusivity of metals at high temperatures, J. Appl. Phys 25, 58 (1954).

38. Thermophysical Properties Research Center Data Book 1, Table 1020 (1965).

39. Barratt, T., Thermal and electrical conductivities of some of the rarer metals and alloys, Proc. Phys. Soc. London 26, 347 (1913).

40. Barratt, T. and Winter, R. M., Das thermische Leitvermögen von Drähten und Stäben, Ann. Phys. 77, 1 (1925).

41. Bode, K-H., Messung der Wärmeleitfähigkeit von reinem Platin zwischen 0°C und 100°C, PTB Mitteilungen Nr. 5, 416 (1964).

42. Powell, R. W., Tye, R. P., and Woodman, M. J., Thermal conductivities and electrical resistivities of the platinum metals, Platinum Metals Rev. 6, 138 (1962).

43. Grüneisen, E. and Goens, E., Untersuchungen an Metallkristallen V. Elektrizitäts und Wärmeleitung von ein- und viel-kristallinen Metallen des regularen Systems, Z. Phys. 44, 615 (1927).

44. Mendelssohn, K. and Rosenberg, H. M., The thermal conductivity of metals at low temperatures, II. The transition elements, Proc. Phys. Soc. 65, 388 (1952).

45. White, G. K. and Woods, S. B., Electrical and thermal resistivity of the transition elements at low temperatures, Phil. Trans. Roy. Soc. 251A, 273 (1959).

White, G. K. and Woods, S. B., Thermal and electrical conductivity of rhodium, iridium, and platinum," Can. J. Phys. 35, 248 (1957).

46. Bode, K. H. and Fritz, W., Eine neue Apparatur zur Messung der Wärmeleitfähigkeit von Metallen, Zeit. angew Phys. 10, 470 (1958).

47. Carter, F. E., The platinum metals and their alloys, Am. Inst. Mining Met. Engrs. Inst. Metals Div. Tech. Publ. No. 70, 1 (1928).

48. Johansson, C. H. and Linde, J. O., Kristallstruktur, elektrischer Widerstand, Thermokrafte, Wärmeleitfähigkeit, magnetische Suszettibilitä, Härte und vergutüngserscheinungen des systems AuPt in Vergindung mit dem Zustandsdiagramm, Ann. Phys. 5, 762 (1930).

49. Mikryukov, V. E., Thermal and Electrical Conductivities of Metals and Alloys (in Russian) (Metallurgizeat, Moscow ,1959).

50. Jaeger, F. M. and Rosenbohm, E., The exact formula for the true and mean specific heats of platinum between 0° and 1600°C, Physica 6, 1123 (1939).

51. Kubaschewski, O. and Evans, L. Ll., Metallurgical Thermochemistry (Pergamon, London, 1956).

52. Powell, R. W. and Tye, R. P., High alloy steels for use as a thermal conductivity standard, Brit. J. Appl. Phys. 11, 195 (1960).

53. Powell, R. W. and Tye, R. P., Thermal and electrical conductivities of nickel-chromium (nimonic) alloys, The Engineer, 729 (1960).

54. Accinno, D. J. and Schneider, J. F., Platinel--a noble metal thermocouple to replace Chromel-Alumel, Engelhard Ind., Inc., Tech. Bul. 1, 53 (1960).

55. Freeze, P. D. and Olsen, L. O., Thermoelectric and mechanical stability of Platinel II thermocouples in oxidizing atmospheres, Tech. Doc. Report ASD-TDR-62-835 (1962).

56. Zysk, E. D., A review of recent work with the Platinel thermocouple, Engelhard Ind., Inc., Tech. Bul. 4, 5 (1963).

57. Olsen, O. L., and Freeze, P. D., Reference tables for the Platinel II thermocouple, J. Res. NBS 68C, 263 (1964).

58. Callen, H. B., The application of Onsager's reciprocal relations to thermoelectric, thermomagnetic, and galvanomagnetic effects, Phys. Rev. 73, 1349 (1948).

59. De Groot, S. R., Thermodynamics of Irreversible Processes (Interscience Publishers, Inc., New York, 1951).

60. Domenicali, C. A., Irreversible thermodynamics of thermoelectric effects of inhomogeneous, anistropic media, Phys. Rev. 92, 877 (1953).

61. Domenicali, C. A., Irreversible thermodynamics of thermoelectricity, Rev. Mod. Phys. 26, 237 (1954).

62. Domenicali, C. A., Stationary temperature distribution in an electrically heated conductor, J. Appl. Phys. 25, 1310 (1954).

63. Leech, J. W., Irreversible thermodynamics and kinetic theory in the derivation of thermoelectric relations, Can. J. Phys. 37, 1044 (1959).

64. Ziman, J. M., Electrons and Phonons (Clarendon Press, Oxford, 1960).

65. Beaumont, C. F. A, Connection between macroscopic and microscopic transport phenomena in solid conductors, Am. J. Phys. 33, 547 (1965).

66. El-Saden. M. R., Theory of nonequilibrium thermodynamics with application to the transport processes in a solid, Trans. ASME, J. Heat Transfer, Paper No. 65-HT-1 (1965).

67. Onsager, L., Reciprocal relations in irreversible processes, Part I, Phys. Rev. 37, 405 (1931).

68. Onsager, L., Reciprocal relations in irreversible processes, Part II, Phys. Rev. 38, 2265 (1931).

69. Huntington, H. B. and Ho, S. C., Electromigration in metals, J. Phys. Soc. Japan 18, Supplement II, 202 (1963).

70. Ho, S. C., Hekenkamp, T. and Huntington, H. B., AEC Document Code No. RPI-1044-1, Contract HT(30-1)-1044 (1 April 1964).

71. O'Boyle, D., Observations of electromigration and the Soret effect in tungsten, J. Appl. Phys. 36, 2849 (1965).

72. Callen, H. B., Thermoelectric and thermomagnetic effects in electrochemical constants, NBS Circular 524, 141 (1953).

73. MacDonald, D. K. C., Thermoelectricity-- An Introduction to the Principles (John Wiley & Sons, Inc. New York · London, 1962).

74. Davidson, P. M., The theory of the Thomson effect in electrical contacts, Proc. Inst. Elec. Engrs. 96, Part 1, 293 (1949).

75. Llewellyn-Jones, F., The Physics of Electrical Contacts (University Press, Oxford, 1957).

76. Watson, T. W. and Flynn, D. R., NBS, Private Communication (January 1966).

77. Kirby, R. K., NBS, Private Communication to D. R. Flynn (December 1965).

78. Wichers, E., The History of Pt 27, Temperature, Its Measurement and Control in Science and Industry, Vol. 3, Part 1, Reinhold Publishing Corp., New York, 259, (1962).

79. Vines, R. F., The platinum metals and their alloys, (The International Nickel Co., Inc. 1941).

80. Evans, J. P., NBS, Private Communication (August 1966).

81. Laubitz, M. J., The thermal conductivity of platinum from 300 to 1100 °K, Proc. Fifth Conf. on Thermal Conductivity, (Denver), Paper III-B-1 (1965).

82. Watson, T. W., NBS, Private Communication (January, 1966).

83. Martin, J. J., Sidles, P. H., and Danielson, G. C., Thermal diffusivity of platinum, Report No. IS-1261, contribution No. 1810 of the Ames Laboratory of the U.S. Atomic Energy Commission.

84. Wilson, A. H., The Theory of Metals (University Press, Cambridge 1954).

85. American Institute of Physics Handbook, Second Edition, P. 4-13 (McGraw-Hill Book Co., 1963). The values given in this reference have been adjusted to correspond to temperatures expressed on the International Practical Temperature Scale of 1948. The original reference is to the work of W. F. Roeser as given in Temperature, Its Measurement and Control in Science and Industry, p. 1312 (Reinhold Publishing Corp., New York, N. Y., 1941)

86. Halpern, C. and Flynn, D. R., Private Communication (August 1966).

87. Watson, T. W. and Robinson, H. E., Thermal conductivity of some commercial iron-nickel alloys, Transaction ASME Journal of Heat Transfer, 83C, 403, (1961).

88. Flynn, D. R., Robinson, H. E., and Martz, I. L., Current status of Pyroceram Code 9606 as a thermal conductivity reference standard, Proc. Fourth Conf. on Thermal Conductivity (San Francisco), Paper I-F (1964).

89. Moore, J. P., Metals and Ceramics Div. Ann. Progr. Rept. June 30, 1966 ORNL-3970.

90. Tye, R. P., Dynatech, Private Communication (June 1966).

91. Lander, J. J., Measurements of Thomson coefficients for metals at high temperatures and of Peltier coefficients for solid-liquid interfaces of metals, Phys. Rev. 74, 479 (1948).

92. Jolley, L. B. W., Summation of Series, 2nd revised ed. (Dover Publications Inc., New York, 1960).

93. McFee, R., Optimum input leads for cryogenic apparatus, Rev. Sci. Instr. 30, 98 (1959).

94. Neighbor, J. E., Leads power in calorimetry, Rev. Sci. Instr. 37, 497 (1966).

95. Mallon, R. G., Optimum electrical leads of aluminum and sodium for cryogenic apparatus, Rev. Sci. Instr. 33, 564 (1962).

96. Sobol, H. and McNicol, J. F., Evaporation of Helium I due to current-carrying leads, Rev. Sci. Instr. 33, 473 (1962).

97. Stein, R. P., A solution of the steady linear heat-flow equation with heat generation and conductivity an arbitrary function of temperature., J. Appl. Mech. 26, 685 (1959).

98. Ginnings, D. C. and West, E. D., Heat lead problem in calorimetry, Rev. Sci. Instr. 35, 965 (1964).

99. Watson, G. N., A Treatise of the Theory of Bessel Functions, 2nd ed. (University Press, Cambridge and The Macmillan Co., New York 1948)

100. Peavy, B. A., Determination and smoothing of Fourier coefficients representing sectionally discontinuous functions on a finite surface, To be published.

101. Laubitz, M. J., National Research Council of Canada, Private Communication (August 1966). These values are revised from those which were given in [81] and will be published shortly.


DEPARTMENT OF COMMERCE
NATIONAL BUREAU OF STANDARDS